



BOOK OF ABSTRACTS

Joint 74th ICCP and 39th TSOP Meeting

**“Organic Petrology in the Energy Transition Era:
Challenges ahead”**

**17 – 24 September 2023
Conference & Cultural Center
of the University of Patras
Rio-Patras, Greece**

Bulletin of the Geological Society
Special Publication No. 12, 2023
Publisher: Geological Society of Greece
ISBN 978-618-86841-0-2
ISSN 2945-1426





Joint 74th ICCP and 39th TSOP Meeting
17th – 24th September 2023, Patras, Greece



**Organic Petrology in the Energy Transition Era:
Challenges ahead**

Bulletin of the Geological Society of Greece, Sp. Publ. 12

With the Support of



UNIVERSITY OF
PATRAS
ΠΑΝΕΠΙΣΤΗΜΙΟ ΠΑΤΡΩΝ



EUROPE DIRECT
Περιφέρεια Δυτικής Ελλάδας
Region of Western Greece

Our Sponsors



**HELPE
UPSTREAM**



Public
Power
Corporation



KOZANIS' MINING Co. G.P.



LaborScience



Joint 74th ICCP and 39th TSOP Meeting
17th – 24th September 2023, Patras, Greece

**Organic Petrology in the Energy Transition Era:
Challenges ahead**



Bulletin of the Geological Society of Greece, Sp. Publ. 12



Joint 74th ICCP and 39th TSOP Meeting
17th – 24th September 2023, Patras, Greece



**Organic Petrology in the Energy Transition Era:
Challenges ahead**

Bulletin of the Geological Society of Greece, Sp. Publ. 12

Dear Colleagues,

we both welcome you to the Joint 74th ICCP and 39th TSOP Meeting taking place in our University here in Patras!

After 1993 in Chania and 2005 again in Patras, it is now the third time in ICCP's history that the annual meeting is held in Greece, whereas for the TSOP members this is the first gathering in our country; and this time in a Joint Meeting aiming to enhance the interaction among the members of the Organic Petrology community. During this event we do hope to continue keeping the tradition of both ICCP and TSOP, namely the international exchange of scientific information directly or indirectly related to Organic Petrology and the fruitful discussions in a friendly atmosphere.

*The Joint Meeting has the very modern and demanding title: '**Organic Petrology in the Energy Transition Era: Challenges ahead**'. The recent political decisions concerning the decarbonization of the energy sector in Europe, as well as the war between Ukraine and Russia have severely affected the global energy market differentiating the energy mix of many countries towards the increase of the renewables' share, the abandonment of coal exploitation, and the volatilization of the oil and gas prices. All these definitely affect our scientific discipline and the organic petrologists as well, despite the fact that in several emerging economies coal still plays and will continue playing an important role in covering the energy demand. Subjects dealing with a wide spectrum of applications of coal and, in general, organic matter like in fertilizer manufacturing, energy storage, biocarbon utilization etc., are nowadays gaining interest beyond the traditional uses such as the petroleum exploration, the cement and steel manufacturing, the gasification, and even the primary power generation. It is our duty to explore new application fields of Organic Petrology and to stay tuned with the forthcoming developments. These subjects will be addressed in the presentations and discussions during the Meeting.*

At this point, we would like to express our gratitude to all the contributors to the success of the Meeting: the members of both the Organizing and the Scientific Committee, our sponsors, the graduates of our Department of Geology for their assistance and, of course, the speakers, the poster presenters and you all who have traveled from many countries to participate in the meeting.

Wishing you to enjoy all the activities scheduled in the frame of our Joint Meeting, as well as the stay in Patras,

Kimon Christanis

Stavros Kalaitzidis



Joint 74th ICCP and 39th TSOP Meeting
17th – 24th September 2023, Patras, Greece

**Organic Petrology in the Energy Transition Era:
Challenges ahead**



Bulletin of the Geological Society of Greece, Sp. Publ. 12

Organizing Committee

Chair

Prof. em. Dr. **Kimón Christanis**, Department of Geology, University of Patras

Executive Secretary

Assoc. Prof. Dr. **Stavros Kalaitzidis**, Department of Geology, University of Patras

Members

Prof. Dr. **Andreas Georgakopoulos**, Department of Geology, Aristotle University of Thessaloniki

Prof. Dr. **Nikolaos Pasadakis**, Institute of Geoenergy, FORTH

Dr. **Aristofanis Stefatos**, Hellenic Hydrocarbons and Energy Resources Management Company (HEREMA)

Dr. **Ioannis Oikonomopoulos**, Hellenic Petroleum Upstream S.A.

Dr. **Dimitrios Rallakis**, Department of Geology, University of Patras

Dr. **Stefanos Papazisimou**, Directorate of Environment and Spatial Planning, Region Western Greece

Dr. **Nicolaos Koukouzas**, Chemical Process and Energy Resources Institute, CERTH

Mr. **Markos Xenakis**, Hellenic Survey of Geology and Mineral Exploration



Joint 74th ICCP and 39th TSOP Meeting
17th – 24th September 2023, Patras, Greece

**Organic Petrology in the Energy Transition Era:
Challenges ahead**



Bulletin of the Geological Society of Greece, Sp. Publ. 12

Scientific Committee

Prof. em. Dr. **Kimon Christanis**, University of Patras, Greece

Dr. **Carolina Fonseca**, Federal University of Rio de Janeiro, Brazil

Dr. **Thomas Gentzis**, Core Laboratories, USA

Dr. **Paul Hackley**, USGS, USA

Assoc. Prof. Dr. **Stavros Kalaitzidis**, University of Patras, Greece

Prof. Dr. **Ali Ihsan Karayiğit**, Hacettepe University, Turkey

Prof. Dr. **Polla Khanaqa**, Kurdistan Inst. for Strategic Studies & Scientific Research, Iraq

Dr. **Grzegorz Lis**, University of Wrocław, Poland

Prof. Dr. **João Graciano Mendonça Filho**, Universidade Federal do Rio de Janeiro, Brazil

Dr. **Ioannis Oikonomopoulos**, Hellenic Petroleum S.A., Greece

Dr. **Henrik I. Petersen**, GEUS, Denmark

Dr. **Joana Ribeiro**, University of Coimbra, Portugal

Dr. **Sandra Rodrigues**, The University of Queensland, Australia

Prof. Dr. **Hamed Sanei**, Aarhus University, Denmark

Dr. **George Siavalas**, Shell Global Solutions International B.V., The Netherlands

Dr. **Bruno R.V. Valentim**, University of Porto, Portugal

Dr. **Nicola J. Wagner**, University of Johannesburg, South Africa

Dr. **Malgorzata Wojtaszek-Kalaitzidi**, Institute of Energy & Fuel Proc. Technology, Poland

Dr. **Lei Zhao**, China University of Mining and Technology, Beijing, China

Prof. Dr. **Dragana Životić**, University of Belgrade, Serbia



Table of contents

Meeting Overview Schedule	1
----------------------------------	----------

Opening Session

A. Stefatos	3
<i>Hydrocarbon Exploration integrated into Greece's trajectory towards a net-zero carbon future</i>	
A. Chatziapostolou, M. Xenakis	4
<i>The contribution of the Hellenic Survey of Geology and Mineral Exploration in coal research in Greece</i>	

TSOP Technical Sessions

Technical Session A	5
G. Smith, L. Johnson, I. Sadd	6
<i>Depositional and climate control of organic facies: Ordovician, Early-Middle Triassic and Cretaceous-Eocene in the Canning, Roebuck and Gippsland Basins, Australia</i>	
A. Wheeler, U. Heimhofer, J.S. Esterle, R. Littke	7
<i>Coal petrology, palynology and carbon isotope record of the Aramac Coal Measures (Galilee Basin, Australia)</i>	
L. Shao	8
<i>Palaeo-peatlands as organic carbon pools in geological history: Quantitative estimation from net primary productivity</i>	
W. Yang, W. Li	9
<i>Observation and quantitative analysis of the effect of enhanced tectonic deformation on the nanostructural alteration of coal</i>	
B. Sun, C. Liu	10
<i>Nano-sized phase in different coal lithotype and their fractions under pyridine treatment</i>	
D. Song, Y. Li, Y. Zhai	11
<i>Desorption rate of methane in coal matrix and its main controlling factors</i>	



S. Pandey, V.A. Mendhe, P. Shukla <i>Petrographic study of palynomorphs and macerals to assess the kerogen in Gondwana and Tertiary coal seams, India</i>	12
Technical Session B	13
A. Damodhar Kamble <i>Reactivity assessment of coal, lignite and biomass organic constituents through detailed petrography: An implication to gasification, carbon conversion and syngas</i>	14
G.P. Lis, I. Jelonek, M. Mastalerz, T. Topór <i>Exploring the influence of maturity evolving maceral composition on shale porosity: Example from the Lower Paleozoic shale from the Baltic Basin (Poland)</i>	15
Y. Li, D. Song, H. Wang, X. Guo, Z. Ren <i>The selective effect of pore-fracture evolution during the process of liquid nitrogen cyclic fracturing in coal</i>	16
N. Xu, Q. Wang, P. Li, M.A. Engle <i>Towards the identification of coal macerals through deep learning</i>	17
Technical Session C	18
Z. Guo, B. Sun <i>Geochemistry of tuff layers and its implications for Li-Zr (Hf)-Nb (Ta) enrichments in Cisuralian coal seams, Shanxi Province, North China</i>	19
M. Costa, H. Moura[†], A. Pinto de Jesus, D. Flores <i>Petrographic, geochemical and mineralogical characterization of coals from the Carboniferous Douro Basin: São Pedro da Cova and Pejão Coalfields</i>	20
P.C. Hackley, R.J. McAleer, A.M. Jubb, B.J. Valentine, J.E. Birdwell <i>Cathodoluminescence differentiates sedimentary organic matter types</i>	21
V.I. Makri, K. Kokkinopoulou, N. Pasadakis <i>Rock-Eval based kerogen kinetics and the effect of rock matrix</i>	22
M. Garcia-Gonzalez, T.S. Palmera-Henao <i>Thermal maturation of the La Luna Formation in the Middle Magdalena Basin, Colombia</i>	23
A. Liu, H. Sanei, N.H. Schovsbo, X. Zheng, L. Bian <i>Influence of thermal intrusion on solid bitumen in the Alum Shale, Central Sweden</i>	24
Technical Session D	25
S. Mohebaty, F. Goodarzi, P.K. Pedersen, T. Gentzis <i>Elemental composition and facies analysis of the Late Cenomanian-Early Turonian Second White Specks and adjacent oil shales, Western Interior Seaway, Canada</i>	26



**Organic Petrology in the Energy Transition Era:
Challenges ahead**

Bulletin of the Geological Society of Greece, Sp. Publ. 12

- C. Fonseca, J. Torres Souza, A.D. de Oliveira, J. de Oliveira Mendonça, J.G. Mendonça Filho, L. Borghi** 27
Organic matter characterization of a sedimentary succession of the Barra Velha Formation carbonates from the Santos Basin, offshore Brazil
- Z. Zhou, H.I. Petersen, N.H. Schovsbo, A. Rudra, H. Sanei** 28
Spatial and temporal changes in the organic matter supply during the Cenozoic basin evolution in the Danish North Sea
- I. Oikonomopoulos, T. Gentzis, H. Carvajal-Ortiz, E. Tripsanas** 29
New insights into oil-to-source rock correlation of oils and asphalt seeps from Zakynthos Island and the west coast of Peloponnese, Western Greece

Joint ICCP-TSOP Symposium

- A. Rudra, H.I. Petersen, H. Sanei** 32
Molecular structure and long-term stability of biochars
- H.I. Petersen, H. Deskur, A. Rudra, S. Bachmann Ørberg, D. Krause-Jensen, H. Sanei** 33
Insight into the composition and permanence of biochar produced from pyrolysis of land plant and macroalgae biomass
- M. Wojtaszek-Kalaitzidi, M. Rejdak, M. Książek, S.Y. Larsen, S. Kalaitzidis** 34
Olive kernel biochar and charcoal "in-fusion" in coke matrix vs. biocoke quality
- M. Misz-Kennan, Z. Milakovska, M.J. Fabiańska, M. Stefanova, D. Więclaw, G. Vladislavov** 35
Pyrolytic alterations in organic matter of lignite gangue rocks from Troyanovo-3 Mine dump area (Mini Maritsa Iztok, Bulgaria)
- M. Zielińska, E. Szram, M. Misz-Kennan, M. Fabiańska, D. Plašienka, R. Aubrecht, M. Molčan Matejová, T. Potočný** 36
Organic matter research from the Pieniny Klippen Belt (Central Western Carpathians)
- A. Drobniak, M. Mastalerz, I. Jelonek, Z. Jelonek** 37
Interlaboratory study: Testing reproducibility of solid biofuel component identification using reflected light microscopy
- V.A. Mendhe** 38
Petrographic facets of Middle Eocene lignite with implications to coalbed methane potential from northern part of Cambay Rift Basin, India
- P. Shukla, V.A. Mendhe, S. Pandey** 39
Influence of lithotypes and petrographic constituents on methane and CO₂ sorption of coal from Early Permian-Gondwana deposits, India
- X. Zheng, R.Ø. Stenshøj, H.I. Petersen, H. Sanei** 40
Evaluation of the effect of supercritical CO₂ injection on remaining oil in depleted chalk reservoirs, Danish North Sea



G. Smith, L. Johnson, I. Sadd <i>Exotic liptinite macerals – what are they and why such good generative potential?</i>	41
X. Xie, Y. Liu, Y. Xu <i>The characteristics comparisons of Cambrian source rocks in South China and Alum Shale in Europe</i>	42
T. Larikova, I. Sýkorová, M. Havelcová, B. Kříbek <i>Radiolytic alteration of uraniferous organic matter and base-metal mineralization in Bytiz, Příbram district, Czech Republic</i>	43
T. Adsul, S. Ghosh, M.D. O’Beirne, J.P. Werne, W.P. Gilhooly III, J. Houghton, D. Fike, P.C. Hackley, J.J. Hatcherian, A. Kumar Varma <i>Decrypting paleomire conditions of superhigh-organic-sulfur coals from Meghalaya, India</i>	44
D.M. de Lima, J.G. Mendonça Filho, C. Fonseca, A.D. de Oliveira, J. de Oliveira Mendonça, P.A. Gonçalves <i>Organic facies variability and paleoenvironmental characterization of the Codó and Itapecuru Formations (Aptian-Albian) of Parnaíba Basin, Brazil</i>	45
P. Khanaqa, S. Kalaitzidis, W. Riegel <i>Organic petrographical features of Miocene Meliadi-Moschopotamos lignite, Macedonia, northern Greece</i>	46
S. Biswas, N.J. Wagner, O.M. Moroeng <i>Mineralogy and organic petrography of the No. 6 coal seam, Soutpansberg Coalfield, South Africa: Evidence for hydrothermal activity</i>	47
Z. Büçkün, M. Çolak <i>Petrological, mineralogical and geochemical proxies to the organic matter dispersed in the sedimentary rocks in Turgut area, Yatağan Basin, SW Türkiye</i>	48
P. Papadopoulou, G. Iliopoulos, K. Perleros, S. Kalaitzidis, K. Christanis, N. Zouros <i>Contribution of organic petrography in the study of volcanoclastic sequences: The case of West Acrocheiras section, Petrified Forest of Lesvos, Greece</i>	49

Posters

A.G. Borrego, J.E. Ortiz, Y. Sánchez-Palencia, J.L.R. Gallego, T. Torres <i>Petrographic composition of Las Conchas Mire in relation to palaeoclimate proxies</i>	51
A. Zdravkov, A. Bechtel, D. Groß, K. Stojanović <i>Reconstruction of peat-forming paleoenvironments within the Oligocene Bobov Dol Basin, SW Bulgaria: Insights from organic petrology</i>	52
A. Zdravkov, D. Groß, A. Bechtel, K. Stojanović, I. Kojić <i>Paleoenvironmental settings of peat formation within Padesh Graben, SW Bulgaria, deduced from maceral analysis and geochemical properties of Suhostrel coal</i>	53



**Organic Petrology in the Energy Transition Era:
Challenges ahead**

Bulletin of the Geological Society of Greece, Sp. Publ. 12

- B. Demberelsuren, L. Jargal, S. Lkhagva-Ochir, B.-O. Erdenetsogt, R. Ganzorig, T. Zorigbold, O. Tugj, T. Khash-Erdene, J. Otgonbaatar** 54
Mineral matter content, distribution, and characteristics of the Ukhaakhudag coal deposit, Mongolia
- J.E. Ogala, K. Perleros, E. Kyriazaki, M. Aggelopoulos, O.I. Ejeh, S. Kalaitzidis, K. Christanis** 55
The coal beds between Obomkpa and Iseele-Azagba from Southern Nigeria: A petrographical, mineralogical and geochemical approach
- R. Melo, E. Font, J. Ribeiro** 56
Signature of wildfires in soils using organic petrology and geochemistry: Case studies from Portugal
- J. Ribeiro, M. Ribeiro, J. Erbolato Filho** 57
Petrographic identification of contaminant particles in soil around a coal-fired thermal power plant (Sines, Portugal)
- C. Chrysakopoulou, K. Perleros, M. Wojtaszek-Kalaitzidi, L. Papadopoulou, N. Kantiranis, S. Kalaitzidis** 58
Mineralogical, chemical and petrographical investigation of airborne dust material nearby coal-fired power plants: A case study from Upper Silesia, Poland
- P. Meyvisch, K.N. Mertens, C. Fonseca, J.G. Mendonça Filho, M. Reolid, L.V. Duarte, S. Louwye** 59
First macromolecular characterization of fossil Choanoflagellates
- J. Wang, R. Xiao, Y. Zhao, J. Zhang** 60
Migration and transformation of uranium during uranium-rich coal combustion
- A.C. Santos, I. Kuźniarska-Biernacka, A. Guedes, B. Valentim** 61
Characterization of Fe-bearing morphotypes from coal combustion ash samples targeting their application in catalytic reactions
- M. Misz-Kennan, M.J. Fabiańska, J. Ciesielczuk, E. Szram, D. Więclaw** 62
Weathering impact on organic petrography, mineralogy and geochemistry of coal wastes – Case studies from the Upper Silesian Coal Basin, Poland
- N. Makri, A. Iordanidis[†], N. Kouvrakidis, K. Christanis, S. Kalaitzidis** 63
Mineralogical, petrographical and geochemical investigation of fly & bottom ashes from Agios Dimitrios Power Plant, W. Macedonia, Greece
- P.A. Gonçalves, M. Corga, S. Aires, J. de Oliveira Mendonça, J.G. Mendonça Filho, D. Flores** 64
The contribution of palynofacies analysis in archeological studies
- M. Životić, D. Stojiljković, N. Nikolić, D. Bajuk-Bogdanović, D. Životić** 65
The behaviour of Kolubara and Kostolac lignite during devolatilisation process: A petrographical approach
- B. Valentim, C. Badenhurst, A. Guedes, E. Mousa, K. Moreira, A.C. Santos, G. Ye** 66
Applied organic petrography to spent lithium-ion batteries (LiB) recycling

**Organic Petrology in the Energy Transition Era:
Challenges ahead**

Bulletin of the Geological Society of Greece, Sp. Publ. 12

- Z. Jelonek, I. Jelonek, A. Drobnik, M. Mastalerz** 67
Distinguishing fossil inertinite from modern charcoal in microscopic images
- I. Matlala, M. Moroeng, N. Wagner** 68
Characterization of the Highveld coal's macromolecular structure and their float products using Raman spectroscopy
- M. Mroczkowska-Szerszeń, K. Ziemianin, L. Dudek, B. Adamczyk, M. Dudek** 69
Investigations of structural and chemical changes during pyrolysis of biomass by means of optical, spectroscopic and porosimetric methods
- J. Hatcherian, T. Adsul, P. Hackley, S. Ghosh, A. Kumar Varma** 70
Impact of pyrite-sourced sulfur on catagenesis in gilsonite undergoing hydrous pyrolysis
- I. Jelonek, Z. Jelonek, A. Drobnik, M. Mastalerz** 71
Composition verification of biofuels produced from herbaceous and woody biomass using petrographic analysis
- G. Predeanu, V. Slăvescu, M.F. Drăgoescu, P. Samoilă, A. Fiti** 72
Microscopic assessment of some biomass chars
- G. Predeanu, M. Wojtaszek-Kalaitzidi, I. Suárez Ruiz, M. Bălănescu, A. Gómez Borrego, M.A. Diez, L. Garcia, M.D. Ghiran, P. Hackley, S. Kalaitzidis, J. Kus, D. Mancisidor, M. Mastalerz, M. Misz-Kennan, S. Pusz, S. Rodriguez, G. Siavalas, A.K. Singh, P. Tomillo, A. Varma, A. Zdravkov, D. Životić** 73
Microscopic characterization of carbon materials derived from coal and biomass and their interaction phenomena in making high grade products
- X. Guo, Y. Tang, C. Eble, H. Schobert, S. Wang** 74
Study on thermal properties differences of coal from insight of nano carbon structure characteristics
- S. Wang, L. Zhao, Y. Shao, Z. Dong** 75
The graphitization characteristics of coal macerals
- S. Kędzior** 76
The occurrence of methane in the deep parts of the Carboniferous Formations in the Upper Silesian Coal Basin, Poland. Case Study of the Orzesze-1 deep exploratory well
- J. Kus, P.C. Hackley** 77
CLSM thermal maturity of Tasmanites-rich Devonian Ohio Shale, northern Appalachian Basin, USA
- A. Ortiz-Loaiza, P.A. Gonçalves, J.G. Mendonça Filho, D. Flores** 78
Origin and thermal maturity of organic matter in Lower-Middle Jurassic rocks from the Lusitanian Basin (Portugal): A case study from the São Pedro de Moel-2 well
- A. Schito, D. Muirhead, P. Hackley, J. Parnell, R. Galimberti, L. Mascheroni** 79
Understanding the effects of heating rate, stress and fluids in maturation of carbonaceous materials by Raman spectroscopy
- A. Zdravkov, N. Botoucharov, D. Groß, I. Kostova, A. Bechtel, D. Apostolova** 80
Origin of organic matter and hydrocarbon generation potential of Early-Mid Jurassic argillaceous rocks from North Bulgaria



Joint 74th ICCP and 39th TSOP Meeting
17th – 24th September 2023, Patras, Greece



**Organic Petrology in the Energy Transition Era:
Challenges ahead**

Bulletin of the Geological Society of Greece, Sp. Publ. 12

J. Reyes, L.J. Knapp, O.H. Ardakani, K. Ishikawa <i>Enumeration of Rock-Eval and organic petrography results from artificially matured core samples with varying TOC and S contents</i>	81
Author Index	82

	Sunday - Joint ICCP-TSOP day 17/9/2023		Monday 18/9/2023	Tuesday 19/9/2023		Wednesday 20/9/2023	Thursday 21/9/2023	Friday 22/9/2023	Saturday 23/9/2023	Sunday 24/9/2023	
8:30 - 9:00			Registration ICCP-TSOP			ICCP-TSOP Mid-Conference Excursion to Delphi or Mycenae			Joint ICCP-TSOP Field Trip (Either one-day to Zakynthos Island or 2-days NW Greece)		
9:00 - 9:30			Joint ICCP-TSOP Opening Session		ICCP Session		TSOP Technical Session A	Joint ICCP-TSOP Symposium			ICCP Session
9:30 - 10:00			Coffee Break		Coffee Break		Coffee Break	Coffee Break			
10:00 - 10:30			ICCP GA	TSOP Short Course	ICCP Session		TSOP Technical Session B	Joint ICCP-TSOP Symposium			ICCP Session
10:30 - 11:00			Joint Lunch		ICCP Lunch		TSOP General Meeting & Business Lunch	Lunch			Lunch
11:00 - 11:30			ICCP Session		ICCP Session		TSOP Technical Session C	Joint ICCP-TSOP Symposium			ICCP-TSOP Microscopy Session
11:30 - 12:00	ICCP Council	TSOP Council	Coffee Break		Coffee Break		Coffee Break	Coffee Break			
12:00 - 12:30			ICCP Session		ICCP Session		TSOP Technical Session D	Joint ICCP-TSOP Symposium			ICCP Closing Plenary Session
12:30 - 13:00			Joint ICCP-TSOP Poster Session					TSOP Closing Ceremony			
13:00 - 13:30			ICCP Council		Student Event						
13:30 - 14:00	Joint ICCP-TSOP Ice Breaker party							Joint Conference Dinner			
14:00 - 14:30											
14:30 - 15:00											
15:00 - 15:30											
15:30 - 16:00											
16:00 - 16:30											
16:30 - 17:00											
17:00 - 17:30											
17:30 - 18:00											
18:00 - 18:30											
18:30 - 19:00											
19:00 - 19:30											
19:30 - 20:00											
20:00 - 20:30											
20:30 - 21:00											
21:00 - 21:30											
21:30 - 22:00											
22:00 - 22:30											



Joint 74th ICCP and 39th TSOP Meeting
17th – 24th September 2023, Patras, Greece

**Organic Petrology in the Energy Transition Era:
Challenges ahead**



Bulletin of the Geological Society of Greece, Sp. Publ. 12

Opening Session



Joint 74th ICCP and 39th TSOP Meeting
17th – 24th September 2023, Patras, Greece



**Organic Petrology in the Energy Transition Era:
Challenges ahead**

Bulletin of the Geological Society of Greece, Sp. Publ. 12

**Hydrocarbon Exploration integrated into Greece's trajectory
towards a net-zero carbon future**

Aristofanis Stefatos

CEO Hellenic Hydrocarbons and Energy Resources Management Company (HEREMA)

Corresponding Author: a.stefatos@herema.gr

Last year (2022) was a year with a profound impact on the energy sector. In light of past year's events, which exacerbated Europe's already complex energy crisis, the EU, as well as many countries around the world, were forced to rethink their energy security management and the pace of their energy transition. In this context, HEREMA's role and contribution became more than ever relevant and was brought in the spotlight, as it seeks to ensure domestic production of hydrocarbons, that can deliver sustainability and security of energy supply, while generating national revenue to sponsor and promote a smooth transition to a more sustainable green energy system, where renewable energy sources will increasingly assume a leading role.

A key component of this effort, is to accelerate the exploration program of our country's hydrocarbon potential, with an emphasis on natural gas. Within only 13 months, we have completed 7 marine geophysical surveys and, in cooperation with the lessees, we are accelerating the transition to the next phase of exploratory drilling. The exploration expenditure was increased by 150% compared to the minimum expenditure commitments under the concession contracts and all programs were delivered at the highest environmental standards and ahead of schedule. The potential exploitation of national energy resources holds the prospect of safeguarding the country's energy independence and energy security, unlocking a sector with enormous economic potential that can help to bear the costs of the green transition and ultimately protecting national, economic and social interests at a time of unprecedented increases in energy costs for households and industry.

Undoubtedly, the long-term solution is an energy system powered by renewable sources and new energy technologies. However, this transition will require time. And this is where natural gas comes in, which will play an essential role as a "fuel bridge" in the future, allowing us to replace other fossil and more polluting fuels. Therefore, natural gas will continue to play an essential role in our country's energy mix for the decades to come. Developments in recent years have also helped to form this consensus.

HEREMA is rapidly implementing its strategy in all its areas of responsibility, including our recently expanded scope that includes carbon capture and storage (CCS) as well as the preparation of the National Program for the development of offshore wind farms (OWF). HEREMA has transformed into a key player in the promotion of Greece's energy potential, which will contribute to our country's development as an energy supply centre and its timely transition to a strengthened and sustainable energy system. Our priority is to contribute to the successful implementation of our country's ambitious energy plan for a green transition and energy security, utilizing our national energy resources that can boost the economy, further enhance the positive investment climate and create new jobs, whilst operating with transparency and a sense of responsibility to contribute to the timely shift to an enhanced and sustainable energy system.



**The contribution of the Hellenic Survey of Geology and Mineral Exploration
in coal research in Greece**

Adamantia Chatziapostolou, Markos Xenakis*

Hellenic Survey of Geology and Mineral Exploration, Acharnae, Greece

* Corresponding Author: markxen@igme.gr

The Hellenic Survey of Geology and Mineral Exploration (HSGME) was contributing to the systematic exploration of energy resources in Greece for the last seven decades. An intense coal exploration period was triggered by the 1973 energy crisis, with the aim to discover new deposits and to increase the mineable coal reserves for power generation. After the discovery of the large lignite-bearing basins of Florina-Ptolemais-Kozani in NW Greece and of Megalopolis in Peloponnese, the research was expanded to inventorize and evaluate all the proven coal reserves of Greece (Koukouzas et al., 1997).

During the period from 1975-2003 and within the framework of HSGME's research programs for solid fuels, 2,664 core drillings were performed, with a cumulative length of > 472 km and an average drilling depth of about 177 m. From the extensive research, 137 lignite deposits distributed in 74 lignite-bearing basins, were systematically studied. Summarizing the results of this campaign, about 6.7 Gt coal reserves were discovered, out of which 4.5 Gt proved being recoverable reserves. In the above proven coal reserves the peat reserves of the Philippi peatland, which are 4.3 Gm³ being equivalent to 1.7 Gt of the Ptolemais-type lignite, are not included.

Since the 1950's, the participation of lignite in power generation has been continuously increasing, reaching the peak of 80% in 1994. The annual lignite production reached the maximum of 70 Mt in 2002. In recent years, the use of natural gas and renewable energy sources in power generation has significantly increased, whereas the lignite share is constantly decreasing. Last year (2022), the lignite share in power generation was 13.7% only (Eurocoal, 2022). Multi-year research projects were initiated in the field of non-power coal uses in order to exploit small coal deposits and to manufacture products of high added value such as soil-amendment media, sorbents for water treatment, air cleaning, urban wastes etc.

With the onset of the decarbonization era, HSGME ceased coal exploration. In the last 4 years all the available information and data of the Greek coal deposits are systematically compiled in a digital database. The aim of this project is the preparation of an interactive, open-access website with digital maps of the coal-bearing basins, the coal deposits, the core loggings, etc. and all the available quantitative and qualitative data (Chatziapostolou and Xenakis, 2022).

References

- Eurocoal - European Association for Coal and Lignite. 2022. Annual report, 23 pp.
Koukouzas, C., Foscolos, A.E., Kotis, T., 1997. Research and Exploration of Coal in Greece: A View to the Future. *Energy Resources* 19, 335-347.
Chatziapostolou, A., Xenakis, M., 2022. Database Design, Implementation and Management of the Greek Lignite Potential. 16th International Congress of the Geological Society of Greece, 17-19 October 2022 - Patras, Greece, Bulletin of the Geological Society of Greece, Sp. Publ. 10, Ext. Abs. GSG2022-099.



Joint 74th ICCP and 39th TSOP Meeting
17th – 24th September 2023, Patras, Greece

**Organic Petrology in the Energy Transition Era:
Challenges ahead**



Bulletin of the Geological Society of Greece, Sp. Publ. 12

TSOP Technical Session A

Tuesday, 19.9. 2023

- | | |
|-------------|--|
| 09:00-09:15 | Welcome – General Business |
| 09:15-09:30 | Depositional and climate control of organic facies: Ordovician, Early-Middle Triassic and Cretaceous-Eocene in the Canning, Roebuck and Gippsland Basins, Australia
<u>G. Smith</u> , L. Johnson, I. Sadd |
| 09:30-09:45 | Coal petrology, palynology and carbon isotope record of the Aramac Coal Measures (Galilee Basin, Australia)
<u>A. Wheeler</u> , U. Heimhofer, J.S. Esterle, R. Littke |
| 09:45-10:00 | Palaeo-peatlands as organic carbon pools in geological history: Quantitative estimation from net primary productivity
L. Shao |
| 10:00-10:15 | Observation and quantitative analysis of the effect of enhanced tectonic deformation on the nanostructural alteration of coal
W. Yang, <u>Wu Li</u> |
| 10:15-10:30 | Nano-sized phase in different coal lithotype and their fractions under pyridine treatment
<u>B. Sun</u> , C. Liu |
| 10:30-10:45 | Desorption rate of methane in coal matrix and its main controlling factors
<u>D. Song</u> , Y. Li, Y. Zhai |
| 10:45-11:00 | Petrographic study of palynomorphs and macerals to assess the kerogen in Gondwana and Tertiary coal seams, India
<u>S. Pandey</u> , V.A. Mendhe, P. Shukla |



Depositional and climate control of organic facies: Ordovician, Early-Middle Triassic and Cretaceous-Eocene in the Canning, Roebuck and Gippsland Basins, Australia

Greg Smith^{1*}, Lukman Johnson^{1,2}, India Sadd^{1,3}

(1) Curtin University, Perth, Australia; (2) now Fugro, Perth, Australia; (3) now Santos, Perth, Australia

* Corresponding Author: Gregory.c.smith@curtin.edu.au

Plants are very selective in where they live and they also evolve with geological time. This makes them excellent indicators of climate change, depositional environments, water table/sea level, rate of subsidence and sediment age. Recent studies at Curtin University have shown how significant this can be for source rocks and to indicate climate impact.

The organic matter in the Ordovician Goldwyer Formation, Canning Basin W.A. is dominated by graptolites (vitrinitic) and liptinites (cryptospores, acritarchs, chitinozoans and liptodetrinite), with minor *G. prisca* (telalginite) and probable bacterial colonies and mats (lamalginite) in the groundmass. They occur in thin calcareous, siliceous and mudstone beds deposited in an equatorial climate with high sea-levels. The calcareous beds have low organic matter, mainly graptolites, and represent more oxidative deeper water environments. The best source rocks are thin organic-rich mudstones representing anoxic shallow water, restricted sediments and they have distinctive Mass Spectrogram (MS) signatures.

The organic matter in the Early Triassic Kockatea Shale, Perth Basin, W.A. was deposited just after the P-T extinction event in restricted shallow marine settings. It is dominated by acritarchs and algae with little land plant input and forms excellent source rock. In contrast, the Middle Triassic Caley Member, Roebuck Basin W.A. forms a good source rock but contains a very different organic assemblage with very high liptinite plus vitrinite contents deposited in an extensive delta. It shows a distinct change with progradation of the delta from low organic matter mudstones with Liptinite (L) \approx Vitrinite (V), to carbonaceous mudstones (L>V), to coaly mudstones (V>L), to organic rich cannel coals (L>>V), with coals at the top of the regression (V>L). The Vitrinite and Liptinite is very different to Carboniferous and Permian organic matter being derived from specially adapted Lycopods, Seed Ferns and Ferns that colonized the late Early-Middle Triassic after the P-T land plant extinction and the cutinite, megaspores and Tasmanites have distinctive MS signatures.

A marked organic facies change occurs in the Gippsland Basin from the Late Cretaceous/Early Eocene to the Middle Eocene/Miocene that coincided with the Eocene to Oligocene transition (EOT) controlled by climate, basin tectonics and sedimentary facies. The older coals are durains with high telovitrinite:detrovitrinite (TV:DV), a gelified DV groundmass, high inertinite from seasonal wet-dry conditions, clays and low pyrite, deposited in alluvial plain/upper delta plain facies. The younger coals include thick ombrogenous peats developed in lower coastal plains mainly upward drying clarain lithotypes with moderate TV:DV and upwards increasing L. More distal back-barrier marshes form thinner clarain and cannel peats with perhydrous high detrovitrinite:telovitrinite and liptinite (14-26%) and together with back barrier lagoon mudstones are very good source rocks.

Coal petrology, palynology and carbon isotope record of the Aramac Coal Measures (Galilee Basin, Australia)

Alexander Wheeler^{1*}, Ulrich Heimhofer¹, Joan S. Esterle², Ralf Littke³

(1) Institute for Geology, Leibniz University Hannover, Callinstraße 30, D-30167 Hannover, Germany;

(2) School of Earth and Environmental Sciences, The University of Queensland, QLD 4072, Australia;

(3) Energy and Mineral Resources Group (EMR), Institute of Geology and Geochemistry of Petroleum and Coal, Lochnerstr. 4-20, RWTH Aachen University, 52056 Aachen, Germany

* Corresponding Author: wheeler@geowi.uni-hannover.de

The Aramac Coal Measures in the Galilee Basin represent the early transition from a cold to a cool-temperate climate at the terminus of the Late Palaeozoic Ice Age (LPIA). The aim of this study is to examine the record of deglaciation and the establishment of the peat-forming *Glossopteris*-flora. Two boreholes, Longreach 1-1B and Muttaburra 1, were sampled to compare palynological and carbon isotope records alongside coal petrology.

Palynological samples yield high abundances of striate bisaccate pollen derived from glossopterids, along with spores represent fern, horsetail and lycopsid undergrowth. Aquatic palynomorphs are rare but are indicative of freshwater conditions with no marine influence. These results reflect the quick establishment of *Glossopteris*-flora following the glaciation. Coals from both sections show a degree of variability can be observed in the coals between each borehole. Coal seams in both holes show relatively low maturity for Australian Permian coals (vitrinite reflectance between 0.5% and 0.6%). Muttaburra 1 features fewer and thinner coal seams than Longreach 1-1B. Coals from Longreach 1-1B tend to have a higher abundance of minerals and variable vitrinite/inertinite ratios. Coals in Muttaburra 1 feature higher inertinite proportions. The liptinite component is made up mainly of sporinite and cutinite, but exsudatinitite is also present filling pore space in the fusinites. The thin seams in the lower part of the Aramac Coal Measures feature higher proportions of liptinite, which tends to decrease upsection. With regards to intraseam variability, increases in inertinite can be observed in some seams in Longreach 1-1B, but not observed in Muttaburra 1. Organic carbon isotope values are within the expected range for C3 terrestrial plants. These values show an apparent cyclicity which may be related to climatic changes and humidity changes affected by the P1 and P2 glaciations.

The timing of the deposition of the Aramac Coal Measures coincides with the P2 glaciation. Peat-formation either occurred distally from the position of the ice sheets or during brief interglacial phases. The high inertinite proportions indicate fire and/or fungal degradation of within the mire. Sedimentological evidence suggests permafrost was present during the formation of at least some proportion of the coal seams.



Joint 74th ICCP and 39th TSOP Meeting
17th – 24th September 2023, Patras, Greece



**Organic Petrology in the Energy Transition Era:
Challenges ahead**

Bulletin of the Geological Society of Greece, Sp. Publ. 12

**Palaeo-peatlands as organic carbon pools in geological history: quantitative estimation
from net primary productivity**

Longyi Shao

College of Geoscience and Surveying Engineering, China University of Mining and Technology (Beijing),
Beijing 100083, China

Corresponding Author: ShaoL@cumtb.edu.cn

Peatlands, as one of the important ecosystems, have the ability of long-term carbon sequestration and are an extremely important carbon pool, which plays a vital role in the global carbon cycle. Palaeo-peatlands are the main storage for terrestrial carbon and important records of palaeoclimate. Net primary productivity (NPP) of the palaeo-peatland refers to the fixed carbon of peatland in the primary production process; studying the NPP in palaeo-peatlands is of great significance for understanding the formation, development, and evolution of palaeo-peatlands.

Geologists examine the stratigraphic cycles using palaeoclimate proxy records and link the recognized sedimentary oscillations to the Milankovitch cycles. Information recorded by the geophysical logs can be an ideal palaeoclimate proxy, which is commonly used in the study of cyclostratigraphy. The logging response of gamma ray, density, and resistivity can reflect the variation in ash yield and the V/I (vitrinite to inertinite) ratio in a coal seam. Spectral analyses of geophysical data from thick coal seams can help identifying the significant signals of Milankovitch period parameters, and then the period of coal deposition can be calculated. Further considering the carbon loss during coalification, the long-term average carbon accumulation rate and net primary productivity (NPP) of palaeo-peatlands in coal seam can be estimated.

The source of carbon in vegetation including palaeo-peatlands, is atmospheric CO₂, fixed through photosynthesis. Therefore, the different atmospheric CO₂ levels in different geological periods should result in different NPP values of palaeo-peatlands. Several case studies for the Late Permian, Middle Jurassic, Early Cretaceous and Holocene showed that the NPPs of palaeo-peatlands were mainly controlled by the atmospheric CO₂ contents. The higher NPP values are associated with the higher atmospheric CO₂ contents. Therefore, it can be suggested that the NPP values could be a possible proxy of global atmospheric CO₂ during geological history.

Reference

Shao, L.Y., Wen, He., Gao, X.Y., Spiro, B., Wang, X., Yan, Z.M., Large, D.J., 2022. Identification of Milankovitch cycles and calculation of net primary productivity of paleo-peatlands using geophysical logs of coal seams. *Acta Geologica Sinica* (English Edition) 96(6), 1830–1841. DOI: 10.1111/1755-6724.14966



Observation and quantitative analysis of the effect of enhanced tectonic deformation on the nanostructural alteration of coal

Wenbin Yang, Wu Li*

Key Laboratory of Coalbed Methane Resource & Reservoir Formation Process, Ministry of Education, China
University of Mining and Technology, Xuzhou 221008, China

* Corresponding Author: liwu@cumt.edu.cn

During the burial history of coals, a series of tectonic processes can lead to the development of tectonically deformed coals (TDC). The mechanochemical effect of tectonic deformation of coal results to the change of chemical structure at the molecular level (Hou et al., 2017). In this study, the morphological features and the structural parameters of bituminous coals underwent different degrees of tectonic deformation (i.e., cataclastic coal in a brittle deformation environment, scaly coal of a transitional/shear deformation environment, and wrinkle coal in a ductile deformation environment), were examined. The study involved high-resolution transmission electron microscopy (HRTEM) analysis, mainly including the size, the alignment ordering, the curvature and the development of stacked layers of aromatic structures, by combining also other chemical structural parameters (Li et al., 2017). The results prove that the order of response of the evaluated coal structural parameters differs with increasing degree of tectonic deformation, i.e., first, mainly the preferential orientation of the aromatic structures is increasingly higher and the curvature of the aromatic lamellae decreases as a result of enhanced tectonic deformation. Additionally, no significant changes in the size of the aromatic structure could be observed in this case. Frictional heat phenomena and even ductile rheology possibly occur upon exposure to strong tectonic deformation (Song et al., 2022, and references therein), but in the study cases the effect of tectonic deformation on the dimensions of the aromatic structure is limited, and its visible change may require more intense stress deformation or higher temperature. To some extent, this also reflects the nature of the tectonic deformation environment, to which the coals were subjected. In addition, the stacked layer structures resulted from strong tectonic deformation are observed only in small localized and very limited areas. Factors such as the original structural characteristics of coal and the nature of tectonic stresses (e.g., stress partitioning, intensity and the direction of action) often lead to the development of the observed localized/non-homogeneous structural ordering.

References

- Hou, Q., Han, Y., Wang, J., Dong, Y., Pan, J., 2017. The impacts of stress on the chemical structure of coals: a mini-review based on the recent development of mechanochemistry. *Science Bulletin* 62(13), 965-970.
- Li, W., Jiang, B., Moore, T.A., Wang, G., Liu, J.G., Song, Y., 2017. Characterization of the chemical structure of tectonically deformed coals. *Energy & Fuels* 31(7), 6977-6985.
- Song, Y., Jiang, B., Vandeginste, V., Mathews, J.P., 2022. Deformation-related coalification: Significance for deformation within shallow crust. *International Journal of Coal Geology*, 103999.

Nano-sized phase in different coal lithotype and their fractions under pyridine treatment

Beilei Sun^{1,2*}, Chao Liu^{1,2}

- (1) Department of Earth Science and Engineering, Taiyuan University of Technology, Taiyuan, China;
(2) Shanxi Key Laboratory of Coal and Coal-measure Gas Geology, Taiyuan, China

* Corresponding Author: sunbeilei@tyut.edu.cn

Nano-minerals are common carriers of the hazardous trace elements, which have been incorporated into coal research in recent years. Vitrain, clarain and durain from two Pennsylvanian-age coals of North China were handpicked to investigate the nano mineral composition. Nanometric-sized phases were characterized using energy-dispersive X-ray spectrometer (EDS) and high-resolution transmission electron microscopy (HR-TEM) images.

A range of mineral crystals and agglomerates phases have been identified in vitrain, clarain and durain. The Al-Si bearing crystal (i.e., kaolinite and boehmite) is the most common nanometric-sized minerals in studied coals, occurring as flake-like, rod-like and scattered-ball particles. The size of these Al-Si bearing nano-minerals are in range of 1-200 nm, and these minerals are usually carriers of Na, Mg, Fe and Ti. Calcium-bearing nano-mineral with size of 50-200 nm, including calcite and apatite, were scattered in vitrain occurring as rod-like. Anatase with length of 5-50 nm, the smallest particle among the identified minerals were detected in all vitrain, clarain and durain. Zircon grains in size of around 100 nm existed in dull coal, and some Pb-Se minerals around 100 nm were identified in clarain coal.

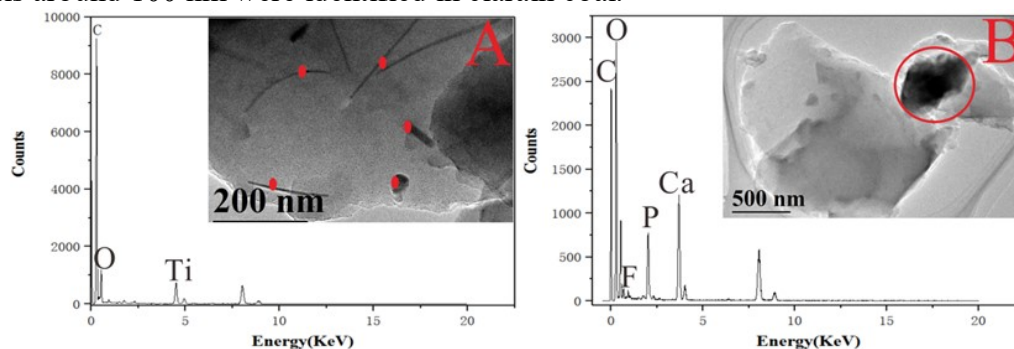


Figure 1. Nanometric-sized anatase in durain (A) and fluorapatite in clarain (B).

In order to further understand the nano-mineral origin, different fractions (i.e., extractions and residues) of these samples were prepared under pyridine solvent treatment. The nano-sized phases were predominantly Ca (Si, Al, Na)-Fe(Ti)-Cl-S nm and Ca-(Fe)-S-(F, Cl) agglomerates (20-50 nm and 100-500 nm in size) and clays with size of 100-500 nm in exactions. Nanometric-sized clays and anatase, and rarely quartz and REY-bearing minerals were also identified in residues. Based on an analysis of the nano-sized phase in extractions and residues, it can be stated that nano-scale minerals in coal lithotype may be from detrital input during peatification and/or diagenesis during coalification.

Acknowledgment: This work has been partially supported by National Key Research and Development Program of China (2021YFC2902002) and the National Natural Science foundation of China (Grant No. 41602178). Dr. Yunxia Liu and Mr. Peng Jia were thanked for the sample treatment and HRTEM-EDX analysis.

Desorption rate of methane in coal matrix and its main controlling factors

Dangyu Song*, Yunbo Li, Yingquan Zhai

Henan Polytechnic University, Jiaozuo city, China

* Corresponding Author: dangyusong@hpu.edu.cn

Methane in coal is mainly adsorbed in the coal matrix micropores. Desorption and diffusion are the initial migration stages in CBM production. In the past, people were concerned about the diffusion of methane in coal matrix pores. Due to the complexity of coal matrix pore structure, both desorption and diffusion of gas occur in matrix micropores, and it is hard to completely separate these two stages. In this study, the release of methane from micropores before continuous flow is defined as the desorption stage, and the desorption rate is used to measure the transport efficiency of the gas molecular flow. Based on the desorption volume-time data obtained from the high-pressure methane isothermal adsorption/desorption experiments, the desorption rates of methane in coal with different pore structures were systematically investigated, and the following findings and conclusions were drawn:

- (1) High-pressure methane isothermal adsorption/desorption experiments were conducted on three aliquots of the same coal with different particle sizes (Fig. 1a), and the desorption volume-time curves were fitted using the Banham thermodynamic model to derive the desorption rate equation with time. Three parameters were proposed to evaluate the desorption rate: desorption rate constant k , initial relative desorption rate, and desorption time corresponding to the median desorption volume.
- (2) The desorption rates of different particle sizes showed similar variation patterns with time, exhibiting an exponential decrease (Fig. 1b). The differences between samples are mainly reflected in the initial desorption rate and the rate of decrease in desorption rate over time.
- (3) Pressure difference is a key external factor determining the desorption rate, and the desorption rate decreases rapidly with the decrease of pressure difference (Fig. 1c).
- (4) Pore structure of mesopores and macropores is a key intrinsic factor controlling the desorption rate. Larger specific surface area of mesopores and macropores, as well as shorter distances of methane migration within micropores, can significantly enhance methane desorption rate.

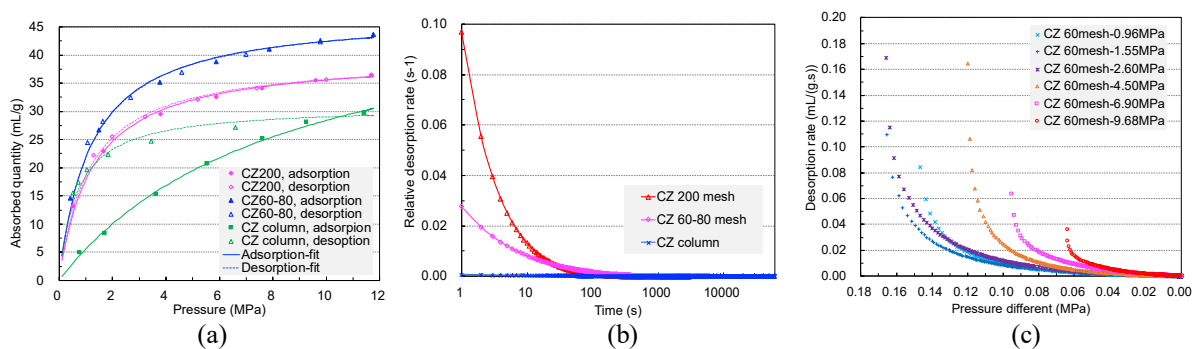


Figure 1. (a) Adsorption/desorption curve of methane in coal; (b) Methane desorption rate *versus* time curve; (c) Variation of desorption rate with pressure difference.



Petrographic study of palynomorphs and macerals to assess the kerogen in Gondwana and Tertiary coal seams, India

Shashanka Pandey^{1,2*}, Vinod A. Mendhe^{1,2}, Priyanka Shukla^{1,2}

(1) CSIR- Central Institute of Mining and Fuel Research, Dhanbad-826015, Jharkhand, India; (2) Academy of Scientific and Innovative Research (AcSIR), Ghaziabad-201002, Uttar Pradesh, India

* Corresponding Author: pandeyshashank194@gmail.com

The demand for energy is continuously increasing and therefore, it is necessary to explore and develop alternative energy resources like CBM, shale gas, oil shale, tight sand, etc. Recently, the extraction of kerogen from lignite, coal, oil shale, and carbonaceous shale through destructive distillation emerged as a potential source of hydrocarbon. Kerogen is a fraction of sedimentary organic matter mainly containing carbon and volatile matter. India has significant lignite, coal, and carbonaceous shale deposit in Gondwana and Tertiary formations spread over the country. There is very limited information available on kerogen occurrence, preservation, and extraction in the Indian context. In this study, lignite and bituminous coal samples obtained from Tertiary and Gondwana deposits are analyzed for geochemical, maceral and lithotype compositions, as well as for kerogen content and palynomorphological features. The moisture, ash, volatile matter and fixed carbon yields of lignite vary in the range from 5.98-7.73, 22.46-36.62, 34.96-37.91, and 20.65-36.6 wt.% and coal varies in the range from 5.39-10.71, 14.93-53.37, 22.73-37.58, 18.52-43.36 wt.%, respectively. The huminite, liptinite, and inertinite contents of lignite vary from 36-72, 7-22 and 9-45 vol.%, respectively, whereas these of vitrinite, liptinite, and inertinite of coal from 7.3-52.2, 1-17 and 4.6-18 vol.%, respectively. The role of petrographic constituents, volatile matter yield and various palynomorphs for kerogen genesis has been evaluated. The petrographic ternary facies indicated kerogen generation pattern in lignite and coal. Vitrain and liptinite-rich lignite and coal has released relatively higher kerogen. Lignite having high moisture and volatile matter yield are a good source of kerogen. Various palynomorphs and their significance in kerogen preservation and accumulation, as well as the relationships among macerals, kerogen content and palynomorphs are discussed. Different extraction procedures like destructive thermal distillation and solvent extraction suitable for lignite and coal, are also described.



Joint 74th ICCP and 39th TSOP Meeting
17th – 24th September 2023, Patras, Greece

**Organic Petrology in the Energy Transition Era:
Challenges ahead**



Bulletin of the Geological Society of Greece, Sp. Publ. 12

TSOP Technical Session B

Tuesday, 19.9. 2023

- 11:30-11:45 Reactivity assessment of coal, lignite and biomass organic constituents through detailed petrography: An implication to gasification, carbon conversion and syngas
A. Damodhar Kamble
- 11:45-12:00 Exploring the influence of maturity evolving maceral composition on shale porosity: Example from the lower Paleozoic shale from the Baltic Basin (Poland)
G.P. Lis, I. Jelonek, M. Mastalerz, T. Topór
- 12:00-12:15 The selective effect of pore-fracture evolution during the process of liquid nitrogen cyclic fracturing in coal
Y. Li, D. Song, H. Wang, X. Guo, Z. Ren
- 12:15-12:30 Towards the identification of coal macerals through deep learning
N. Xu, Q. Wang, P. Li, M.A. Engle



Joint 74th ICCP and 39th TSOP Meeting
17th – 24th September 2023, Patras, Greece



**Organic Petrology in the Energy Transition Era:
Challenges ahead**

Bulletin of the Geological Society of Greece, Sp. Publ. 12

Reactivity assessment of coal, lignite and biomass organic constituents through detailed petrography: An implication to gasification, carbon conversion and syngas

Alka Damodhar Kamble

KLEF – Department of Engineering Chemistry (KLEF Deemed to University), Greenfield Vaddeswaram,
Guntur – 522302, Andhra Pradesh, India

Corresponding Author: dralkadamodhar@kluniversity.in, alka.kamble@gmail.com

Recently, the gasification of coal, co-gasification of coal and biomass, oxyfuel and coal to liquid (CTL) have emerged as potential near future clean energy technologies to obtain syngas comprising hydrogen, CO, methane and other combustible gases. The heterogeneity of coal composition and low density of biomass are major issues for carbon conversion to syngas. In this study, high-ash coal from Gondwana seams, low-ash lignite from Tertiary deposits, and biomass waste like rice husks, sawdust, and press mud have been chemically, petrographically and spectroscopically evaluated for micro understanding and their sensitivities during gasification in a fluidized bed gasifier. The coal, lignite, biomass, and blend bottom ash after gasification were examined through detailed micro-petrography. The change in organo-inorganic constituents and their relationship with carbon conversion to generate syngas and the efficiency of gasification have been established. The petrographic constituents of coal and lignite, the lignocellulose of biomass, the water and the volatile content directly control the gasification process. The petrographic constituents like vitrinite, liptinite, biomass lignocellulose, and various oxides favored the gasification process. It is summarized that the huminite macerals, mainly textinite, and ulminite, of lignite played a significant role in lignite to syngas conversion. Hence, finally, it is concluded that gasifying high-ash coal is feasible with the blending of vitrinite-rich coal and biomass, whereas lignite is the most suitable raw material, having great reactivity suitable for gasification. The outcome of the study provides detailed information on coal, lignite macerals and biomass lignocellulose reactivity during gasification and is useful for the commercial implementation of large-scale gasification projects in India.

**Exploring the influence of maturity evolving maceral composition on shale porosity:
Example from the lower Paleozoic shale from the Baltic Basin (Poland)**

Grzegorz P. Lis^{1*}, Iwona Jelonek², Maria Mastalerz³, Tomasz Topór⁴

(1) University of Wrocław, Wrocław, Poland; (2) University of Silesia, Sosnowiec, Poland; (3) Indiana University, Bloomington IN, USA; (4) Oil and Gas Institute-National Research Institute, Cracow, Poland

* Corresponding Author: grzegorz.lis@uwr.edu.pl

Pore network within organic matter rich shales is responsible for transport, sorption, and gas storage capacity, the latter very important for unconventional shale gas reservoirs. Shale porosity consists of inorganic mineral matrix pores and pores hosted within organic matter. Organic hosted pores are the most important for shale gas storage capacity; they evolve in response to increasing thermal maturity, change in maceral composition, and hydrocarbon generation.

The lower Paleozoic shales from the Baltic Basin were recently targeted for exploration of unconventional resources of hydrocarbons. So far, the exploration results have not been promising, even though the shale has elevated organic matter content of several wt.%, and sometimes reaching more than 15 wt.%. Thermal maturity of the shale ranges from immature in the NE region of the Baltic Basin, gradually increasing to overmature in the SW of the basin, allowing for the opportunity to observe evolving maceral composition and pore network.

Organic petrography was applied to monitor maceral composition changes, while low pressure gas sorption (both N₂ and CO₂) was used for porosity and surface area measurements. Maceral composition in low maturity samples is dominated by liptinites with some solid bitumen present. Increasing maturity within the oil window results in a decrease and eventual disappearance of liptinites and an increase of solid bitumen content. This change is accompanied by decreasing porosity and specific surface area. The decreasing porosity can be attributed to compaction with increasing burial and also plugging of the pore system with secondary solid bitumen. Further increase in maturity within the gas window results in a slight increase in porosity and specific surface area, which can be attributed to the hydrocarbon generation from solid bitumen associated by secondary porosity development within organic matter. Further maturity increase in overmature samples results in a slight porosity decrease, which again can be attributed to compaction.

Organic petrography also revealed the presence of graptolites within the studied shales. Observations of a wide maturity range of graptolites indicate they behave differently than other primary macerals. While other primary macerals eventually convert to solid bitumen, graptolites persist through increasing maturity and are present even in overmature samples. Thermal endurance of graptolites may suggest they contribute to a lesser degree towards hydrocarbon generation than remaining macerals. The lower Paleozoic shale from the Baltic Basin can be locally enriched in graptolites, as often visible macroscopically within the cores. Graptolite enrichment contributes to the shale's organic richness, but their low hydrocarbon generation potential could be one of the reasons the exploration results are lower than expected.

Acknowledgements: This study was funded by the National Science Centre, Poland, project 2019/35/B/ST10/00385.

The selective effect of pore-fracture evolution during the process of liquid nitrogen cyclic fracturing in coal

Yunbo Li^{1,2,3*}, Dangyu Song^{1,2,3}, Haifeng Wang^{1,2,3}, Xingxin Guo^{1,2,3}, Zixian Ren^{1,2,3}

(1) Institute of Resource and Environment, Henan Polytechnic University, Jiaozuo 454000, China; (2) Key Laboratory of Biogenic Traces and Sedimentary Minerals of Henan Province, Jiaozuo 454003, China; (3) Key Laboratory of Biogenic Traces and Sedimentary Minerals of Henan Province, Jiaozuo 454003

* Corresponding Author: liyunbo@hpu.edu.cn; yunboli@163.com

To gain a better understanding of the fracturing process in low-permeability reservoirs with varying degrees of coalification under liquid nitrogen freeze-thaw experiments (LNFT), we collected coals from mining areas in Qinghai, Shanxi, and Shaanxi provinces. By conducting a combination of experiments such as low-temperature N₂/CO₂ adsorption, high-pressure mercury intrusion (MIP), X-ray computed microtomography (μCT), low-field nuclear magnetic resonance experiments (NMR), and permeability testing, we analyzed the expansion characteristics of pores and fractures in coal and their impact on permeability during the LNFT process. The results are as follows: (1) LNFT effectively increases the porosity of coal. Compared to the original coal, the pore volume of coal after LNFT increases by 70.41-100.17% in the 0.3-20000 nm range. However, the fracturing effect is mainly concentrated in the mesopores (>2 nm) and macropores (>50 nm) range. The conversion of small-scale pores to larger-scale pores during the LNFT process is the main reason. (2) LNFT exhibits a selective effect on pore and fracture development. In the case of low- to medium-rank coals, the modification primarily focuses on the mesopores and macropores, while for anthracite coals, the modification concentrates on the macropores and fractures. Dry samples primarily experience the extension of existing fractures, while samples with moisture show simultaneous expansion of primary fractures and generation of new fractures, resulting in the formation of a dense network of microfractures. (3) The modification of coal rock through LNFT demonstrates a stage-wise effect, with a rapid increase in the early stages of fracturing. However, as the number of LNFT increases, the magnitude of improvement decreases, leading to a weaker fracturing effect. Changes in coal permeability are synchronized with the evolution of fractures. (4) The fracturing of coal using liquid nitrogen is the result of the combined effects of water-ice phase transition volume expansion, liquid nitrogen phase transition fracturing, and low-temperature freeze expansion fracturing. To enhance the effectiveness of LNFT in low-permeability reservoirs, a pre-injection of water into the coal seam can be conducted to reduce coal seam plasticity. Subsequently, a large-volume LNFT operation can be implemented to achieve optimal reservoir permeability enhancement. Our research provides new technological references for the efficient development of coalbed methane in low-permeability coal seams.

Towards the identification of coal macerals through deep learning

Na Xu¹, Qingfeng Wang¹, Pengfei Li¹, Mark A. Engle²

(1) College of Geoscience and Survey Engineering, China University of Mining and Technology (Beijing), Beijing 100083, China; (2) Department of Earth, Environmental and Resource Sciences, University of Texas at El Paso, El Paso, Texas 79968, USA

* Corresponding Author: xuna1011@gmail.com

In recent years, significant effort has been made in automated coal macerals identification [1-2]. One method to improve the performance of the coal macerals identification is the use of deep learning algorithms. In this paper, a semi-supervised semantic segmentation model [3] was used for pixel-level identification of coal macerals. To verify the performance of coal macerals identification using semi-supervised semantic segmentation model, the results are compared with the other three existing image segmentation methods, including K-means [4], Gaussian mixture model (GMM), [5] and convolutional neural network (CNN) model [6]. For the Inertinite group, the semi-supervised model achieves a pixel accuracy of 0.96 while K-means, GMM and CNN achieve values of 0.75, 0.78, and 0.69, respectively. In terms of intersection over union, the semi-supervised model achieves 0.90 while K-means, GMM, and CNN achieves 0.79, 0.80, and 0.82. For the Vitrinite group, the semi-supervised model achieves 0.91-pixel accuracy while K-means, GMM, and CNN achieve 0.68, 0.67, and 0.77, respectively. In terms of intersection over union, the semi-supervised model achieves 0.88-pixel accuracy while K-means, GMM and CNN achieve 0.80, 0.77, and 0.72, respectively. For the Liptinite group, the semi-supervised model achieves 0.70-pixel accuracy while K-means, GMM, and CNN achieve 0.60, 0.74, and 0.66, respectively. In terms of intersection over union, the semi-supervised model achieves 0.68 while K-means, GMM and CNN achieve 0.10, 0.24, and 0.24, respectively. The results show that our proposed semi-supervised model markedly outperforms the current image segmentation methods.

References

- [1] Scott, A.C., 2002. Coal petrology and the origin of coal macerals: a way ahead? *International Journal of Coal Geology* 50, 119-134.
- [2] O'Brien, G., Jenkins, B., Esterle, J., Beath, H., 2003. Coal characterisation by automated coal petrography. *Fuel* 82, 1067-1073.
- [3] Hung, W.-C., Tsai, Y.-H., Liou, Y.-T., Lin, Y.-Y., Yang, M.-H., 2018. Adversarial learning for semi-supervised semantic segmentation. arXiv preprint arXiv: 1802.07934.
- [4] Burney, S.A., Tariq, H., 2014. K-means cluster analysis for image segmentation, *International Journal of Computer Applications* 96.
- [5] Huang, Z.-K., Chau, K.-W., 2008. A new image thresholding method based on Gaussian mixture model. *Applied Mathematics and Computation* 205, 899-907.
- [6] Kanezaki, A., 2018. Unsupervised image segmentation by backpropagation. In: 2018 IEEE International Conference on Acoustics, Speech and Signal Processing (ICASSP), IEEE, pp. 1543-1547.



Joint 74th ICCP and 39th TSOP Meeting
17th – 24th September 2023, Patras, Greece



**Organic Petrology in the Energy Transition Era:
Challenges ahead**

Bulletin of the Geological Society of Greece, Sp. Publ. 12

TSOP Technical Session C

Tuesday, 19.9. 2023

- 14:30-14:45 Geochemistry of tuff layers and its implications for Li-Zr (Hf)-Nb (Ta) enrichments in Cisuralian Coal Seams, Shanxi Province, North China
Z. Guo, B. Sun
- 14:45-15:00 Petrographic, geochemical and mineralogical characterization of coals from the Carboniferous Douro Basin: São Pedro da Cova and Pejão Coalfields
M. Costa, H. Moura[†], A. Pinto de Jesus, D. Flores
- 15:00-15:15 Cathodoluminescence differentiates sedimentary organic matter types
P.C. Hackley, R.J. McAleer, A.M. Jubb, B.J. Valentine, J.E. Birdwell
- 15:15-15:30 Rock-Eval based kerogen kinetics and the effect of rock matrix
V.I. Makri, K. Kokkinopoulou, N. Pasadakis
- 15:30-15:45 Thermal maturation of the La Luna Formation in the Middle Magdalena Basin, Colombia
M. Garcia-Gonzalez, T.S. Palmera-Henao
- 15:45-16:00 Influence of thermal intrusion on solid bitumen in the Alum Shale, Central Sweden
A. Liu, H. Sanei, N.H. Schovsbo, X. Zheng, L. Bian

Geochemistry of tuff layers and its implications for Li-Zr (Hf)-Nb (Ta) enrichments in Cisuralian coal seams, Shanxi Province, North China

Zhanming Guo¹, Beilei Sun^{1,2*}

(1) Department of Earth Science and Engineering, Taiyuan University of Technology, Taiyuan, China;
(2) Shanxi Key Laboratory of Coal and Coal Measure Gas Geology, Taiyuan, China

* Corresponding Author: sunbeilei@tyut.edu.cn

Tuffs, typically of alkali origin, may contain valuable trace elements that could be potentially utilized and used as indicators in the search for unconventional ore deposits. Tuff layers were found in Cisuralian coal seams, Qiaotou Section, Shanxi Province, North China (Wu et al., 2021). This study aims to characterize the trace element concentrations of tuffs and their contribution to the trace elements enrichments in the coal seams. A total of 61 benches, including thirty-six no-coal benches (five layers of tuff, thirty-one partings) and 25 coal benches, were collected from Taiyuan Formation, from these five tuffs and 25 coal benches were analyzed for major oxides and trace elements determination.

Tuff layers have extremely high average concentrations of Li (207 µg/g) and high field strength elements (HFSE) like Zr (352 µg/g), Nb (43.8 µg/g), Hf (10.8 µg/g) and Ta (3.40 µg/g), displaying concentrations ten times higher than those of world hard coals, whereas Th and U are present in concentrations close to ten times of the average found in world hard coals (Ketriss and Yudovich, 2009). All coal benches have weighted average concentrations of Li (65.9 µg/g), Zr (200 µg/g), Nb (12.2 µg/g), and Hf (5.28 µg/g). Compared with world hard coals, there are only significant enrichments ($5 < CC < 10$) of Sr, Zr, Hf, Pb and U in coal benches (Fig. 1).

The TiO₂ vs Al₂O₃ diagram has been widely used as a provenance indicator for sedimentary, due to immobility of the Al and Ti during superficial weathering, hydrothermal alteration, and volcanic processes. This diagram suggests that intermediate rocks would be a potential detrital source for the coal benches, whereas the mafic igneous source would be responsible for these tuff layers origins. It is not expected that these mafic tuff layers host such high concentrations of HFSE that were considered to be usually related to alkali volcanic ash in coal (Fig. 2).

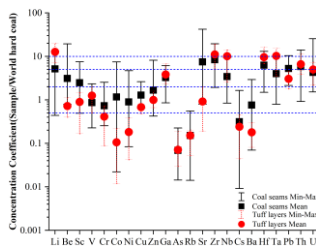


Figure 1. Boxplots of the Concentration Coefficients of 22 trace elements of coal seams (black) and tuff layers (red).

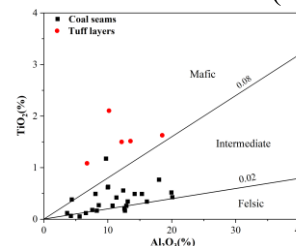


Figure 2. TiO₂ versus Al₂O₃ discrimination diagrams for the tuff layers and coal benches (after Hayashi et al., 1997).

References

- Hayashi, K.I., Fujisawa, H., et al., 1997. Geochemistry of ~1.9 Ga sedimentary rocks from northeastern Labrador, Canada. *Geochimica et Cosmochimica Acta* 61, 4115–4137.
- Ketriss, M.P., Yudovich, Ya.E., 2009. Estimations of Clarkes for Carbonaceous biolithes: World averages for trace element contents in black shales and coals (Article). *International Journal of Coal Geology* 78/2, 135–148.
- Wu, Q., Ramezani, J., et al., 2021. High-precision U-Pb age constraints on the Permian floral turnovers, paleoclimate change, and tectonics of the North China block. *Geology* 49(6), 677–681.



Petrographic, geochemical and mineralogical characterization of coals from the Carboniferous Douro Basin: São Pedro da Cova and Pejão Coalfields

Mariana Costa*, Helena Moura[†], Ary Pinto de Jesus, Deolinda Flores

Departamento de Geociências, Ambiente e Ordenamento do Território da Faculdade de Ciências da Universidade do Porto, Portugal, e Instituto de Ciências da Terra - Polo da Universidade do Porto, Portugal

* Corresponding Author: mariana.costa@fc.up.pt

The São Pedro da Cova and Pejão Coalfields are hosted in the Douro Carboniferous Basin (DCB) and were historically and economically important for its coal exploitation. The DCB, aged from Lower Gzhelian, is a pull-apart basin and corresponds to the largest terrestrial Carboniferous outcrop in Portugal. This study aims to present petrographic, geochemical, both organic and inorganic, and mineralogical data of 24 coal samples obtained from São Pedro da Cova and 18 coal samples from the Pejão Coalfields.

Vitrinite random reflectance (between 4.51% and 5.76% in São Pedro da Cova, and between 3.54% and 5.30% in Pejão) classifies these coals as anthracite A (high rank coals) according to ISO 11760 (2018). Regarding the maceral composition, expressed in volume percent on a mineral-matter-free basis (mmf), vitrinite is the main component of the organic fraction in both coalfields, ranging from 91-99% in the São Pedro da Cova Coalfield and between 94 and 100% of the organic fraction in Pejão Coalfield. Considering the mineral content, in the São Pedro da Cova Coalfield, it varies between 0% and 9.8%, while in the Pejão Coalfield, it ranges 5% to 85%. In both coalfields the mineral matter is composed of quartz, iron oxides, clay minerals, both framboidal and epigenetic pyrite, iron oxides, and carbonates that grow within organic matter in the form of concretions which indicates that they are syngenetic. The proximate and ultimate analyses, reported in weight percentage, are in accordance with the rank of these coals, except for seven samples of the Pejão Coalfield, that have an ash yield higher than 50%, classifying these samples as carbonaceous rocks.

The major and trace element composition of the studied samples are in accordance with the mineralogy identified by SEM-EDS. In the São Pedro da Cova Coalfield illite and muscovite were identified. The most abundant sulfide is pyrite, but galena, sphalerite, chalcopyrite and cinnabar were also observed. The carbonate concretions are mainly ankerite. Regarding the phosphates, fluorapatite, xenotime, monazite and gorceixite were identified. The presence of gorceixite is important, since it is associated with hydrothermal fluid circulation. In the Pejão Coalfield, although similar, the coal shows some differences as, within the sulfides, arsenopyrite was also identified, while gorceixite was not. Bournonite and tetrahedrite were occasionally recognized associated to pyrite. Concerning the phyllosilicates, muscovite, vermiculite, kaolinite and possibly biotite were distinguished. The differences in the mineralogical and geochemical compositions of these coals in both coalfields seem being related with the mineralizations existing in the region, confirming the circulation of hydrothermal fluids.

Acknowledgments: The author M. Costa benefits from a PhD scholarship granted by FCT Ref: 2022.11145.BD. This work was supported by national funds through ICT, projects UIDB/04683/2020 and UIDP/04683/2020.

Cathodoluminescence differentiates sedimentary organic matter types

Paul C. Hackley^{1*}, Ryan J. McAleer¹, Aaron M. Jubb¹, Brett J. Valentine¹, Justin E. Birdwell²

(1) U.S. Geological Survey, Reston VA, USA; (2) U.S. Geological Survey, Denver CO, USA

* Corresponding Author: phackley@usgs.gov

High-resolution scanning electron microscopy (SEM) visualization of sedimentary organic matter (SOM) is a widely utilized petrographic approach for better understanding of fluid generation, transport, and storage processes in mudrock. However, despite thousands of studies incorporating SEM approaches, the inability of SEM to differentiate SOM types (e.g., primary *versus* secondary SOM), has hampered the pace of discovery and scientific advancement. In this study, we show that SEM-cathodoluminescence (CL, electron-induced photon emission) properties can be used to identify and characterize SOM types from immature to peak-oil window thermal conditions. Shale and mudrock samples (n=11) representing a broad array of sedimentological character (clastic *versus* carbonate), depositional environment (lacustrine *versus* marine), geologic age (Paleoproterozoic to Eocene), kerogen type (Types I, II), and petrographic organic matter assemblage (vitrinite, inertinite, liptinite, and solid bitumen) were investigated. Fluorescence (photon-induced photon emission) intensity of SOM and CL intensity showed an almost one-to-one correspondence, with certain exceptions which are potentially related to radiolytic alteration. Fluorescence and CL intensity also displayed an inverse correlation against reflectance and Raman spectral properties, i.e., as fluorescence and CL intensity decreased, the reflectance and Raman carbon peaks of SOM types systematically increased in the same sample. Therefore, because CL emission can be used as a proxy for fluorescence emission from SOM, CL emission during SEM visualization can be used to differentiate fluorescent SOM (liptinite maceral group, some solid bitumen) from non-fluorescent SOM (vitrinite and inertinite maceral groups, high maturity solid bitumen). That is, CL emission can be used in SEM-based petrographic studies as a visual means to quickly differentiate SOM types without employing correlative optical microscopy. Use of SEM-CL represents a potential breakthrough improvement over prior schemes for SEM-based identification of SOM types using petrographic textures, and could be widely and rapidly adapted for SEM petrographers with access to a CL detector.

Rock-Eval based kerogen kinetics and the effect of rock matrix

Vagia Ioanna Makri^{1,2*}, Katerina Kokkinopoulou², Nikos Pasadakis^{1,2}

(1) Institute of GeoEnergy, Foundation for Research and Technology, (FORTH/IG), Chania, Greece; (2) School of Mineral Resources Engineering, Technical University of Crete, Chania, Greece

* Corresponding Author: vayanna@ig.forth.gr

Studying kerogen kinetics is important for comprehending the thermal history of source rocks and enhancing the precision of petroleum systems modeling. Kerogen is the insoluble organic matter present in sedimentary rocks, which undergoes complex chemical and physical transformations over geological time under increasing temperature and pressure. This field of study involves analysing reaction mechanisms, determining kerogen transformation rates, and utilizing kinetic models to understand hydrocarbon generation processes.

Traditionally, petroleum systems modeling has relied on kinetic models of studied kerogen families which could be found in commonly used software databases. While this approach is efficient in terms of time consumption, inaccuracies may arise due to compositional differences of kerogen and rock mineralogy.

Rock-Eval pyrolysis has been widely employed for the characterization of source rocks and their maturity level. The Rock-Eval pyrolysis curve (S2) is indicative of the quantity of hydrocarbons generated from the thermal decomposition of organic matter within the sample. By fitting kinetic models to the Rock-Eval pyrograms (S2 data), reaction kinetic parameters such as activation energy and frequency factor can be estimated efficiently.

To evaluate the ability of utilizing Rock-Eval pyrograms for determining kinetic parameters, a set of source rock samples from the fold and thrust belt of Western Greece was analysed. Comparisons were made between the results obtained from the source rocks, the extracted source rocks, and the source rocks treated with hydrochloric acid, highlighting the influence of the matrix. Rock-Eval kinetic results were further compared to those obtained from thermal gravimetry pyrolysis experiments (TGA).

This study confirms the effectiveness of utilizing Rock-Eval S2 pyrograms for determining kinetic parameters and demonstrates the influence of organofacies variations on the accuracy of hydrocarbon generation models.

Thermal maturation of the La Luna Formation in the Middle Magdalena Basin, Colombia

Mario Garcia-Gonzalez^{1*}, Tania S. Palmera-Henao²

(1) Escuela de Geología Universidad Industrial de Santander, Bucaramanga, Colombia; (2) Laboratorio de Geoquímica del petróleo LGP, Piedecuesta, Santander, Colombia

* Corresponding Author: mgarciag@uis.edu.co

The La Luna Formation is considered as the main oil source rocks in the Middle Magdalena Basin of Colombia. This Upper Cretaceous Formation presents high TOC values between 3 and 15% and high HI values from 300 to 900 mg HC/g rock. The vitrinite reflectance (Ro) values range from 0.3 to 0.5% in the eastern part of the MMB, and from 0.5 to 1.0% in the center of the basin, where the La Luna Formation lies 3 to 4.5 km beneath the surface according to the findings from several exploration wells. Despite the relatively low Ro values in the eastern part of the MMB, this formation is in the Oil Generation Window as it is demonstrated by the presence of oil within mudstone and shale layers of the La Luna Formation; the amorphous organic matter and the oil within foraminifera chambers, as well as the oil filling fractures and microfractures show yellow and orange fluorescence.

The Umir Formation is overlaying the La Luna Formation, however, the Ro values of coal beds in the Umir Formation exhibit higher Ro values than the Ro values of the older and underlying La Luna Formation; this situation indicates that the La Luna Formation presents suppression of the vitrinite reflectance and therefore, determining the maturation stages of this formation requires a calibration of the Ro values using several techniques and other geochemical maturation parameters such as Rock-Eval pyrolysis and Ro measurement on bitumen found in the La Luna Formation, as well as Ro calibration using Ro values from coal beds present in the overlaying Umir Formation.

One dimension (1D) thermal maturation models of the La Luna Formation in the MMB show inconsistent results between the measured Ro values and the calculated Ro values of this formation, indicating that high heat flow during the Upper Cretaceous rifting process should be considered to obtain a match between calculated and measured Ro values in the MMB. This contradiction can be solved by calculating the radiogenic heat flow production due to the high Uranium and Thorium concentration reported in the La Luna Formation. A new thermal model that includes the radiogenic heat production within the La Luna Formation can explain the maturation stages of the La Luna Formation in the Middle Magdalena Basin.

The non-conventional reservoirs of the La Luna Formation are considered to contain the biggest oil and gas resources in the MMB; therefore, assessing its maturation stages distribution in the MBB will allow delineation of the main oil and gas shale prospects in this basin.

Influence of Thermal Intrusion on Solid Bitumen in the Alum Shale, Central Sweden

Anji Liu¹, Hamed Sanei^{1*}, Niels H. Schovsbo², Xiaowei Zheng¹, Leibo Bian^{1,3}

(1) Lithospheric Organic Carbon (LOC) Group, Department of Geoscience, Aarhus University, Høegh-Guldbergs gade 2, 8000C Aarhus, Denmark; (2) Department of Geoenergy and Storage, Geological Survey of Denmark and Greenland (GEUS), Øster Voldgade 10, 1350 Copenhagen K, Denmark; (3) Research Institute of Petroleum Exploration and Development, PetroChina, Beijing 100083, China

* Corresponding Author: sanei@geo.ac.dk

This study investigates the geochemical and petrological characteristics of solid bitumen in the DBH 15/73 core from the Furongian (upper Cambrian) and Miaolingian (middle Cambrian) Alum Shale in central Sweden. The shale here was intruded by Permo-Carboniferous diabase approximately 100 m above. The results show that the solid bitumen in DBH samples could be classified as follows: bituminite, diagenetic solid bitumen (DSB), initial-oil solid bitumen (IOSB), primary-oil solid bitumen (POSB) and solid bitumen inside apatite nodules based on their morphology and random solid bitumen reflectance (BR_o). The immature Miaolingian shale contains bituminite and DSB, with measured BR_o ranging from 0.40% to 0.48%. The Furongian shale is enriched with IOSB and POSB indicating a maturity gradient from marginally mature to peak oil generation from the bottom to the top stratigraphically. The IOSB (BR_o : 0.54-1.08%) exhibits characteristics of uneven heating such as oxidation rim, melted maceral, abnormal maturity around fractures. In addition, POSB (BR_o : 0.63-2.01%) displays flow structures, and its migration is evidenced by its occurrence in the overlying organic-poor Ordovician Lanna limestone and the underlying Kakeled Limestone Bed. The sum of POSB and IOSB is determined through maceral point counting. We suggest that POSB is the main bitumen type (1.54-7.13 vol.%) and IOSB is the minority (0.05-0.31 vol.%) in the Furongian shale indicating rapid thermal evolution of the organic matter within the oil generation window. The free hydrocarbon (Rock-Eval S1) and T_{max} anomalies are observed in Furongian shale. We hypothesis that the migration of POSB and generated oil results in a decrease of free hydrocarbon (S1). The low T_{max} value appears to be a result of microbially mediated oxidation and high uranium content, leading to an underestimation of thermal maturity and kerogen conversion.

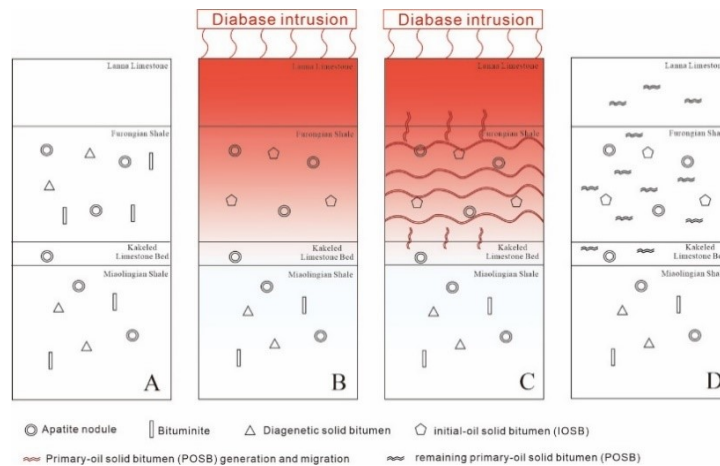


Figure 1. Models illustrating the genesis of solid bitumen in the well DBH 15/73 that is intruded by diabase. A: diagenesis stage. B: catagenesis stage. C: oil generation window. D: after thermal intrusion.



Joint 74th ICCP and 39th TSOP Meeting
17th – 24th September 2023, Patras, Greece

**Organic Petrology in the Energy Transition Era:
Challenges ahead**



Bulletin of the Geological Society of Greece, Sp. Publ. 12

TSOP Technical Session D

Tuesday, 19.9.2023

- 16:30-16:45 Elemental composition and facies analysis of the Late Cenomanian-Early Turonian Second White Specks and adjacent oil shales, Western Interior Seaway, Canada
S. Mohebati, F. Goodarzi, P.K. Pedersen, T. Gentzis
- 16:45-17:00 Organic matter characterization of a sedimentary succession of the Barra Velha Formation carbonates from the Santos Basin, offshore Brazil
C. Fonseca, J. Torres Souza, A.D. de Oliveira, J. de Oliveira Mendonça, J.G. Mendonça Filho, L. Borghi
- 17:00-17:15 Spatial and temporal changes in the organic matter supply during the Cenozoic basin evolution in the Danish North Sea
Z. Zhou, H.I. Petersen, N.H. Schovsbo, A. Rudra, H. Sanei
- 17:15-17:30 New insights into oil-to-source rock correlation of oils and asphalt seeps from Zakynthos Island and the west coast of Peloponnese, Western Greece
I. Oikonomopoulos, T. Gentzis, H. Carvajal-Ortiz, E. Tripsanas

**Elemental composition and facies analysis of the Late Cenomanian-Early Turonian
Second White Specks and adjacent oil shales, Western Interior Seaway, Canada**

Somayeh Mohebat¹, Fariborz Goodarzi², Per K. Pedersen¹, Thomas Gentzis^{3*}

(1) Department of Geoscience, University of Calgary, Calgary, AB T2N 1N4, Canada; (2) FG & Partners Ltd., 219 Hawside Mews Heights NW, Calgary, AB T3G 3J4, Canada; (3) Core Laboratories, Petroleum Services, 6316 Windfern Road, Houston, TX 77040, USA

* Corresponding Author: thomas.gentzis@corelab.com

Two cores from the Cretaceous Second White Speckled (2WS) formation, the underlying Belle Fourche and the overlying Carlile formations, and the interval of the Oceanic Anoxic Event 2 (OAE2) were studied. The 2WS oil shale consists of limestone and marlstone. The limestone is associated with shallow marine facies. It contains Inoceramid shell debris deposited during enhanced water column mixing periods that promoted benthic carbonate productivity, increased bottom-water oxygenation, and reworking. The marlstone is associated with the open marine facies and includes sand-sized coccolith aggregates with varying planktonic foraminifera deposited under low oxygen conditions. Hierarchical component analysis identified two main families. The Belle Fourche and Carlile family is referred to as coastal marine facies. The 2WS oil shale is divided into three sub-facies, namely deep marine, open shelf-lower, and shallow shelf-upper. Bioturbation, lack of lamination, and scarcity of fossils in the Carlile indicate deposition in a restricted basin with minimal circulation. Sand laminae and higher bioturbation in the Belle Fourche indicate higher energy and shallow water facies with high riverine and terrigenous input. Variations in Cr, Ni+V, and Th/U vs. authigenic U show that the coastal facies reflect an anoxic environment, those in the shallow and open shelf marine facies in a suboxic-anoxic, and those in the deep marine facies in a suboxic environment. The coastal facies have high Al₂O₃, SiO₂, and low CaCO₃ content. Based on Mn/Ca vs. Sr/Ca, the temperature of water decreased from the coastal facies toward the shallow shelf and open shelf facies. The P/Ti ratio, an indication of OM production and preservation, is greater in the shallow shelf and open shelf marine facies and the highest in the deep marine facies. Clays decreased from 80% to 5% in the shallow shelf and open shelf facies. The 2WS shale was deposited during a long-lived transgression comprised of higher order shallowing upward parasequences that are accompanied by a shift from pelagic to benthic carbonate productivity. There is an increase in carbonates and decrease in siliciclastics (SiO₂, clays) toward the eastern shoreline. Facies associations show an overall decrease in grain size, energy level, and bioturbation from east to west within the study area, with increasing distance from the eastern shoreline. Lateral changes of similar facies are controlled by water depth (i.e., sea level fluctuations). During deposition of the limestone lithofacies, the abundance of pelagic activity and oxygenated bottom water conditions resulted in very low TOC quantity of dominantly Type III kerogen. During deposition of the marlstone lithofacies, high marine productivity, coupled with low oxygen bottom water conditions, resulted in an enrichment of micronutrient trace elements (Zn, Ni) and the effective OM preservation with high contribution of oil-prone type II kerogen. The 2WS oil shale present along the eastern margin of the Western Interior Seaway was deposited on a low gradient shallow and broad carbonate ramp, marked by wave energy, minimal fluvial input, and under moderate climatic conditions.

Organic matter characterization of a sedimentary succession of the Barra Velha Formation carbonates from the Santos Basin, offshore Brazil

Carolina Fonseca^{1,2*}, Jaqueline Torres Souza^{1,2}, António D. de Oliveira²,
Joalice de Oliveira Mendonça^{1,2}, João G. Mendonça Filho², Leonardo Borghi¹

(1) Laboratório de Geologia Sedimentar (Lagesed), Departamento de Geologia, Instituto de Geociências, Universidade Federal do Rio de Janeiro, Rio de Janeiro, Brazil; (2) Laboratório de Palinofácies e Fácies Orgânica (LAFO), Departamento de Geologia, Instituto de Geociências, Universidade Federal do Rio de Janeiro, Rio de Janeiro, Brazil

* Corresponding Author: carolina@lafo.geologia.ufrj.br

The Santos Basin is the largest basin in the eastern margin of Brazil, being considered one of the main basins of hydrocarbon exploration and production. The Piçarras-Itapema/Barra Velha petroleum system was generated in lacustrine shales with intercalated carbonates of the Piçarras Formation and accumulation in carbonatic reservoirs of the Itapema and Barra Velha formations (pre-salt interval petroleum system). The Aptian lacustrine carbonates of the Barra Velha Formation are recorded in several South Atlantic basins, representing one of the largest palaeo-lake systems known in the geological record. Here, a multi-proxy approach was applied to the characterization of the organic matter of 52 borehole samples from a sedimentary succession of the Barra Velha Formation, including organic geochemical (Total Organic Carbon - TOC, Sulfur and insoluble residue – IR) and petrographic (Palynofacies and Organic Petrology) techniques.

The studied samples from the Barra Velha Formation display a TOC content ranging from 0.08 to 10.77 wt.% (average 0.99 wt.%), sulfur content between 0.02 and 2.33 wt.% (average 0.34 wt.%), and insoluble residue with values <1 to 72 wt.% (average 15 wt.%).

In whole rock polished sections (perpendicular to bedding plane), under reflected white and blue incident lights, the samples are dominated by bituminite under the form of bands, threads and elongated lenses exhibiting a yellow, orange or brown fluorescence, and by great quantities of solid bitumen. The solid bitumen displays no/weak fluorescence, appears mostly filling voids within the mineral matrix, appearing either as thin films surrounding the minerals or as more massive, elongated particles parallel to the bedding plane. Solid bitumen presents mean random reflectance values from 0.37 to 0.50%Rr (equivalent vitrinite reflectance 0.63-0.71%VReq). Sporinite, inertinite and zooclasts were also identified.

Under transmitted white and incident blue lights, the kerogen is dominated by the Amorphous Group. This group is characterized by: (i) bacterial AOM that forms uniform cohesive plate-like particles with sharp and distinct (sometimes angular) outlines displaying a strong yellow fluorescence; (ii) bacterial AOM exhibiting a strong yellow fluorescence, a diffuse outline and a thin, low density, sheet-like aspect (pelicular type); and, (iii) Zoomorph-derived AOM displaying a brown fluorescence. It is also possible to identify the presence of zoomorphs, sporomorphs and solid bitumen.

Acknowledgements: This research was carried out in association with the ongoing R&D project registered as ANP 23009-4, PRESAL-II – Impacto dos controles tectonoestratigráficos na qualidade e distribuição de reservatórios do intervalo Pré-sal da bacia de Santos (UFRJ/Shell Brazil/ ANP), sponsored by Shell Brazil.

Spatial and temporal changes in the organic matter supply during the Cenozoic basin evolution in the Danish North Sea

Zhiheng Zhou¹, Henrik I. Petersen², Niels H. Schovsbo², Arka Rudra¹, Hamed Sanei^{1*}

(1) Lithospheric Organic Carbon (LOC) Group, Department of Geoscience, Aarhus University, Aarhus, Denmark; (2) Geological Survey of Denmark and Greenland (GEUS), Øster Voldgade 10, 1350 Copenhagen K, Denmark

* Corresponding Author: sanei@geo.au.dk

The mudstones of the Upper Eocene – Middle Miocene Lark Formation in the Danish North Sea have not been the subject of a detailed organic petrographic and geochemical investigation despite its importance for paleoclimate studies and as a regional seal for potential CO₂ storage sites. This study investigates the characteristics and quantity of organic matter in 391 samples of cuttings obtained from 7 wells from the Danish North Sea.

The Hawk pyrolysis was conducted on all cuttings samples while reflected light and fluorescence microscopy was conducted on 38 pellets for determining the reflectance of primary huminite (HRo), the volume percentage of huminite and inertinite (H+I, vol.%) and the intensity ratio of red to green light of alginite (R/G quotient). The results show that the organic matter in the Lark Formation is generally immature (T_{max} < 430°C, HRo mean value = 0.3%, R/G mean value = 0.51) and mainly consists of Type III kerogen which is dominated by huminite macerals, with the total organic carbon (TOC) content ranging from 0.33 wt.% to 7.34 wt.% (mean value = 2.54 wt.%).

In a north distal site, we observed a long-term decrease in hydrogen index (HI) caused by the increase in TOC outpaced S₂ during Oligocene to Early Miocene. In the south distal sites in the Danish Central Graben, we noticed the increase in HI resulted from the jump in TOC and S₂ during Early Miocene to Middle Miocene. The increase in TOC was proved to be the result of the increased influx of terrestrial organic matter as we established the positive correlation (R²>0.95) between the volume percentage of total organic carbon (TOC, vol.%) and that of huminite and inertinite (H+I, vol.%). This increased influx proved further being the result of changes in organic matter supply from N to NE and then ENE direction during the Cenozoic Basin Evolution in the Danish North Sea.



New insights into oil-to-source rock correlation of oils and asphalt seeps from Zakynthos Island and the west coast of Peloponnese, Western Greece

Ioannis Oikonomopoulos¹, Thomas Gentzis², Humberto Carvajal-Ortiz²,
Efthymios Tripsanas¹

(1) Helleniq Energy Holdings SA, Helpe Upstream S.A., 4A Gravias, Marousi, Athens, 15125, Greece;

(2) Core Laboratories, LP, Reservoir Geology, 6316 Windfern Road, Houston, TX 77040, USA

* Corresponding Author: ioikonomopoulos@upstream.helleniq.gr

Western Greece is considered a frontier area for hydrocarbon exploration. An active petroleum system is documented through the identification of world-class Jurassic source rock intervals, hydrocarbon indications (e.g., surface seeps and oil shows in wells) and by the discovery of the Katakolo oil field, offshore west Peloponnese. The subject of the present study is the origin of oils along the west coast of Peloponnese and on SW Zakynthos Island. The 67 samples analyzed include oils from shallow wells on Zakynthos, oils, asphalts, and oil-impregnated limestones taken from outcrops along the west coast of Peloponnese, core and cuttings from source rock (SR) intervals, and from outcrops throughout western Greece. The samples were examined by Rock-Eval 7S for sulfur speciation, Gas Chromatography (GC), Gas Chromatography-Mass Spectrometry (GC-MS) for the identification of biomarkers, carbon stable isotopes on saturate and aromatic compounds, and sulfur isotopes. GC analysis showed that the oils were biodegraded, which excluded the use of n-alkanes and isoprenoids from further consideration. Instead, the isotopic and molecular parameters were used to derive at the similarities and differences among the oils and their extracts by multivariate statistical methods such as Principal Component (PC) and Hierarchical Cluster (HC) analyses.

Results showed that the oils from Zakynthos and SW Peloponnese are not correlated to Miocene SR intervals, which is the current interpretation. The oils are strongly correlated to the Jurassic SR intervals of the Ionian Basin, including the most external part of the Thrust and Fold Belt (TFB). Based only on GC-MS data, correlations suggest that the oils from Keri on Zakynthos and those from NW Peloponnese are part of the same family. A strong correlation is also seen between the above oils and the U Triassic/L Jurassic Pantokrator shales (PSh) in Epirus. Seeps surrounding the Kyparissiakos Gulf (Block 10) also show a strong correlation with M-U Jurassic SR from the outcrops within the Ionian Basin and the Paxi-Gaios 1X well (PxGa-1X).

Previous studies showed an indirect oil-source correlation between oils from Keri and oils from SW Peloponnese near Marathopolis, suggesting that the above oils are correlated to Miocene age SR in an evaporitic basin. However, results from the current study point to a strong correlation (>0.95) between the oils from Marathopolis and the PSh and the M-U Jurassic SR from PxGa-1X. In addition, many of the wells drilled in the past at Keri indicate multiple oil shows in the carbonate section. This is consistent with deeply buried SRs at the Triassic and Jurassic level, as also indicated by the current study. Samples from the Psh are rich in organic sulfur moieties, particularly in S₂-org sulfur, which is also corroborated by organic petrography under UV light. The organic sulfur-rich nature of the kerogen Type II in Jurassic SR intervals, is shown by the high Sulfur Index (SI) of >100. The high SI, in combination with the kerogen low activation energies suggest an earlier onset of the oil window for these source rocks.

Joint ICCP-TSOP Symposium

Thursday, 21.9.2023

09:00-13:00 Joint ICCP-TSOP Symposium

09:00-09:20 Molecular structure and long-term stability of biochars

A. Rudra, H.I. Petersen, H. Sanei

09:20-09:40 Insight into the composition and permanence of biochar produced from pyrolysis of land plant and macroalgae biomass

H.I. Petersen, H. Deskur, A. Rudra, S. Bachmann Ørberg, D. Krause-Jensen, H. Sanei

09:40-10:00 Olive kernel biochar and charcoal "in-fusion" in coke matrix vs. biocoke quality

M. Wojtaszek-Kalaitzidi, M. Rejdak, M. Książek, S.Y. Larsen, S. Kalaitzidis

10:00-10:20 Pyrolytic alterations in organic matter of lignite gangue rocks from Troyanovo-3 Mine dump area (Mini Maritsa Iztok, Bulgaria)

M. Misz-Kennan, Z. Milakovska, M.J. Fabiańska, M. Stefanova, D. Więclaw, G. Vladislavov

10:20-10:40 Organic matter research from the Pieniny Klippen Belt (Central Western Carpathians)

M. Zielińska, E. Szram, M. Misz-Kennan, M. Fabiańska, D. Plašienka, R. Aubrecht, M. Molčan Matejová, T. Potočný

10:40-11:00 Interlaboratory study: Testing reproducibility of solid biofuel component identification using reflected light microscopy

A. Drobnik, M. Mastalerz, I. Jelonek, Z. Jelonek

11:30-11:50 Petrographic facets of Middle Eocene lignite with implications to coalbed methane potential from Northern Part of Cambay Rift Basin, India
V.A. Mendhe

11:50-12:10 Influence of Lithotypes and Petrographic Constituents on Methane and CO₂ Sorption of Coal from Early Permian-Gondwana Deposits, India

P. Shukla, V.A. Mendhe, S. Pandey

12:10-12:30 Evaluation of the effect of supercritical CO₂ injection on remaining oil in depleted chalk reservoirs, Danish North Sea

X. Zheng, R.Ø. Stenshøj, H.I. Petersen, H. Sanei



**Organic Petrology in the Energy Transition Era:
Challenges ahead**

Bulletin of the Geological Society of Greece, Sp. Publ. 12

12:30-12:50 Exotic liptinite macerals – what are they and why such good generative potential?

G. Smith, L. Johnson, I. Sadd

14:30-14:50 The characteristics comparisons of Cambrian source rocks in South China and Alum Shale in Europe

X. Xie, Y. Liu, Y. Xu

14:50-15:10 Radiolytic alteration of uraniferous organic matter and base-metal mineralization in Bytiz, Příbram district, Czech Republic

T. Larikova, I. Sýkorová, M. Havelcová, B. Kříbek

15:10-15:30 Decrypting paleomire conditions of superhigh-organic-sulfur coals from Meghalaya, India

T. Adsul, S. Ghosh, M.D. O'Beirne, J.P. Werne, W.P. Gilhooly III, J. Houghton, D. Fike, P.C. Hackley, J. Hatcherian, A. Kumar Varma

15:30-15:50 Organic facies variability and paleoenvironmental characterization of the Codó and Itapecuru Formations (Aptian-Albian) of Parnaíba Basin, Brazil

D.M. de Lima, J.G. Mendonça Filho, C. Fonseca, A.D. de Oliveira, J. de Oliveira Mendonça, P.A. Gonçalves

16:30-16:50 Organic petrographical features of Miocene Meliadi-Moschopotamos lignite, Macedonia, northern Greece

P. Khanaqa, S. Kalaitzidis, W. Riegel

16:50-17:10 Mineralogy and organic petrography of the No. 6 coal seam, Soutpansberg Coalfield, South Africa: Evidence for hydrothermal activity

S. Biswas, N.J. Wagner, O.M. Moroeng

17:10-17:30 Petrological, mineralogical and geochemical proxies to the organic matter dispersed in the sedimentary rocks in Turgut area, Yatağan Basin, SW Türkiye

Z. Büçkün, M. Çolak

17:30-17:50 Contribution of Organic Petrography in the study of volcanoclastic sequences: the case of West Acrocheiras section, Petrified Forest of Lesvos, Greece

P. Papadopoulou, G. Iliopoulos, K. Perleros, S. Kalaitzidis, K. Christanis, N. Zouros

17:50-18:00 TSOP Closing Ceremony

Molecular structure and long-term stability of biochars

Arka Rudra^{1*}, Henrik I. Petersen², Hamed Sanei¹

(1) Lithospheric Organic Carbon, Department of Geoscience, Aarhus University, Aarhus, Denmark;

(2) Geological Survey of Denmark and Greenland (GEUS), Copenhagen, Denmark

* Corresponding Author: arudra@geo.au.dk

Biochars are increasingly used to improve the productivity of agricultural soils as well as for long-term carbon sequestration (Petersen et al., 2023). The wastes from biomass are used to manufacture biochar as a clean and sustainable environmental solution. The pyrolysis of biomass generates biofuel, which can be utilized for generating energy and solid biochar. However, there lacks an understanding about the structural stability of the biochars generated through various pyrolytic processes. The objective of the study is to understand the molecular structural remnants of the biochar from different biomasses and assess the long-term stability of the macromolecule. For this, various agricultural biomass, food wastes and urban sludge are pyrolysed at temperatures ranging from 450-900°C and converted into biochars, which are further analyzed with a pyrolysis-gas chromatography-mass spectrometry. The biochars were flash pyrolysed at 700°C (0.2 min) and the pyrolysis products were studied by GC-MS. The GC temperature was initially set at 50°C, and then ramped up to 300°C at a rate of 10°C/min.

The results show that the pyrolysates from the studied biochars produced at lower temperatures (400-500°C) contain larger, 3-4 ring aromatic compounds (PAH) as well as their methylated compounds. Aliphatic compounds are entirely missing. Pyrolysates from the lower pyrolysis temperatures are susceptible to produce secondary compounds, leading to formation of alkylated aromatic compounds.

The degree of methylation and aromaticity of biochars produced from different biomass is likely to be function of the ratio of labile:refractory carbon of the feedstock as well as the maximum temperature of pyrolysis at which biochars have been produced. Therefore, biochars produced at low temperatures having large macromolecular size and linked via methyl chains are susceptible to break off at the methylated bonds and further susceptible to microbial and thermal degradation. With the increasing biochar production temperatures, the degree of methylation decreases along with more condensation of the macromolecule. Therefore, the pyrolysates show no methyl bonds and only scarce amount of single or two ring aromatic compounds. Biochars having such condensed macromolecular structure can be utilized as long-term carbon sequestration.

Reference

Petersen, H.I., Lassen, L., Rudra, A., Nguyen, L.X., Do, P.T.M., Sanei, H., 2023. Carbon stability and morphotype composition of biochars from feedstocks in the Mekong Delta, Vietnam. *Int. J. Coal Geol.* 271, <https://doi.org/10.1016/j.coal.2023.104233>

Insight into the composition and permanence of biochar produced from pyrolysis of land plant and macroalgae biomass

Henrik I. Petersen^{1*}, Helena Deskur², Arka Rudra³, Sarah Bachmann Ørberg⁴, Dorte Krause-Jensen⁴, Hamed Sanei³

(1) Geological Survey of Denmark and Greenland (GEUS), Copenhagen, Denmark; (2) NIRAS, Aalborg, Denmark; (3) Lithospheric Organic Carbon, Department of Geoscience, Aarhus University, Aarhus, Denmark; (4) Department of Ecoscience - Marine Ecology, Aarhus University, Aarhus, Denmark

* Corresponding Author: hip@geus.dk

Production of biochar from pyrolysis under anoxic or oxygen-deficient conditions of agricultural waste products and aquatic biomass has increasing focus due to a wide range of beneficial applications of biochar. The formation of biochar can reduce CO₂ emissions by sequestration of carbon from the biosphere pool to the geological carbon cycle with long-term storage potential. Biochar is also a byproduct of sustainable biofuel production as a substitute to fossil fuel. Characterization of biochar, including carbon stability in the soil, has primarily been based on elemental composition and incubation experiments. However, organic petrographic and geochemical methods are preferable since they are standardized, well-established and can set biochar properties into the context of the geological bacterial and heat-induced organic carbon evolution in the Earth's crust (Petersen et al., 2023).

This study provides organic petrographic and geochemical results from pyrolysis at different heating rates and maximum temperatures for different macroalgal species and agricultural waste products. The morphotype composition of the biochars reflects both the structural nature and the chemical composition of the biomass, and the maximum pyrolysis temperature. The biochars derived from agricultural waste products show that increasing end-temperature yields a higher proportion of porous morphotypes and an increase in TOC content. The macroalgal species yield different quantities of biochar and hydrocarbons (biofuel) at the same heating rate and end-temperature. However, a fast-heating rate produces the most hydrocarbons and generally least biochar, while it is the opposite for slower heating rates.

Biochar mean reflectance from agricultural waste products increases from <2.33% at 500°C to >4.35% when pyrolyzed at 700°C or higher at a heating rate of 10°C/min, indicating a highly stable polyaromatized condensed carbon structure. In accordance with this, the fraction of labile organic carbon is near zero and the Hydrogen Index very low. The highest biochar mean reflectance of the macroalgae pyrolyzed at a faster heating rate is 2.91% despite an end-temperature of 650°C, suggesting the heating rate also influences biochar stability.

The results highlight the strength of using organic petrography and geochemistry to describe feedstock pyrolysis yields, biochar morphotype composition, and carbon stability within the context of the deep geological carbon cycle.

Reference

Petersen, H.I., Lassen, L., Rudra, A., Nguyen, L.X., Do, P.T.M., Sanei, H., 2023. Carbon stability and morphotype composition of biochars from feedstocks in the Mekong Delta, Vietnam. *Int. J. Coal Geol.* 271, <https://doi.org/10.1016/j.coal.2023.104233>

Olive kernel biochar and charcoal "in-fusion" in coke matrix vs. biocoke quality

Małgorzata Wojtaszek-Kalaitzidi^{1*}, Michał Rejdak¹, Michał Książek²,
Sten Y. Larsen³, Stavros Kalaitzidis⁴

(1) Institute of Energy and Fuel Processing Technology, Zabrze, Poland; (2) SINTEF AS, Trondheim, Norway;
(3) Eramet Norway AS, Trondheim, Norway; (4) Department of Geology, University of Patras, Patras, Greece

* Corresponding Author: mwojtaszek@itpe.pl

Using biomass as a blend component for metallurgical coke production is a way to reduce the CO₂ emission from ferroalloys industry. The coke used in ferroalloys production has different quality requirements what gives a chance of using biomass in bigger scale than in metcoke for the blast furnace. Not every biomass type behaves similarly in coking process. To be able to use greater share of biomass in the coking blend and to achieve required coke quality at the same time, it is necessary to select the biomass component with the optimal structural features.

Since biomass substances do not plasticize during the pyrolysis process, they are inert. The solid residue from the coking process is therefore one of the components of the coke matrix that can be identified and characterized under an optical microscope. During the pyrolysis process, the coal substance liquefies, thus enabling the molecular arrangement of the coke matrix, which leads to an increase in its optical anisotropy. Biomass components do not have this ability, therefore they are an isotropic component with a low degree of order. Moreover, their addition reduces the plasticity of the coals, and thus worsens the conditions for the ordering of the coal substance. Due to this fact, many types of biomass components in fresh and carbonized form were tested. Two the most promising biomass types were selected to continue the research: olive kernel and commercial charcoal. Both biomass components differ in a way how they build-in the anisotropic coke matrix. This difference is a result of the different biomass components' structural character. The quality of the obtained coke depends on the built-in mechanism.

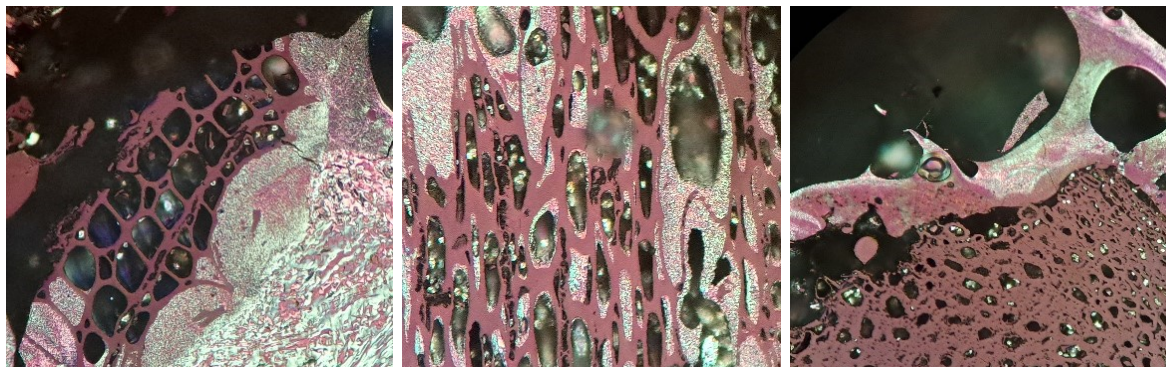


Figure 1. The exemplary photomicrographs of the way how the biomass component is built-in the coke matrix (from left: in-fused, saturated, capsulated).

Acknowledgements: The research leading to these results has received funding from the Norway Grants 2014-2021 via the National Centre for Research and Development. Project is co-funded by the Norwegian Financial Mechanism 2014-2021 based on the contract no: NOR/POLNOR/BioCoke4FAI/0070/2019-00.

More information: www.biocoke4fai.pl

Pyrolytic alterations in organic matter of lignite gangue rocks from Troyanovo-3 Mine dump area (Mini Maritsa Iztok, Bulgaria)

Magdalena Misz-Kennan^{1*}, Zlatka Milakovska², Monika J. Fabiańska¹, Maya Stefanova³, Dariusz Więclaw⁴, Georgi Vladislavov⁵

(1) Faculty of Natural Sciences, University of Silesia in Katowice, Poland; (2) Geological Institute, Bulgarian Academy of Sciences, Sofia, Bulgaria; (3) Institute of Organic Chemistry with Centre of Phytochemistry, Bulgarian Academy of Sciences, Sofia, Bulgaria; (4) AGH University of Science and Technology, Kraków, Poland; (5) Troyanovo-3 Mine OOD, Mini Maritsa Iztok EAD, Mednikarovo, Bulgaria

* Corresponding Author: magdalena.misz@us.edu.pl

The Troyanovo-3 Mine occupies the SE part of the Maritsa Iztok Basin (MIB). The mean thickness of the coal-overlying sediments is on average 70-80 m but southwards, close to the basin rim, it is often 8-10 m. Carbonaceous mudstone and lignite of high ash yield were deposited in the dump area of the Troyanovo-3 Mine.

Samples collected at the Troyanovo-3 Mine represent coals (lignite) and coal wastes stored 6-10 years after excavation and underwent mild heating, smoldering. Organic matter (OM) is dominated by huminite macerals. Macerals of liptinite and inertinite are relatively rare. Huminite macerals sometimes contain cracks and/or are paler in colour. Rarely signs of plasticity or devolatilisation pores occur indicating a low heating rate. The reflectance of unaltered OM is 0.19-0.25%; the reflectance of altered OM can reach 0.53% but in the case of individual particles it might exceed 1%. Organic matter co-occurs with dominating clay minerals and pyrite usually occurring as framboidal particles. Pyrite content varies from 0.2-8.8% and its oxidation might contribute to self-heating of coal and coal wastes.

The bituminous fraction of gangue rocks comprised a wide range of compounds from aliphatic and aromatic hydrocarbons and polar derivatives. Two populations of samples can be distinguished, (i) lignite and wastes corresponding to the common level of thermal maturity of the early geochemical diagenetic stage, (ii) much more mature samples that were exposed to self-heating/smoldering. The (i) set samples contained only small amounts of *n*-alkanes, high concentrations of diterpenoids such as 16 α (H)-phylocladane, kauren-15-ene, and abietane derivatives. Pentacyclic triterpanes and aromatic hydrocarbons, both substituted and unsubstituted, were mostly absent. Among polar compounds ferruginol, benzoic aldehyde derivatives, and fatty acids predominate. The second group (samples SN1, SN2, SN7, SN8, SN9, SN14, and SN6) showed the obvious signs of higher temperature impact such as high concentrations of *n*-alkanes with a pyrolytic Gaussian peaks outline, presence of alkyl aromatic hydrocarbons including C₁-C₅ naphthalenes and C₁-C₂ phenanthrenes, absent in the first sample set. Their distribution is mature and does not conform with the generally immature organic matter of rocks investigated. Lighter phenolic compounds that comprised phenol, cresols, and xylenols were present only in the samples of the (ii) set whereas absent in (i) samples. Opposite, higher phenolic compounds derived from lignin weathering such as guaiacol were found in the (i) set. Altogether the features suggest thermal stress during self-heating that affected the (ii) samples.

Acknowledgements: The study was performed in the frame of the Project KP-06-H64/5 at the National Science Fund (Ministry of Education and Science of Bulgaria).



Organic matter research from the Pieniny Klippen Belt (Central Western Carpathians)

Magdalena Zielińska^{1*}, Ewa Szram¹, Magdalena Misz-Kennan¹, Monika Fabiańska¹,
Dušan Plašienka², Roman Aubrecht², Marína Molčan Matejová², Tomáš Potočný²

(1) University of Silesia in Katowice, Poland; (2) Comenius University in Bratislava, Slovakia

* Corresponding Author: magdalena.zielinska@us.edu.pl

Jurassic-Cretaceous shales of the flysch and pelagic formations from the Pieniny Klippen Belt, being a constituent of the Central Western Carpathians, were analyzed to evaluate the type of organic matter, the origin and the depositional environment. The Pieniny Klippen Belt formations were deposited 120 million years in the northern sector of the Tethys Ocean. Results from the 24 samples established the organic geochemical characteristics and identified the kerogen type and thermal maturity of organic matter based on their petrographic approach as observed under incident white light and blue light excitation.

Both petrographic microscopy and biomarker parameters showed that the shales contain organic matter of terrigenous and marine origin preserved in the sediments under various depositional conditions at different depths beneath the shelf. The organic matter represented by three maceral groups, is typical for flysch sediments of the Szlachtowa Formations. It signifies mixed organic matter origin, proved by the presence of yellow fluorescing liptinite macerals with the addition of vitrinite and inertinite particles. The organic petrography of pelagic sediments represented by the Opaleniec and Skrzypny Formations revealed a low abundance of organic matter represented mainly by the inertinite group with the addition of vitrinite and liptinite remains. Bimodal distribution at $n\text{-C}_{16}\text{-}n\text{-C}_{18}$ and $n\text{-C}_{23}\text{-}n\text{-C}_{28}$ with the predominance of long-chain over short-chain n -alkanes in the flysch sediments also confirmed various sources for the organic matter within the epicontinental basin. The lack of homologues from $n\text{-C}_{11}$ to $n\text{-C}_{14}$ indicates the biodegradation of organic matter. The marine origin of the pelagic deposits of the Opaleniec and Skrzypny Formations was testified in the distribution of n -alkanes as the dominance of short-chains with a low contribution of middle- and long-chain n -alkanes, which may suggest their mainly planktonic/bacterial origin. The steranes were uncommon in the samples; only single sterane peaks were observed. Aromatic hydrocarbons such as dimethyl- and trimethylnaphthalenes, usually show low concentrations, but only in the flysch samples. The Pr/Ph ratio values range from 1.00 to 3.72 (av. of 2.27), indicating that organic matter was deposited in a marine environment and preserved under suboxic and oxic conditions.

The kerogen type-III identification obtained using the cross-plot of Pr/ $n\text{-C}_{17}$ versus Ph/ $n\text{-C}_{18}$, corresponds to the thermally mature organic matter being at early/middle catagenesis of the oil window. These results are consistent with vitrinite reflectance values in the range of 0.60% to 1.03% measured on indigenous vitrinite particles.

Funding: This research was funded by three projects: from the National Science Centre in Poland, No. 2019/03/X/ST10/00336, from the NAWA (Polish National Agency for Academic Exchange), No. BPN/BSK/2021/1/00029/U/00001, and from the Slovak Research and Development Agency No. SK-PL-21-0030).



Interlaboratory study: Testing reproducibility of solid biofuel component identification using reflected light microscopy

Agnieszka Drobnik^{1,2,3*}, Maria Mastalerz^{2,3}, Iwona Jelonek^{1,3}, Zbigniew Jelonek^{1,3}

(1) University of Silesia in Katowice, Institute of Earth Sciences, ul. Będzińska 60, 41-200 Sosnowiec, Poland;

(2) Indiana Geological and Water Survey, Indiana University, 1001 E. 10th St., Bloomington, IN, 47405, USA;

(3) Centre for Biomass Energy Research and Education, ul. Będzińska 60, 41-200 Sosnowiec, Poland

* Corresponding Author: agnieszka.drobnik@us.edu.pl

Considering global market trends and environmental climate, increased biomass use for energy is expected to continue. As more diverse materials are being utilized to manufacture solid biomass fuels, it is critical to implement quality assessment methods to thoroughly test these fuels. One such method is reflected light microscopy, which has the potential to complement and enhance current standard testing, leading to improving fuel quality assessment and, ultimately, preventing avoidable air pollution.

An interlaboratory study (ILS) was conducted to test the reproducibility of biomass fuel component identification using a reflected light microscopy (RLM) technique. The exercise was conducted on 30 photomicrographs showing biomass and various undesired components of solid biofuels, which were purposely added to contaminate wood pellets and charcoal-based grilling fuels.

Forty-six organic petrographers from all over the world had various levels of difficulty identifying the marked components and, as a result, the percentage of correct answers ranged from 52.2 to 94.4%. Among the most difficult components to distinguish were different petroleum products and various types of inorganic matter. This erroneous identification resulted from a lack of sufficient morphological descriptions which would unquestionably characterize the components; ambiguities of the nomenclature; limitations of the analytical and exercise method; and insufficient experience of the participants.

The results of the exercise led to proposing a simplified classification of the biomass fuel components, and concluding that while RLM has significant potential to enhance the quality assessment of the fuels, the technique still requires refinement before it can be standardized. Future research must be conducted to refine the nomenclature, develop a microscopic morphological description of the components, and conduct a follow-up ILS.



Petrographic facets of Middle Eocene lignite with implications to coalbed methane potential from northern part of Cambay Rift Basin, India

Vinod A. Mendhe

CSIR – Central Institute of Mining and Fuel Research, Dhanbad - 826 015, Jharkhand, India

Corresponding Author: vamendhe@cimfr.nic.in; vamendhe@gmail.com

Evaluation of the coalbed methane (CBM) prospects of the lignite reserves from the Middle Eocene age, located at depths ranging from 1200 to 1700 m in the Kalol and Kadi Formations of the Northern part of the Cambay rift basin in Gujarat, India, is carried out in order to meet any future exigencies through petrographic parameters. In this study, a total of 19 lignite core samples were collected from five exploratory vertical drilling boreholes at different locations, with varying depths including Kalol, Sobhasan top, and Sobhasan bottom seams. The lithology and formation log of five boreholes shows that the three seams consistently maintain their thickness and lateral continuity throughout the Shobhasan area of the Mehsana district. The in-situ gas content values were determined to range from 2 to 8 m³/t, surprisingly high given the low rank of the coal. The huminite, liptinite and inertinite on mineral matter free basis varies from 78.3-96.5, 1.3-12.6 and 0.9-10.2 vol.%, respectively. The pyramidal shape of liptinite observed in lignite seams may be due to the contribution of plant evolving specific liptinite components and their geochemical gelification. The appearance of micrinite in lignite samples may indicate the expulsion of hydrocarbons from the organic matter. The mean huminite reflectance measured on ulminite is placed in a very narrow range of 0.32-0.56%. The V-step reflectogram of Sobhasan bottom, Sobhasan top and Kalol seams are symmetrical in nature having clear one peak. The lignite samples facies plot of tissue preservation index and gelification index, which fall in three distinct regions, which point out depositional conditions of various lignite seams viz. Sobhasan bottom seam (marshy - limnic condition), Sobhasan top seam (dry forest swamp – limnic – marshy condition) and Kalol seam (limnic-marshy condition). The lignite samples placed in marshy depositional conditions having larger gas content. The organic petrological facies (huminite, liptinite and inertinite) and subfacies (Humotelinite (HT) and Humodetrinite (HD)) were delineated on the basis of petrographic constituents. It appears that petrographic reactive components viz. vitrinite and liptinite help in the generation and storage of coalbed gas (predominantly methane). Also, it is inferred that lignite seams have undergone organic gelification of thermogenic material in the mire, where an increase in gelification may occur due to increased favourable activity of bacteria as well as a probable increase in the concentration of Na⁺, K⁺ and Ca⁺⁺ in groundwater. The minimum gelification of organic matter in HT-TE (Textinite) and HD-AT (Atrinite), liptinite-rich organic subfacies may be due to favourable conditions for the preservation of petrographically structured organic materials. It may also occur due to anaerobic bacterial activity in moist conditions. The groundwater may contain smaller amounts of Na⁺, K⁺ and Ca⁺⁺ ions. Overall, the petrographic components, depositional facies and favourable groundwater conditions supported the lignite deposits and gas generation in the northern part of the Cambay Basin, Gujarat, India.



Influence of lithotypes and petrographic constituents on methane and CO₂ sorption of coal from Early Permian-Gondwana deposits, India

Priyanka Shukla^{1,2*}, Vinod A. Mendhe^{1,2}, Shashanka Pandey^{1,2}

(1) CSIR – Central Institute of Mining and Fuel Research, Dhanbad - 826 015, Jharkhand, India; (2) AcSIR - Academy of Scientific and Innovative Research, Ghaziabad - 201002, Uttar Pradesh, India

* Corresponding Author: priyankabhu410@gmail.com

CO₂ storage in the different geologic formations is a feasible option to reduce GHG emissions to the atmosphere. The most feasible and techno-economical accepted method is CO₂ injection in deep unmineable coal beds with enhanced methane recovery. CO₂ has a greater affinity with coal, shale and associated rock compared to methane. However, detailed information on the coal reservoir is crucial before CO₂ injection. In this study, high volatile bituminous coal samples derived from the Barakar Formation have been analyzed for lithotype, geochemical, petrographic and pore characteristics. Estimated the volume percentage of lithotypes, e.g., vitrain, clarain, claro-vitarin, durain, claro-durain, etc. Also, determined the volume percentage of each petrographic constituent. The different litho-bands were separated and analyzed for geochemical and high-pressure CH₄ and CO₂ adsorption isotherm. Assessed the maximum CH₄ and CO₂ sorption capacity of different lithotypes. It is observed that vitrain has comparatively higher adsorption capacity followed by claro-vitrain, clarain and durain. The desorption isotherm indicated claro-vitrain and vitrain have maximum gas diffusivity controlled by pore distribution and cleat/fracture system. However, durain has shown the least sorption and diffusion characteristics, mainly influenced by fusinite content, geochemically altered organic and inorganic material. The pore distribution studies have been carried out through micropetrography, FE-SEM photographs, and low-pressure BET sorption isotherms. These different pore distributions have been used to formulate the empirical formula to assess the diffusivity of coal and associated rocks. Established the relationship of the CH₄ and CO₂ sorption properties with different macerals, lithotypes, pore size, surface area and pore volume. Examined the role of a fractal, i.e. internal pore surfaces' in gas sorption of the different lithotypes matrix system. Finally, it is summarized that the content of vitrain and meso- to macro- pore matrix systems in early Permian coal seams directly controls the CH₄ and CO₂ storage. Moreover, the moisture, volatile matter and secondary mineral content minutely influenced the sorption mechanism. The study shall help to develop procedures for CO₂ injection and ECBM recovery from Gondwana coal seams in India.

Evaluation of the effect of supercritical CO₂ injection on remaining oil in depleted chalk reservoirs, Danish North Sea

Sherry (Xiaowei) Zheng^{1*}, Rasmus Ø. Stenshøj², Henrik I. Petersen², Hamed Sanei¹

(1) Lithospheric Organic Carbon (LOC) Group, Department of Geoscience, Aarhus University, 8000 Aarhus C, Denmark; (2) Department of GeoEnergy and Storage, Geological Survey of Denmark and Greenland (GEUS), 1350 Copenhagen K, Denmark

* Corresponding Author: zhengxiaowei@geo.au.dk

Geological storage of CO₂ is an important strategy for reducing the atmospheric CO₂ at scale. The depleted oil and gas reservoirs in the North Sea have shown significant carbon storage capacity, however, a potential risk is that the injected supercritical CO₂ (scCO₂) interact with the residual oil. This may lead to displacement of movable oil fractions and clogging by non-movable solid bitumen/asphaltenes.

The remaining oil fractions in a core plug from the Maastrichtian Tor reservoir in the Halfdan Field, Danish North Sea, have been investigated before and after scCO₂ flooding under reservoir conditions to examine the effect of scCO₂ injection on the hydrocarbons. Besides, 24 core chip samples through the Tor reservoir (M1 and M2 units) were analyzed to unravel the remaining oil composition. The analytical work included reflected light microscopy, Extended Slow Heating (ESH[®]) pyrolysis, extract composition and Gas Chromatography (GC), and Thermal desorption-GC/MS.

The scCO₂ flooding experiment indicates that scCO₂ can effectively solubilize and mobilize all lighter oil fractions, leaving behind the heavy immiscible asphaltene/solid bitumen. After scCO₂ flooding immobile asphaltene, oil and solid bitumen aggregates were physically trapped at various points and primarily at the outlet section due to a sudden change in pressure. Extracts of the remaining oil through the M1 and M2 units of the Tor reservoir show a fairly uniform extract composition and GC traces, although some variation in asphaltene content and *n*-alkane distribution is recorded in certain levels within the M1 unit. Furthermore, all GC traces have a pronounced Unresolved Complex Mixture (UCM) hump. ESH oil fractions of all samples show that asphaltene/solid bitumen is the dominant oil fraction, ranging from 1.49-3.30 vol.% (ave. 2.00 vol.%). Levels within the M1 unit contain a higher saturation of non-movable oil. These levels are enriched in asphaltene/solid bitumen and could potentially constitute layers with higher pore throat clogging risk that could have an adverse effect on scCO₂ flow. The asphaltene (%) in the extractable organic matter (EOM) do not correlate with the asphaltene/solid bitumen fraction (vol.%) derived from ESH pyrolysis. The reason is supposedly that EOM asphaltene is soluble in organic solvent and likely belong to the bitumen fraction, while the non-movable asphaltene/solid bitumen fraction is more similar to solid kerogen that is insoluble in organic solvents.

These results will help de-risk scCO₂ injection issues related to presence of remaining oil in depleted oil reservoirs considered for CO₂ storage.

Exotic liptinite macerals – what are they and why such good generative potential?

Greg Smith^{1*}, Lukman Johnson^{1,2}, India Sadd^{1,3}

(1) Curtin University, Perth, Australia; (2) now Fugro, Perth, Australia; (3) now Santos, Perth, Australia

* Corresponding Author: Gregory.c.smith@curtin.edu.au

The origin of some liptinite macerals such as sporinite, cutinite, suberinite, resinite and telaginite is well understood because they can be directly related to plant phyterals. More obscure and mysterious is the origin and composition of the liptinite macerals bituminite, lamalginite and exsudatinitite that are controlled by sedimentary facies, burial diagenesis and low temperature-pressure metamorphism (coalification). Analysis of these macerals by nano-scale ToF-SIMS shows they are largely composed of hydrocarbons and hence form extremely good source rocks.

Bituminite was described as amorphous bitumen then bituminite by Teichmüller (1950; 1974). Some authors have suggested it is probably derived from cyanobacterial mats (Glikson, 1984; Cook & Sherwood, 1991) though high magnification, organic analyses have eluded previous studies. Analyses of bituminite groundmass in Ordovician mudrocks, using fluorescence microscopy and Tof-SIMS, indicate bituminite is composed of elongate organic bodies (~2 µm x 5 µm) isolated, clumped or aligned as bedding plane sheets (Johnson *et al.*, 2023). They probably do represent cyanobacteria (or blue-green algae, though they are not algae) and have characteristic Mass Spectrogram signatures. Cyanobacteria are photoautotrophic prokaryotes with variable morphology from single cells to colonies to filamentous forms that form bacterial mats. This explains the various morphology from micron sized bodies, or clusters (cf micro-telalginite) to laminated groundmass (cf micro-lamalginite). This suggests some Lamalginite is not algal. Also, nano-scale Tof-SIMS in these shales does not show bituminite impregnated in the clays as commonly inferred but occurring as separate bodies.

Exsudatinitite is less enigmatic and occurs over a wide range of ranks and lithofacies. Consequently, Tof-SIMS analyses show a range of compositions as expected for a secondary maceral though a general characteristic is their very low oxygen content (Sadd *et al.*, 2023). Most liptinites are capable of producing exsudatinitite but especially large phytoclasts of cutinite, sporinite (megaspores), resinite and fracture fill in bituminite and detrovitrinite.

References

- Cook, A., Sherwood, N., 1991. Classification of oil shales, coals and other organic-rich rocks. *Organic Geochemistry* 17(2), 211-222.
- Glikson, M., 1984. Transmission electron microscopy and C-isotope composition of oil shales with particular reference to Australian deposits. ANU PhD thesis, unpublished.
- Johnson, L., Smith, G., Iqbal, M., van Hattum, J., Taylor-Walsh, R., 2023. A new bacterial origin for the hydrocarbon-bearing zones in the Goldwyer Formation on the Broome Platform, Canning Basin, WA, from Nanoscale ToF-SIMS. AEGC 2023. ASEG. doi:10.5281/zenodo.7980115.
- Sadd, I., Smith, G., Hanich, T., Sun, X., Minken, J., 2023. Organic Depositional Facies Control on Hydrocarbon Occurrence in the early Middle Triassic, Roebuck Basin, WA. AEGC. ASEG.
- Teichmüller, M., 1950. Zum petrographischen Aufbau und Werdegang der Weichbraunkohle. *Geologisches Jahrbuch* 64, 429-488.
- Teichmüller, M., 1974. Über neue Macerale der Liptinit-Gruppe und die Entstehung von Micrinit. *Fortschr. Geol. Rheinl. u. Westf.* 24, 37-64.

The characteristics comparisons of Cambrian source rocks in South China and Alum Shale in Europe

Xiaomin Xie*, Yumin Liu, Yaohui Xu

Hubei Key Laboratory of Petroleum Geochemistry and Environment, School of Resources and Environment, Yangtze University, Wuhan, Hubei 4301002, China

* Corresponding Author: xiaominxie2019@sina.com

The Lower Cambrian Niutitang Fm shale is a shale gas target in south China, and the shale gas resource evaluation is fundamental for shale gas exploration. This Lower Cambrian shale interval is over-mature, and it is difficult to evaluate the hydrocarbon generation potential. The characteristics of Alum Shale with low maturity (%Ro= 0.4~0.5) could be references for Lower Cambrian Shale evaluation in south China. In this study, organic matter compositions and sedimentary environment were carefully compared. The organic matter of Alum Shale is dominated by lamalginite and vitrinite-like mass (VLM) deposited in an euxinic or even sulfurized marine sedimentary environment. The bio-precursors of organic matter in Lower Cambrian contained mainly multicellular macro-benthic algae, planktonic algae and some zooplanktons. Organic matter is well preserved because of the syngenetic hydrothermal silica fluid input, which silicified organisms rapidly and diluted the organic matter. This well-preserved organic matter provided TOC content but probably without hydrocarbon generation potential; no solid bitumens were observed. These could be because these organisms were instantly fossilized in Lower Cambrian and did not experience the bio-degradation and complicated diagenesis. Thus, the characteristics of the low maturity Alum Shale could help analyzing the organic matter in Lower Cambrian Shales, but the characteristics of hydrocarbon generation potential and resources evaluation were difficult or used with cautions to apply in the gas shale resources evaluation in China.

References

- Xie, X.M., Borjigin, T., Qin, J., Zhang, Q., Bian, L., Yin, L., 2015. Depositional environment, organisms components and source rock formation of siliceous rocks in the base of the Cambrian Niutitang Formation, Kali, Guizhou. *Acta Geologica Sinica* 89, 425-439.
- Xie, X.M., Zhu, G.Y., Wang, Y., 2021. The influence of syngenetic hydrothermal silica fluid on organic matter preservation in lower Cambrian Niutitang Formation, South China. *Marine and Petroleum Geology* 129, 105098.

**Radiolytic alteration of uraniferous organic matter and base-metal mineralization in
Bytiz, Příbram district, Czech Republic**

Tatiana Larikova^{1*}, Ivana Sýkorová¹, Martina Havelcová¹, Bohdan Kříbek²

(1) Institute of Rock Structure and Mechanics CAS, Prague, Czech Republic; (2) Czech Geological Survey, Prague, Czech Republic

* Corresponding Author: larikova@irms.cas.cz

Bytiz deposit is a part of the previously mined Příbram uranium and base-metal ore district. It is an example of a vein-type deposit with polyphase hydrothermal mineralization, probably caused by the granitoids of the Central Bohemian Plutonic complex. Six uraniferous bitumen samples from Bytíz with U content up to 37.7% were characterized petrologically, geochemically and mineralogically, and also by infrared and Raman microspectroscopy. The bitumen-bearing samples consist of base-metal sulfides: galena, sphalerite, pyrite, chalcopyrite, and also, minor amounts of tetrahedrite, stibnite, and acanthite, associated with Mn-bearing calcite, quartz, and silicates (chlorite, muscovite). Samples of bitumen contain 4.3% to 55.5% organic carbon, 0.1% to 2.2% hydrogen and 0.01% to 2.15% of total sulphur. Uraniferous bitumen was found in the form of small veins and rarely droplets, and roundish to irregular accumulations, in association with carbonate veins, and in fractures.

U-bearing minerals in the studied samples are presented by uraninite and more rarely coffinite (as pseudomorphs after uraninite). There were found two generation of uraninite in association with bitumen: 1. big grains, filled with organic phase in cracks; and 2. as a part of complex textures inside areas with organic matter; in this case uraninite was probably remobilized. The geochemical distributions of the elements were studied using EPMA and GC/MS throughout the areas of organic matter.

It was found microscopically that more than 80 vol.% of the bitumen from the vein fillings was radiolytically altered. The random reflectance values of unaltered mineral-free amorphous bitumen range from 0.45% to 1.11%. Random reflectance of radiolytically altered bitumen increased from 1.72% to 3.44%.

Radiolytic alteration results in optical properties, composition and formation of various textures: from simple massive to flow, dendritic to very complex morphology. The degree of graphitization of the carbonaceous material was assessed by Raman microspectroscopy. Spectral maps show significant destruction changes of aliphatic C-H bonds and an increase in the content of oxygen functional groups in the vicinity of U minerals. The reflectance and abundance of alteration signs increase with increasing of U concentration. Samples with higher uranium content have a more aromatic character.

Thus, the results show that the concentration of uranium is the main factor influencing the radiolytic alteration of the organic matter; and geochemical analyses confirmed changes in the chemical composition of the samples related to the uranium content.

Decrypting paleomire conditions of superhigh-organic-sulfur coals from Meghalaya, India

Tushar Adsul^{1*}, Santanu Ghosh², Molly D. O'Beirne³, Josef P. Werne³,
William P. Gilhooly III⁴, Jennifer Houghton⁵, David Fike⁵, Paul C. Hackley⁶,
Javin J. Hatcherian⁶, Atul Kumar Varma¹

(1) Coal Geology and Organic Petrology Laboratory, Department of Applied Geology, Indian Institute of Technology (Indian School of Mines) Dhanbad-826004, Jharkhand, India; (2) Department of Geology, Mizoram University, Aizawl-796004, Mizoram, India; (3) Organic and Stable Isotope Biogeochemistry Laboratory, Department of Geology and Environmental Science, University of Pittsburgh, 200 Space Research Coordination Center, 4107 O'Hara Street, Pittsburgh, PA 15260, USA; (4) Department of Earth Sciences, Indiana University-Purdue University Indianapolis, Indianapolis, IN 46202, USA; (5) Department of Earth and Planetary Sciences, Washington University in St. Louis, 1 Brookings Drive, St. Louis, MO 63130-4899; (6) U.S. Geological Survey, Geology, Minerals & Energy Science Center, MS 954 National Center, Reston, VA 20192, USA

* Corresponding Author: tpadsul@gmail.com

The present investigation decrypts the paleomire conditions of the Paleogene superhigh-organic-sulfur (SHOS) coals from Meghalaya, India, using $\delta^{34}\text{S}_{\text{V-CDT}}$ values of the total sulfur ($\delta^{34}\text{S}_{\text{TS-V-CDT}}$) and pyritic sulfur ($\delta^{34}\text{S}_{\text{Py-V-CDT}}$) along with the micropetrography and trace element ratios. Thirty coal samples were collected from the Jaintia Hills in the east, Khasi Hills in the middle, and Garo Hills in the west. From the Jaintia to Garo Hills, the $\delta^{34}\text{S}_{\text{TS-V-CDT}}$ ranges from -21.2‰ to +1.7‰ ($\Delta\delta^{34}\text{S}_{\text{TS-V-CDT}} = 22.9\text{‰}$), -10.0‰ to +18.0‰ ($\Delta\delta^{34}\text{S}_{\text{TS-V-CDT}} = 28.0\text{‰}$), and -8.9‰ to -4.5‰ ($\Delta\delta^{34}\text{S}_{\text{TS-V-CDT}} = 4.4\text{‰}$), respectively. Similarly, the $\delta^{34}\text{S}_{\text{Py-V-CDT}}$ varies from -29.3‰ to +6.2‰ ($\Delta\delta^{34}\text{S}_{\text{Py-V-CDT}} = 35.5\text{‰}$), -21.7‰ to +27.1‰ ($\Delta\delta^{34}\text{S}_{\text{Py-V-CDT}} = 48.8\text{‰}$), and -12.1‰ to -3.7‰ ($\Delta\delta^{34}\text{S}_{\text{Py-V-CDT}} = 8.4\text{‰}$), respectively, in these three hills. The isotopic signatures of the Garo coals suggest sulfur contribution mainly from the parent paleobiota and possibly from sulfides derived from primary sulfate within oxic conditions in a freshwater environment. Sr/Ba values averaging 0.5 and Th/U values > 2.0 further complement the freshwater peat deposition in the Garo Hills. Meanwhile, isotope variations in the Jaintia and Khasi coals indicate bacterial sulfate reduction of sourced seawater sulfate under reducing conditions. Moreover, isotopically depleted pyritic sulfur in the Jaintia coals possibly formed in the water column/near the sediment-water interface (open system). However, mixed $\delta^{34}\text{S}_{\text{Py-V-CDT}}$ values in the Khasi coals imply pyrite formation near the sediment-water interface and deeper in the sediments (open and close hybrid system). Additionally, the presence of microscopic framboidal pyrite (FP) and polyframboids, Sr/Ba values > 0.5, and average Th/U ratios close to 2.0 in the Jaintia samples indicate the marine-influenced euxinic-anoxic depositional environment. Nevertheless, the presence of euhedral pyrites with the alleviated FP in the Khasi coals and their complete absence in the Garo coals may suggest dysoxic-suboxic and suboxic-oxic depositional conditions, respectively. Moreover, an amplified inertinite content ($I^{\text{mmf}} = 9.77\text{--}33.16 \text{ vol.}\%$), possibly induced by atmospheric peat exposure, supplements the suboxic-oxic paleomire in the Garo Hills. Besides, gradually depleting mineral matter content from the Jaintia (13.60 vol.%) to Garo coals (7.36 vol.%) additionally projects a transition from mesotrophic (marginal marine) to raised bog environment (terrestrial), complementing the shift in the paleomire condition of Paleogene coals from eastern (Jaintia) to western (Garo) Meghalayan Hills.

Organic facies variability and paleoenvironmental characterization of the Codó and Itapecuru Formations (Aptian-Albian) of Parnaíba Basin, Brazil

Danielle M. de Lima^{1*}, João G. Mendonça Filho¹, Carolina Fonseca^{1,2},
Antônio D. de Oliveira¹, Joalice de Oliveira Mendonça¹, Paula A. Gonçalves^{1,3}

(1) Laboratório de Palinofácies e Fácies Orgânica (LAFO) da Universidade Federal do Rio de Janeiro, Brazil;
(2) Universidade de Coimbra, MARE – Centro de Ciências do Mar e do Ambiente, ARNET- Aquatic Research Network, Portugal; (3) Instituto de Ciências da Terra – Pólo da Faculdade de Ciências da Universidade do Porto, Portugal

* Corresponding Author: danimarques@lafo.geologia.ufrj.br

The transition between Aptian and Albian stages of the Lower Cretaceous (~113 Ma) in the Parnaíba Basin (NE Brazil), represented by the Codó and Itapecuru formations, was a critical moment in the development of the proto-South Atlantic Ocean. During this time, deposition of lacustrine, shallow marine and fluvio-lacustrine sediments occurred in a large sag-type basin. The objectives of this study is the characterization of the organic matter (OM) of the succession of the 2-TV-1-MA borehole (270 m) for paleoenvironmental interpretation and evaluation of the thermal maturity of the OM by organic petrology and organic geochemistry techniques. The sedimentary succession was divided into 4 depositional systems according to the organic facies variability: (i) the base of the sequence represented by a freshwater lacustrine system (262.65-202.2 m); (ii) the lower middle section (201.75-159.6 m) a sabkha system with the deposition of microbial mats; (iii) the upper middle section (156.4-131.7 m) a deltaic system with incipient marine influence; and, (iv) the upper part of the borehole (112.7-28.1 m) with the emplacement of a fluvio lacustrine system. This study indicates that, in the study area, the deposition of the Codó Formation occurred, initially, in a lacustrine system, which evolved into a hypersaline lacustrine system and later into a fluvial system. The identification of dinoflagellate cysts, *Subtilisphaera* genus, and foraminiferal test-linings corroborated the hypothesis that the first marine incursions probably occurred at the initial stages of deposition of the Codó Formation, possibly from the Tethyan domain (Central Atlantic). The OM of the Itapecuru Formation is characterized by the occurrence of phytoclasts, corroborating previous palynological studies that suggest the development of vegetation during a significant period of its sedimentation, in this area. The organic matter is thermally immature, with vitrinite reflectance ranging from 0.37 to 0.52%VRr.

Acknowledgements: The authors gratefully acknowledge the research and development project “Correlação estratigráfica, evolução paleoambiental e paleogeográfica e perspectivas exploratórias do Andar Alagoas”, sponsored by Shell Brasil Petróleo Ltda, with resources allocated to R&D institutions accredited by the Brazilian National Agency of Petroleum, Natural Gas and Biofuels – ANP (technical cooperation agreement #20219).

**Organic petrographical features of Meliadi-Moschopotamos Miocene lignite,
Macedonia, northern Greece**

Polla Khanaqa^{1*}, Stavros Kalaitzidis², Walter Riegel³

(1) Kurdistan Institution for Strategic Studies and Scientific Research, Sulaimani, Kurdistan, Iraq;
(2) Department of Geology, University of Patras, 26504 Rio-Patras, Greece; (3) Georg-August-Universität
Göttingen, 37077 Göttingen, Germany

* Corresponding Author: polla.khanaqa@kissr.edu.krd

This study presents the organic petrographical features of a lignite deposit, located in Northern Greece, and outcropping between the villages of Meliadi and Moschopotamos, approximately 24 km northwest of Katerini town.

The studied profile at Meliadi consists of a ~20 m thick lignite-bearing sequence; samples were obtained for sedimentological and petrographical examinations. Two main seams are recognized, the lower one being 5 m thick and the upper with 1.5 m thickness, being separated by 12 m of inorganic strata. The age of the lignite is Miocene, as defined by palaeontological studies.

The lower seam is of matrix lithotype, black in colour and macroscopically displays a quite strong gelified texture with luster appearance; furthermore, in many parts it reveals a laminated structure. Maceral analysis of the lower seam indicates that detrohuminite is the predominant maceral subgroup, although the macerals of gelinite and particularly alginite are quite elevated, with the latter reaching up to 40%. The enriched mode of liptinite classifies the lignite seam as a sapropelic (boghead) coal. The average huminite reflectance is of 0.35%, fitting well with the Miocene age.

In terms of palaeoenvironmental conditions the data supports a subaquatic limnic environment for the lower seam, with significant accumulation of algae mats, under reducing conditions, as the elevated pyrite content also indicates. On the contrary, the upper seam displays both matrix and xylite-rich lithotypes, although the latter in minor extent, with detrohuminite being the prevailed maceral sub-group; the liptinite content is quite low, with cutinite being the predominant maceral of this group. The overall data points to a more deltaic-limnotelmatic palaeoenvironmental setting for the upper seam than the lower one.



**Mineralogy and organic petrography of the No. 6 coal seam, Soutpansberg Coalfield,
South Africa: Evidence for hydrothermal activity**

Sanki Biswas, Nicola J. Wagner*, Ofentse M. Moroeng

Department of Geology, University of Johannesburg, PO Box 524, Auckland Park 2006, South Africa

* Corresponding Author: nwagner@uj.ac.za

The Soutpansberg Coalfield is a Karoo-aged intracratonic rift basin in South Africa's Limpopo Province. This study aims to assess samples from the No. 6 coal seam in the Makhado and Voorburg south area of the Soutpansberg Coalfield to determine the peat-depositional conditions, organic matter provenance, and their relation to paleoclimate and tectonic setting based on coal-petrography, mineralogical and SEM-EDX analyses. The coals are classified as medium-rank bituminous coal, with high ash yield (avg. 36.08 wt%; db). Ash yields display increasing trends from the middle upper (MU) to bottom lower (BL) part of the seam, while fixed carbon content values decrease. The maceral composition indicates that most samples are rich in vitrinite (~62%), with some inertinite (~10%) and very low liptinite (~1.4%). However, BL and BU in one core from the Makhado valley area are marked by very high inertinite (avg. 64%) and low vitrinite (avg. 7.3%). The patchy occurrence of inertinite macerals indicates high oxidation conditions or forest fires in peatmire at certain times. The coal facies diagrams indicate that precursor peat of the No. 6 seam started accumulating under mesotrophic hydrological conditions with a limited oxygen supply and low degree of degradation. Megathermal terrestrial plants might be the major component of the vegetation and the peatmire was formed under mildly oxic-to-anoxic wet-forest conditions.

The mineralogical composition indicates that inorganic matter in coal is mostly composed of quartz, kaolinite, siderite, muscovite, dolomite, calcite, and pyrite. The Al_2O_3/TiO_2 ratio shows that clay minerals are derived from felsic igneous rocks of granite or granodiorite composition. The Al-Fe-Mn ternary plot suggests some influence of hydrothermal activity in the post mire as the sample has an $Al/(Al + Fe + Mn)$ value of < 0.4 and $(Fe + Mn)/Ti$ value > 15 . The presence of massive porphyritic-type pyrite in the coal also indicates they may be formed by hydrothermal mineralization instead of sedimentation, strongly indicating the occurrence of hydrothermal activity. The SEM-EDX analyses denoted that As, Ni, Pb, and Co are associated with pyrite. Enriching these elements in coal might be terrigenous during sedimentation/peatification, and/or hydrothermal fluids during igneous intrusion emplacement. The chemical index of weathering (CIW) and chemical index of alteration (CIA) range from 92.04 to 97.66 (avg. 95.40) and 98.25 to 99.67 (avg. 99.26), respectively. The geochemical indices like CIA, CIW, A-CN-K ternary diagram, and SiO_2 vs $\log(K_2O/Na_2O)$ plot show that the paleoclimate conditions were warm and the coal component suffered strong chemical weathering, under passive continental margin depositional environment supporting luxurious vegetation and organic matter preservation. The inferred tectonic setting is consistent with tectonic events seen in East and Central Africa during the Carboniferous to the Permian period.

Petrological, mineralogical and geochemical proxies to the organic matter dispersed in the sedimentary rocks in Turgut area, Yatağan Basin, SW Türkiye

Zeynep Büçkün*, Mümtaz Çolak

Department of Geological Engineering, Dokuz Eylül University, 35390 Buca-İzmir, Türkiye

* Corresponding Author: zeynep.buckun@deu.edu.tr

The 30-km-long and 10-km-wide, coal-bearing Yatağan Basin is located in SW Anatolia, close to the eastern coast of the Aegean Sea, Türkiye. In the NW part of this intermontane basin, the Turgut lignite deposit is hosted occupying a *c.* 80-km²-large area and containing a mineable seam up to 15 m thick. The basement consists of Menderes Massif metamorphites, whereas the Neogene and Quaternary sedimentary filling comprises fluvioterrestrial, limnic and telmatic sediments unconformably overlain the basement. In the northern sector of the Turgut deposit, where the coal seam is *c.* 210 m deep, silicate-rich sedimentary rocks are dominant, whereas in the southern sector, where the coal depth is *c.* 490 m, carbonate-rich rocks are common. The mineable coal seam is distinguished in two beds; the upper one has a mean net calorific value of around 14.5 MJ/kg (on moist, ash-free basis; maf), whereas the lower bed displays slightly lower values (13.5 MJ/kg, maf).

Eight samples obtained from the inorganics over- and underlying the coal seam from four borehole cores, were examined firstly under both the optical microscope, later under the coal-petrography microscope under both incident white light and blue-light excitation. Moreover, XRD, SEM-EDX and ICP-MS analyses were performed to all the core samples. The aim of the study was to examine the dispersed organic matter hosted in the sedimentary rocks in respect of the type and rank along with the diagenetic processes the sedimentary rocks underwent at various depths.

The inorganic sedimentary layers overlying the coal, are of fluviolacustrine origin, whereas the underlying ones are of lacustrine. All the samples obtained from the northern part consist of mainly quartz, feldspar, mica and clay minerals, whereas, calcite, dolomite and aragonite are dominant in these from the southern part. The -2 µm fraction of the samples consists of illite with a less amount of smectite and kaolinite.

The organic matter dispersed in the samples is, in overall, rare. The samples obtained from the coal-overlying strata, include mainly gelohuminite with a minor amount of telohuminite, some cutinite and liptodetrinite; moreover, in the southern deposit sector, inertinite macerals and framboidal pyrite along carbonates are also contained. The random reflectance (R_r) value of eu-ulminite B is around 0.34%. The samples picked up from the underlying strata, include mainly sporinite and alginite (displaying an orange fluorescence), reworked huminite macerals, and framboidal pyrite; in the northern deposit sector carbonates are lacking, whereas in the southern sector liptodetrinite and carbonates are common. The huminite reflectance is *c.* 0.22%. Well-preserved diatom frustules were identified in only one carbonate-rich sample from the deepest part of the basin, pointing to a fluviolacustrine depositional environment.

Contribution of organic petrography in the study of volcanoclastic sequences: The case of West Acrocheiras section, Petrified Forest of Lesvos, Greece

Penelope Papadopoulou^{1,2*}, George Iliopoulos¹, Konstantinos Perleros¹, Stavros Kalaitzidis¹, Kimon Christanis¹, Nikolaos Zouros^{2,3}

(1) Department of Geology, University of Patras, Greece; (2) Natural History Museum of the Lesvos Petrified Forest, Sigri, Greece; (3) Department of Geography, University of the Aegean, Mytilene, Greece

* Corresponding Author: cperleros@gmail.com

The Petrified Forest of Lesvos Island is a Natural Monument and a geosite of international value within the Lesvos Island UNESCO Global Geopark (Greece). Silicified tree trunks, branches and leaves are included at several stratigraphic levels of Sigri Pyroclastic Formation, which consists of several hundred-meter-thick Miocene tuffs and other volcanoclastic sediments intercalating with palaeosoil layers. Six organic-rich samples were obtained from three palaeosoil layers outcropping at a road-cut section and examined conducting maceral analysis and measuring huminite/vitrinite reflectance, in order to acquire information regarding their origin and depositional conditions. This study is ongoing.

In the lower palaeosoil layer, the huminite macerals, mainly ulminite and text-ulminite, display plasticized edges, as an evidence of heat influence. Charred particles being disseminated within the same palaeosoil layer, contain mostly telinite/collotelinite and macrinite. Exposure to heat is evident through desiccation cracks, darker rims and plasticized edges. Macrinite displays cracks and devolatilization pores; it is surrounded by framboidal pyrite of authigenic origin. Huminite mean reflectance is 0.47%, whereas the charred particles (fusinite) display values from 0.7-1.0%.

In the middle layer a black horizon is hosted including large cellular tissues (telinite-like) and detrovitrinite. Plasticized edges point to exposure to heat. Mean vitrinite reflectance is 0.85%. In the same strata, charred particles with thin cell walls (fusinite) are evident of heat affection with cracks, plasticized edges and devolatilization pores. Reflectance values can be distinguished in three groups: fusinite with values 1.1-1.4%, macrinite originating from corphuminite, 0.8-1.0% and the brownish inertodetrinite with 0.5-0.6%. This complies with the second char sample of similar characteristics and reflectance values (0.88-1.12%).

The upper layer consists of mainly carbonaceous particles. Altered telinite/collotelinite A and B are dominant; they display occasionally plasticized edges and desiccation cracks. In fluorescence mode alginite and cutinite are identified; vitrinite A has a weak brown fluorescence. The reflectance of vitrinite A is 0.5% and this of vitrinite B 0.65%. The organic matter in this layer may be deposited in a short-lasting telmatic/limnotelmatic environment, which later was affected by the heat of the overlying pyroclastics.

Summing up, the organic-rich samples from the lower and the middle layers reflect biomass grown and accumulated *in situ*, later being thermally affected at various degrees, whereas detrital input of chars from wildfires in the surrounding took place. The upper layer was deposited as peat, coalified and partially charred by the influence of the pyroclastics on top.



Joint 74th ICCP and 39th TSOP Meeting
17th – 24th September 2023, Patras, Greece

**Organic Petrology in the Energy Transition Era:
Challenges ahead**



Bulletin of the Geological Society of Greece, Sp. Publ. 12

Abstracts of Posters

Petrographic composition of Las Conchas Mire in relation to palaeoclimate proxies

Angeles G. Borrego¹, José E. Ortiz², Yolanda Sánchez-Palencia²,
José L.R. Gallego³, Trinidad Torres²

(1) Instituto de Ciencia y Tecnología del Carbono (INCAR-CSIC), Oviedo, Spain; (2) Biomolecular Stratigraphy Laboratory, ETSIME, UPM, Madrid, Spain; (3) INDUROT and Environmental Biogeochemistry & Raw Materials Group, University of Oviedo, Mieres, Spain

* Corresponding Author: angeles@incar.csic.es

The Las Conchas Mire, at the base of the Cuera Range in Northern Spain, has been regarded as an example of a peatland, where the palaeoclimate variations are obscured by the continuous water runoff — even during drier periods —, the latter being not necessarily accompanied by additional mineral input (Ortiz et al., 2016). The 320-cm-thick, bryophyte-dominated profile covers a time span of 8000 cal yr BP.

The petrographic study of the samples reveals that huminite macerals dominate the profile with liptinite and inertinite yielding typically contents below 3%, except in the bottommost area, where higher content of both maceral groups is observed. This section is also characterized by a fast increase in ash yield towards the bottom, and lower ratio textinite/atrinite representing the phase of depression filling. Once ombrotrophic conditions were established, the maceral composition became more stable.

The major component throughout the profile is textinite indicating a high level of tissue preservation as also inferred from predominance of long chain *n*-alkanoic acids. Three maceral varieties have been counted for textinite (0, A and B) with 0 representing the closest appearance to recent tissues and B the most humified material. The predominant textinite is the A variety, exhibiting high intensity yellow-orange fluorescence. Higher amount of textinite 0 has been recorded in the upper 60 cm of the peat profile suggesting less humified material. The uppermost 20 cm of the profile are clearly enriched in atrinite resulting from tissue destruction in agreement with a drop of the C/N ratio, a bimodal distribution of the *n*-alkanoic acids with significant presence of short-chain homologues attributed to microbes. This is explained as the result of the mire transformation into a meadow through drainage in the last ca. 200 yr.

The homogeneity of the maceral composition throughout the profile supports the findings based on organic geochemical proxies, which suggest a peat profile accumulated during humid periods with short drier periods determined more by the geomorphological setting than the palaeoclimate conditions.

Acknowledgements: Financial support through the projects CGL2013-46458-C1-1-R, and CGL2013-46458-C2-2-R from CICYT is gratefully acknowledged.

Reference

Ortiz JE, Borrego AG, Gallego JLR, Sánchez-Palencia Y, Urbanczyk J, Torres T, Domingo L., Estébanez B., 2016. Biomarkers and inorganic proxies in the paleoenvironmental reconstruction of mires: The importance of landscape in Las Conchas (Asturias, Northern Spain). *Organic Geochemistry* 95, 41-54.

Reconstruction of peat-forming paleoenvironments within the Oligocene Bobov Dol Basin, SW Bulgaria: Insights from organic petrology

Alexander Zdravkov^{1*}, Achim Bechtel², Doris Groß², Ksenija Stojanović³

(1) University of Mining and Geology, Sofia, Bulgaria; (2) Montanuniversität, Leoben, Austria;
(3) University of Belgrade, Serbia

* Corresponding Author: alex_zdravkov@mgu.bg

Up to fourteen sub-bituminous coal beds are hosted within the Oligocene Bobov Dol Basin. Among them, six (numbered I to VI from base to top) are considered economically significant. In this study, ninety samples from five of the main seams (I-V) and a locally mined sub-seam (I^a) were characterized by maceral analysis and ash yield determination. The coal is composed of huminite (avg. 86.6 vol.%), liptinite (avg. 17.5 vol.%) and minor inertinite (avg. 1.5 vol.%). Maceral composition is dominated by gymnosperm-derived telohuminite (up to 72.0 vol.%) with resinite (up to 28.0 vol.%) and exsudatinitite (up to 16.0 vol.%) cell infillings, embedded in attrinitic (avg. 21.0 vol.%) or densinitic (avg. 17.0 vol.%) groundmass. Most samples also contain abundant leaf-derived huminite (phyllo-huminite, up to 29.0 vol.%) in association with cutinite (up to 8.0 vol.%) and fluorinite (up to 5.0 vol.%). Low to moderate ash yields (< 25 wt.% for most samples) coupled with low to moderate values of the maceral indices, namely TPI < 3 (for ~80% of the samples) and GI < 3 (for >53% of the samples), and low values of the GWI < 1 (for 81% of the samples), denote organic matter deposition within an oligo- to mesotrophic topogenous mire with (ground)watertable beneath the peat surface. Reconstruction of paleoenvironmental settings based on maceral analysis (Fig. 1) argues for plant matter accumulation under marginal aquatic (seam I^a) and moderately wet- to dry-forested mires (seams I-V). Abundance of resinite and fluorinite-rich (phyllo-)huminite indicates development of conifer-dominated forests (likely deciduous gymnosperms), perhaps within a background of herbaceous plants and/or deciduous shrubs. The data is compatible with the previously reported preliminary organic geochemical data for part of the seams (Zdravkov et al., 2021).

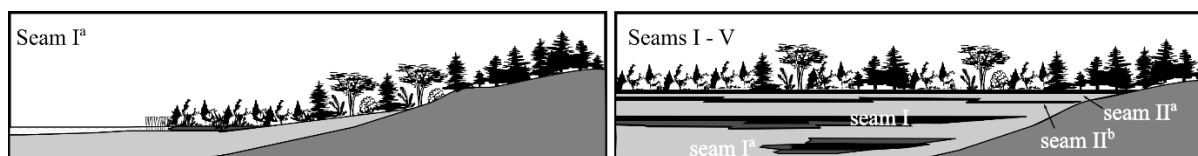


Figure 1. Schematic diagram representing presumed environmental settings during peat formation.

Acknowledgements: Financial support from BNSF through project KP-06-H64/5/2022 is greatly appreciated.

Reference

Zdravkov, A., Bechtel, A., Gross, D., Stojanović, K.A., 2021. Peat-forming depositional environments within the Oligocene Bobov dol Basin, SW Bulgaria. In: Abstract Book, 37th TSOP Annual Meeting (Sofia, 12-14 September, 2021). pp. 123–125.

Paleoenvironmental settings of peat formation within Padesh Graben, SW Bulgaria, deduced from maceral analysis and geochemical properties of Suhostrel Coal

Alexander Zdravkov^{1*}, Doris Groß², Achim Bechtel², Ksenija Stojanović³, Ivan Kojić⁴

(1) University of Mining and Geology, Sofia, Bulgaria; (2) Montanuniversität, Leoben, Austria; (3) University of Belgrade, Serbia; (4) Innovative Centre, Faculty of Chemistry, Belgrade, Ltd.

* Corresponding Author: alex_zdravkov@mgu.bg

Three 0.2-0.6 m thick coal seams, representing seam splits from a locally thicker seam (~1.8 m), comprise the Eocene Suhostrel coal deposit from the S-SW margin of the E₁₋₂-O₁ Padesh Graben. High TOC contents (avg. ~86 wt.%, daf), VR (avg. Ro = 1.05%) and T_{max} (avg. 457°C), argue for high vol. A/medium vol. bituminous coalification rank. Maceral composition is dominated by vitrinite (avg. ~95 vol.%), represented by detrovitrinite (e.g., collodetrinite, avg. 37.5 vol.%, and vitrodetrinite, avg. 19.2 vol.%) and collotelinite (avg. 38.0 vol.%, mostly gelified leaf-derived tissues, e.g. phyllo-vitrinite). Liptinite (avg. ~5 vol.%) includes cutinite and microsporinite. Predominance of mid- and long-chain *n*-alkanes argues for peat formation from a mixture of aquatic macrophytes and terrestrial vascular plants. Low Vegetation Index values (VI = 0.1-3.2, avg. 0.8; Calder et al., 1991) denote major organic matter contribution from vegetation with poor preservation potential. This is compatible with the presence of oleanane, confirming input from angiosperm plants. The absence of resin-derived sesqui- and diterpenoid hydrocarbons argues for an insignificant role of conifers during peat formation. Reconstructed depositional settings (Fig. 1) argue for organic matter deposition under marginal aquatic, marsh/fen-type peatland with meso- to rheotrophic characteristics (Groundwater Index, GWI = 0.3-7.2, avg. 1.4; Calder et al., 1991). High mineral matter contents (ash yields 21-47 wt.%) imply hydrologically active environment with frequent (perhaps seasonal) changes in Eh settings. Low concentrations of hopanoid biomarkers imply limited aerobic degradation of the plant remains. Post-depositional marine influence and downward infiltrating sulfate-rich waters are considered responsible for the presence of dibenzothiophene and its methylated derivatives.

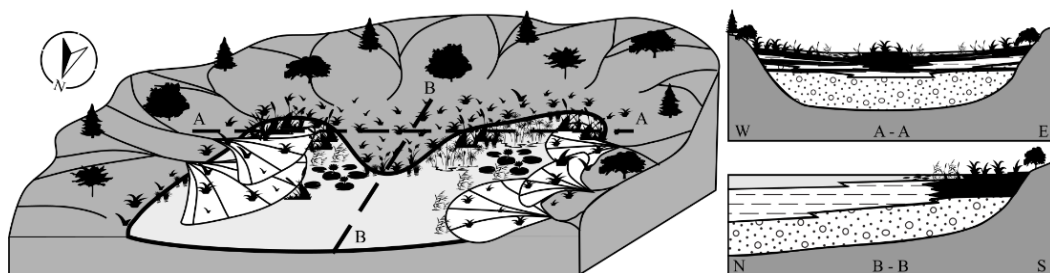


Figure 1. Schematic diagram representing presumed environmental settings during peat formation.

Acknowledgements: Financial support from BNSF through project KP-06-H64/5/2022 is greatly appreciated.

Reference

Calder, J.H., Gibling, M.R., Mukhopadhyay, P.K., 1991. Peat formation in a Westphalian-B piedmont setting, Cumberland Basin, Nova Scotia: implications for the maceral-based interpretation of rheotrophic and raised paleomires. *Bull. Soc. Geol. France* 162, 283-298.

Mineral matter content, distribution, and characteristics of the Ukhaakhudag coal deposit, Mongolia

Batbold Demberelsuren^{1*}, Luvsanchultem Jargal², Said Lkhagva-Ochir¹,
Bat-Orshikh Erdenetsogt², Ranjin Ganzorig¹, Tserennadmid Zorigbold¹, Otgonjargal Tugj¹,
Tumuruu Khash-Erdene¹, Jargal Otgonbaatar¹

(1) Ukhaakhudag coal mine, branch of “Energy Resource” LLC; (2) National University of Mongolia

* Corresponding Author: demberelsuren.b@mmc.mn

The Ukhaakhudag coal deposit lies in Tavantolgoi Basin in South Gobi coal-bearing region, Southern Mongolia. The coal seams are hosted in middle Permian coal-bearing Tavantolgoi Formation. In total, 14 coal seams and 49 coal plies were discovered in this deposit. The coal qualities of the seams are distinguishable, and some seams have coking properties. At the mine site, coal seams are blended and washed by using heavy medium cyclone, spiraling, and froth flotation methods. However, Seam 0 is washed with difficulty and the ash yield of washed Seam 0 exceeds the acceptable level. This high ash yield is probably due to minerals in the coal.

To test this prediction, 13 coal samples from Seam 4 (4C first order ply) and Seam 0 (0AU, 0BR and 0CL second order plies) are studied for mineral matter and its distribution. Seam 4 has good coking properties and is simple to wash; thus, samples from this seam were included in this study to compare with samples from Seam 0. We slightly modified the standard method to determine the mineral matter content of Ukhaakhudag coal. The modified method includes counting grains in two major categories: 1) minerals associated with macerals (fracture-, cell- and pore-filling minerals), and 2) single mineral grains. The grains were classified and counted into 15 categories, such as single mineral grains (quartz, pyrite, carbonates, clay minerals, etc.), which are not associated with macerals, and as quartz, pyrite, carbonates, clay minerals, etc., which filled fractures, cellular cavities, and pores/voids of macerals.

The results reveal that the contents of single minerals and grains of minerals associated with macerals are approximately one and two times higher in the coals from the Seam 0 (0AU, 0BR and 0CL second order plies) than in the coals from Seam 4 (4C first order ply). The content of clay minerals associated with macerals in the coals of the Seam 0 (0AU, 0BR and 0CL second order plies) is relatively high compared to the coals of the Seam 4 (4C first order ply). Clay minerals are distributed in the studied coals, mainly in collodetrinite, filling pores/voids or forming thin layers. Carbonates mainly fill the cell voids of semifusinite, small amounts of collodetrinite pores/voids, and rarely telinite and fusinite cell voids. The content of carbonates associated with macerals is similar (20–60 vol.%) in the coals of the 0AU, 0BR and 4C first, second order plies), whereas it is relatively low in the coals of 0BR second order ply. The content of pyrite associated with macerals is slightly higher in sample 0AU_4 from the upper part of the 0AU second order ply and in samples 4C_2 and 4C_3 from the middle part of the 4C first order ply. Pyrites associated with macerals in the coals from 0AU, 0BR and 0CL second order plies mainly filling fracture in collodetrinite, filling cell. Rarely, the size of the pyrite's grain grows, it is occurred in the framework (appears at the OAU second order ply). In the coals from 4C first order ply, pyrites associated with macerals appear as fine-grained concretions, filling the voids of collodetrinite.

**The coal beds between Obomkpa and Iseele-Azagba from Southern Nigeria:
A petrographical, mineralogical and geochemical approach**

Jude E. Ogala^{1*}, Konstantinos Perleros², Evangelia Kyriazaki², Michalis Aggelopoulos²,
Omabehere I. Ejeh¹, Stavros Kalaitzidis², Kimon Christanis^{2*}

(1) Department of Geology, Delta State University, Abraka, Nigeria; (2) Department of Geology,
University of Patras, Greece

* Corresponding Author: christan@upatras.gr

Twenty-eight (8 organic-rich and 20 inorganic sediment) core samples obtained from six boreholes spread over a *c.* 60-km²-large area in the alluvial plain of Niger River between Obomkpa and Iseele-Azagba, southern Nigeria, were examined and evaluated by means of coal petrography, mineralogical (XRD) and geochemical (XRF) analyses. The aim of this study was to determine the palaeoenvironmental conditions and to reconstruct the depositional setting.

As the samples were received a long time after sampling, moisture could not be determined. The ash and the volatile matter yields of the coal samples vary from 19.9-88.5% (db) and 63.5-67.9% (daf), respectively. Huminite is the dominant maceral group ranging from 60.6-90.6 vol.% (on mineral matter-free basis), with detrohuminite being the major sub-group. Attrinite ranges between 8.4 and 45.8% and densinite from 15.3-43.5%. Ulminite displays values from 18-41.9%, textu-ulminite from 3.1-22.3%, and textinite very low values (<2.8%). Gelohuminite, mainly copohuminite, appears at concentrations <11.5%. The inertinite content is very low (<1.5%). Liptinite macerals are also rare (<6.5%) with cutinite being the most common (<3.7%). The high huminite and low liptinite contents of all the coal samples prove their humic origin. The mean random huminite reflectance of all the coal samples varies between 0.32% and 0.39%.

As sand and kaolin are the main sediments filling in the alluvial plain, the inorganic part of all the studied samples consists of mainly quartz and kaolinite; gypsum, muscovite and sanidine are contained in minor amounts. Accordingly, SiO₂ and Al₂O₃ display values ranging from 15.9-58.4% and up to 21.7%, respectively, followed by Fe₂O₃ (up to 8.8%) and TiO₂ (up to 2.3%). All samples are depleted in the elements Cr, Cu, Ni, Rb, Sc and Sr, and enriched in Ba, Ce, Hf, La, Nb, Pb, V, W, Zn and Zr, when compared with the average values of the continental crust. The contents of all elements, excluding Sr and Y, exceed the values determined for low-rank coals worldwide.

Facies diagrams based on the maceral contents were applied to reconstruct the environmental conditions in the palaeomires. According to the TPI *vs.* GI diagram, the peat-forming vegetation was mostly herbaceous yielding low TPI and medium GI values, and the conditions were limnotelmatic. The GWI *vs.* VI diagram points to herbaceous vegetation on the palaeomire surface and mesotrophic water conditions with intense mineral matter influx from palaeo-Niger River. The area received frequent rainfall along with flooding episodes; thus, peat remained water-logged. Within the several hundred meters thick alluvial sediments, only short periods of limnotelmatic conditions prevailed in the area, yielding coal beds less than 10 m thick. The small number of the available cores distributed over a large area does not allow a more detailed palaeoenvironmental reconstruction.

**Signature of wildfires in soils using organic petrology and geochemistry:
Case studies from Portugal**

Rui Melo^{1*}, Eric Font^{1,2}, Joana Ribeiro^{1,2}

(1) University of Coimbra, Department of Earth Sciences, Coimbra, Portugal; (2) University of Coimbra, Instituto Dom Luiz, Coimbra, Portugal

* Corresponding Author: joana.ribeiro@uc.pt

Wildfires are responsible for the formation of charred organic particles that are deposited and incorporated in soil and/or mobilized to water bodies. The incomplete combustion of biomass is known as a source of polycyclic aromatic hydrocarbons and mercury (Hg) that can be emitted to the atmosphere and be retained in the fire-derived materials in soil, impacting the environment. Moreover, the fire-derived organic matter affects carbon forms and budget in soils, thus playing a role in the carbon cycle. The composition and properties of fire-derived organic matter in soils: i) influence the long term fate and impact of carbon compounds in the environment (e.g., mobilization, degradation, reactivity, stabilization, preservation); and, ii) depend on the fire intensity, which in turns depends on many factors such as type and abundance of biomass, soil properties and atmospheric conditions. This research aims to identify and characterize the organic matter in soils affected by wildfires, contributing to predict potential environmental impacts, incorporation of pyrogenic carbon in the geological record, and fire intensity and its spatial variation. The Hg content of the samples was also determined. This knowledge can be useful in the study of paleofires and their signature in the geological record, as well as in the identification of actions towards mitigation and adaption to climate change. Two wildfires that occurred in Portugal were considered in this study (Pedrogão Grande in 2017; Condeixa-a-Nova in 2022). Soil samples were collected at different depths in burned and unburned areas. The <2 mm fraction was used to prepare polished sections and to measured Hg concentration. The preparation of polished sections and petrographic observations followed the methodologies proposed for the petrographic analysis of coal and dispersed organic matter. Mercury was measured by atomic absorption spectrometer. The results demonstrate the presence of recent and fossil soil organic matter in the unburned areas. The petrographic observation of soils from burned areas allows the identification of non-affected and thermally affected soil organic matter as well as fire-derived particles from the deposition and incorporation of charcoal from biomass combustion. The fire-derived particles have different degrees of alteration evidencing the heterogeneity of the fire intensity across the burned areas. The Hg concentration is generally lower in soils from burned areas, evidencing volatilization during the fire. The petrographic examination of soil proved to be an effective tool to study the effects and changes induced by wildfires in soil, thus affecting their composition and quality, and consequently the land use capacity, and it also gives information about the signature left by wildfires in the geological record.

Acknowledgements: This work was funded by the Portuguese Fundação para a Ciência e a Tecnologia (FCT) I.P./MCTES through national funds (PIDDAC) - UIDB/50019/2020-IDL; PTDC/CTA-GEO/0125/2021; MIT-EXPL/ACC/0023/2021.

Petrographic identification of contaminant particles in soil around a coal-fired thermal power plant (Sines, Portugal)

Joana Ribeiro^{1,2*}, Mónica Ribeiro¹, José Erbolato Filho^{1,3}

(1) University of Coimbra, Department of Earth Sciences, Coimbra, Portugal; (2) University of Coimbra, Institute Dom Luiz, Coimbra, Portugal; (3) University of Coimbra, Natural Radioactivity Laboratory, Coimbra, Portugal

* Corresponding Author: joana.ribeiro@uc.pt

The industrial use of fossil fuels is a human activity affecting soil and the carbon-cycle in the vicinity of utilization facilities. The combustion of coal for power generation is a known source of contaminants that may pose risk to soils. Once in the soil, contaminants can be concentrated or mobilized back to the atmosphere, made available to biota, leached to surface water bodies and aquifers, or transported to other areas by soil erosion. This research aims the petrographic identification of contaminants particles in soils nearby Sines coal-fired thermal power plant, in Portugal, which was recently decommissioned. This site was selected for study because the industrial activity based on coal combustion lasted for decades, between 1985-2021, and during this period the impact on soil in the surrounding area was never investigated. Besides, it is located in an environmentally sensitive area since it is adjacent to a natural park and to the coast of Atlantic Ocean. According to the geological context, the natural soil occurring in the area is classified as arenosol. A total of 27 superficial soil samples (from 0 to 10 cm depth after removal of vegetation debris and gravel) were collected around the outer limit of the entire complex of the power plant facilities. Field observations during sampling reveal that some ash could be mixed with soil or buried in some restricted places in the sampled area and, in these cases, the distinctive material was also collected. One sample was collected farther (≈ 750 m) to the study area but with the same geological background, representing a local reference sample. After sieving, the sample fraction finer than 2 mm was used to prepare polished blocks. The microscopic observations were performed under incident white light and with an oil immersive objective. The identification of organic particles followed the ICCP nomenclature. The petrographic analysis of the reference soil sample allows the observation of organic matter particles of natural origin together with the mineral matter, principally composed of silicates. The microscopic observation of soil samples allows the identification of contaminant coal particles and combustion-derived particles in some samples (char, amorphous agglomerates, and magnetic and glass spheres), being more abundant in the proximity of old storage and disposal sites of coal and coal combustion by-products, respectively, and the area towards the prevailing wind direction (from N-NW to S-SE). The petrographic study also proved the presence of coal-ash, below the superficial soil layer in a specific and spatially limited place. Further work should include the expansion of the soil sampling grid (either in depth and laterally) to define the spatial extent of the contamination left by the coal use in the decommissioned coal-fired thermal power plant.

Acknowledgements: This work was funded by the Portuguese Fundação para a Ciência e a Tecnologia (FCT) I.P./MCTES through national funds (PIDDAC) - UIDB/50019/2020-IDL.

Mineralogical, chemical and petrographical investigation of airborne dust material nearby coal-fired power plants: A case study from Upper Silesia, Poland

Chrysoula Chrysakopoulou¹, Konstantinos Perleros², Małgorzata Wojtaszek-Kalaitzidi³,
Lambrini Papadopoulou¹, Nikolaos Kantiranis¹, Stavros Kalaitzidis^{2*}

(1) Department of Geology, Aristotle University of Thessaloniki, Greece; (2) Department of Geology, University of Patras, Greece; (3) Institute of Energy and Fuel Processing Technology, Zabrze, Poland

* Corresponding Author: skalait@upatras.gr

The objective of this research focuses on air-borne dust from Knurów region in Upper Silesia, Southern Poland, where one coal mine, two coal-fired power plants and one coal-waste dump site are located. The aim is to determine the environmental impacts from the anthropogenic activities, particularly the fly ash dispersion from the coal combustion in the region. Two samples (KN1 and KN2) collected from a domestic gutter system, were subjected to mineralogical and petrographical examination. Ash yields were determined by combustion at 750°C. Magnetic particles were separated, whereas their morphological appearance and chemical composition were determined by SEM-EDX analysis. The mineralogical composition of the whole sample and the magnetic fraction as well, was determined by applying X-ray diffraction (XRD) on randomly oriented powder samples. Additionally, polished blocks of the samples were examined using standard organic petrography techniques.

The proximate analysis proved 78 wt.% ash yield for KN2 sample, suggesting 22% of fossil and fresh organic matter content. The magnetic fraction for samples KN1 and KN2 accounts for 3.02 and 0.53 wt.%, respectively, whereas the major mineral phase of the magnetic fraction is magnetite, followed by minor amounts of hematite but also quartz and other non-magnetic minerals. The magnetic fraction appears in the form of spheres of simple or complex surface structure. The average size of the magnetic spheres of KN1 and KN2 is 12.74 and 16.11 μm, respectively; they mainly consist of Fe (c. 70 wt.%, on average), while Al, Si, Na and Mn are contained in minor amounts. Additionally, the average Mg content of the magnetic spheres from KN1 is three times higher than of these of KN2; Ca appears only at those of KN2 and K only in those of KN1. According to the mineralogical study of the bulk samples, the major mineral phases for KN1 and KN2 are illite and quartz, respectively, while albite, anorthite, magnetite and hematite are found in minor amounts. Chamosite and orthoclase are also present in KN2 in minor amounts. In terms of the petrographical composition, KN2 sample consists mainly of unburnt coal-particles along with chars, sooty and coke particles, accounting for 40 vol.% of the total organic composition. Fresh residues of immature organic matter account for 10 vol.%, whereas mineral matter for 50 vol.%. The average size of the macerals is ~45 μm, three times higher than the average size of the anthropogenic magnetic spheres. Anthropogenic activities in the study area, particularly both the industrial and the domestic coal combustion leaves behind a significant environmental footprint to the urban site of Knurów region.

First macromolecular characterization of fossil Choanoflagellates

Pjotr Meyvisch^{1*}, Kenneth N. Mertens², Carolina Fonseca^{3,4}, João G. Mendonça Filho³,
Matías Reolid⁵, Luís V. Duarte⁴, Stephen Louwye¹

- (1) Ghent University – Department of Geology Ghent Belgium; (2) Ifremer – LITTORAL, Concarneau, France;
(3) Laboratório de Palinofácies e Fácies Orgânica (LAFO) da Universidade Federal do Rio de Janeiro, Brazil;
(4) Universidade de Coimbra, MARE – Centro de Ciências do Mare do Ambiente, ARNET - Aquatic Research Network, Portugal; (5) Departamento de Geología and CEACTEMA, Universidad de Jaén, Spain

* Corresponding Author: pjotr.meyvisch@ugent.be

Choanoflagellates are microeukaryotes that inhabit freshwater and marine environments and have long been regarded as the closest living relatives of Metazoa. Although molecular clock evidence suggests their appearance by late Neoproterozoic, only recently the first identification of fossil choanoflagellates in sediments from the Cretaceous was made (Fonseca et al., 2023). Here, attenuated total reflection (ATR) micro-Fourier-transform infrared (micro-FTIR) spectroscopy was used to achieve the first macromolecular characterization of single-specimen fossil choanoflagellates, and to assess differences and similarities with dinoflagellate cysts from the same sample. ATR micro-FTIR spectra reveal consistent molecular differences between fossil choanoflagellates and dinoflagellate cysts. Both microfossils are composed of a predominantly hydrogen-cross-linked, aliphatic biomacromolecule, with notable contributions of (probably polycyclic) aromatic rings, aromatic ethers, and phenols. However, choanoflagellates were systematically more aliphatic in nature than dinoflagellate cysts. The generally aliphatic-aromatic compounds in fossil choanoflagellates differ from actin found in modern choanoflagellates (Karpov and Leadbeater, 1998) and a cellulose-like carbohydrate in modern dinoflagellates (Versteegh et al., 2012) and were likely a result of (possibly early diagenetic) molecular alteration due to oxidative polymerization, which is a common taphonomical phenomenon in organic fossils (Gupta and Briggs, 2011). Despite taphonomical effects, a parallel molecular analysis of different fossil organisms from the same sample can reveal chemosystematic signatures and, in this case, highlights a different pre-diagenetic macromolecule present in the analyzed fossil choanoflagellates compared to other microeukaryotes. These results provide a first basis to further decrypt the chemospecific signatures of fossil choanoflagellates using complementary analytical methods, as well as to explore the fossilization and preservation behavior of these primitive metazoans. This is necessary to be able to construct chemotaxonomical arguments which could support established morphological affinities of modern and fossil organisms.

References

- Fonseca, C., Mendonça Filho, J.G., Reolid, M., Duarte, L.V., Oliveira, A.D., Sousa, J.T., Lézin, C., 2023. First putative occurrence in the fossil record of choanoflagellates, the sister group of Metazoa. *Scientific Reports* 13, 1242. <https://doi.org/10.1038/s41598-022-26972-8>
- Gupta, N.S., Briggs, D.E., 2011. Taphonomy of animal organic skeletons through time, in: Allison, P.A., Bottjer, D.J. (Eds), Taphonomy. Aims & Scope Topics in Geobiology Book Series, vol 32, Springer, Dordrecht, pp. 199-221.
- Karpov, S.A., Leadbeater, B.S., 1998. Cytoskeleton structure and composition in choanoflagellates. *Journal of Eukaryotic Microbiology* 45(3), 361-367.



Migration and transformation of uranium during uranium-rich coal combustion

Jiang Wang, Rihong Xiao, Yongchun Zhao, Junying Zhang*

State Key Laboratory of Coal Combustion, School of Energy and Power Engineering, Huazhong University of Science and Technology, Wuhan 430074, China

* Corresponding Author: jy Zhang@hust.edu.cn

Uranium is enriched in fly ash during coal combustion, resulting in increased radioactivity level of fly ash. The accumulation and comprehensive utilization of fly ash cannot be underestimated in terms of radiation hazards to the environment and human body. The recycling and harmless treatment of uranium-rich fly ash can not only greatly reduce radioactive hazards, but also serve as a powerful supplement for nuclide resources. Therefore, it is of great significance to explore the migration and transformation characteristics of uranium in the process of coal combustion for the directed regulation and resource utilization of uranium. A detailed study on typical uranium-rich coal in China have been investigated to focus on the occurrence forms of uranium in coal and ash, and to understand the evolution law of uranium in the process of combustion.

Firstly, Lincang coal in Yunnan Province, China (LC coal) with high uranium content and Shengli coal in Inner Mongolia, China (SL coal) with conventional uranium content were selected as experimental coal samples. Through float-sink density separation test, the occurrence forms of uranium in coal were explored. The results show that uranium in LC coal is mainly combined with organic matter, while uranium in SL coal is mainly combined with clay minerals.

Secondly, the form distribution of uranium in the two coal samples during combustion is simulated by thermodynamic calculation. The thermodynamic calculation results show that uranium and alkali earth metal will form corresponding uranate during combustion.

Finally, the drop tube furnace combustion experiment is designed to study the quantitative release of uranium, the distribution in particulate matter and the micro-zone enrichment. After high temperature combustion in drop tube furnace, uranium will be enriched in coal ash. The uranium content in ash is about twice that in coal. Uranium tends to be enriched in small particle size, and the uranium content in PM₁ can reach 3~10 times of that in PM₁₀₊. Uranium will be enriched on the surface of aluminate, iron oxide and calcium oxide with the polymerization of fine particles. Within the particle, uranium will be randomly distributed in silicaluminate minerals, mainly in Si/Ca/Mg enriched minerals.

Characterization of Fe-bearing morphotypes from coal combustion ash samples targeting their application in catalytic reactions

Ana C. Santos^{1*}, Iwona Kuźniarska-Biernacka², Alexandra Guedes¹, Bruno Valentim¹

(1) Earth Science Institute – Porto pole, Department of Geosciences, Environment and Spatial Plannings, Faculty of Sciences, University of Porto, Rua do Campo Alegre s/n, 4169-007 Porto, Portugal; (2) REQUIMTE/LAQV, Department of Chemistry and Biochemistry, Faculty of Science, University of Porto, Rua do Campo Alegre s/n, Porto 4169-007, Portugal

* Corresponding Author: anasantos@fc.up.pt

Iron is one of the main inorganic constituents of coal and is mostly found associated with mineral phases such as sulfides, sulfates, silicates, and carbonates. During coal combustion, the Fe-bearing minerals undergo through thermochemical transformations and may originate Fe-bearing minerals such as magnetite and hematite, and other Fe-bearing phases when coalescence with melt derived from other minerals present in coal takes place. Previous research showed that these Fe-rich fractions can have several applications, namely as excellent catalysts in 4-nitrophenol reduction reaction (toxic compound usually found in industrial wastewater). Therefore, the recovery of Fe-bearing morphotypes besides being beneficial for ash recycling, may result in value-added products. However, it requires a deep knowledge of Fe-bearing phases properties to assess their potential and further improve the efficiency on the targeted applications. In this work an integrated study was made on bulk samples of coal fly ash magnetic concentrates (MC) and respective pellets using a multi-technique approach with reflected light microscopy, scanning electron microscopy with energy dispersive X-ray spectroscopy (SEM/EDS) and microscope-assisted Raman spectroscopy. The MC were collected from six ash samples from Pego Power Plant (Abrantes, Portugal; 2 bottom ash samples, 2 economizer fly ash, 2 fly ash from electrostatic precipitator - ESP) via wet magnetic separation using ferrite (samples MCF) and neodymium (samples MCNd) magnets in sequence. In MCF from ESP fly ash, iron is mainly concentrated in discrete Fe-morphotypes (ferrospheres and magnesiopheres), while in MCF from bottom ash and economizer FA it is often found embedded in aluminosilicate glassy particles. In all MCNd, Fe-morphotypes are scarce and Fe-bearing phases are usually found within glassy agglomerates. The study of the pellets from MCF showed that Fe-morphotypes are mostly massive spheres with microtextures extending from the core particle to its surface, being Fe-bearing crystals of skeletal-dendritic type the most common microstructure. The analysis of the internal structure of these ferrospheres also provided insightful information regarding local scale variations in the chemistry and mineralogy, namely the occurrence martitization, i.e., oxidation of magnetite to hematite, in the edge and within morphotypes, the coexistence of mineral phases, e.g., hematite with magnesioferrite, and trace elements within mineral phases, e.g., magnetite with Mg. These changes can affect the MC application as catalysts, particularly when occurring at particles surface where chemical reactions take place. Nevertheless, the information gathered under this research provides details that can help guiding chemical experiments and overcoming the drawbacks that could arise from Fe-bearing phases heterogeneity.

Acknowledgements: The work was supported through the projects UIDB/04683/2020, UIDP/04683/2020, DRI-India/0315/2020 (Insub), EXPL/CTM-CTM/0790/2021 (PhotoBioTrans), POCI-01-0145-FEDER-007690. ACS for PhD scholarship SFRH/BD/131713/2017 and COVID/BD/151941/2021. IKB for funding through program DL 57/2016 – Norma transitória REQUIMTE/EEC2018/14. Pego power plant (Portugal) for ash samples.

Weathering impact on organic petrography, mineralogy and geochemistry of coal wastes – case studies from the Upper Silesian Coal Basin, Poland

Magdalena Misz-Kennan^{1*}, Monika J. Fabiańska¹, Justyna Ciesielczuk¹,
Ewa Szram¹, Dariusz Więclaw²

(1) Faculty of Natural Sciences, University of Silesia in Katowice, Poland; (2) Faculty of Geology, Geophysics and Environmental Protection, AGH University of Science and Technology, Kraków, Poland

* Corresponding Author: magdalena.misz@us.edu.pl

Coal wastes after depositing in the dumps undergo weathering that changes their properties. The research attempted to determine the impact of weathering on the organic petrography, mineralogy, and geochemistry of coal wastes deposited in dumps in the Upper Silesian Coal Basin (Poland). Organic matter of these wastes differs significantly in rank, from sub-bituminous (the eastern part of the basin) to bituminous (the western part). Waste samples were collected from current production and material deposited in the dumps for 2-20 years before sampling, thus subjected to weathering. Vitrinite macerals dominate, but in some samples the content of all three maceral groups is similar. Weathering was seen in some samples as irregular cracks and paler in colour oxidation rims around the external edge. The reflectance is in the range of 0.49-0.94%, and on average is lower in the eastern wastes ($R_r=0.50\%$) than in the western ($R_r=0.88\%$), reflecting the trends in coalification in the Upper Silesian Coal Basin.

Wastes contain mostly quartz, kaolinite, muscovite+illite-smectite, K-feldspar, chlorite+serpentine, titanium oxides, and pyrite with its oxidation products, which are the only influenced by weathering. Carbonates are more common in western samples and chlorite+serpentine, kaolinite, and illite-smectite+muscovite relatively to quartz. The western samples show lower variability in mineral composition than the eastern ones. The same trends are also for major and trace chemical elements. The ratio between particular clay minerals does not show significant differences for both the studied sites.

Organic matter shows some changes due to low-temperature processes such as oxidation, leaching, and biodegradation. The weathering generally did not affect the values of the Rock-Eval indices (HI or T_{max}), however, oxidation increased the Oxygen Index in less mature samples, possibly due to their higher reactivity. Similarly, biomarker distributions show more pronounced changes in the eastern samples. Lighter *n*-alkanes removal found in both sets is the result of biodegradation since the low water solubility of these compounds. Acyclic isoprenoids, i.e. Pr and Ph, more resistant to bacterial attack were not removed. Alkyl naphthalenes, better water-soluble and of relatively high resistance to biodegradation, were leached. However, despite partial alkyl aromatic hydrocarbons removal, the ratios values seem to be affected only slightly and still reflect the initial maturity of coal waste organic matter.

Thus, the research points out that organic geochemistry is the most sensitive to weathering whereas organic petrography and mineralogy of coal wastes the least.

Acknowledgements: The financial support by the National Science Centre, grant No 2017/27/B/ST10/00680, is gratefully acknowledged.



**Mineralogical, petrographical and geochemical investigation of fly & bottom ashes from
Agios Dimitrios Power Plant, W. Macedonia, Greece**

Niki Makri¹, Andreas Iordanidis^{2†}, Nikolaos Kouvrakidis³, Kimon Christanis¹,
Stavros Kalaitzidis^{1*}

(1) Department of Geology, University of Patras, 26504 Patras, Greece; (2) Department of Mineral Resources Engineering, Faculty of Engineering, University of Western Macedonia, 50100 Kozani, Greece; (3) DEI S.A. Steam Electric Station (SES) Agios Dimitrios-Kozani

* Corresponding Author: skalait@upatras.gr

The disposal of fly and bottom ash is one of the major environmental issues of coal-fired power plants. Ash is a complex mixture of components, many of which can cause adverse effects on the environment during storage and/or disposal and utilization. Furthermore, even though the properties of ash (particularly of the fly ash) make it a useful material for various industrial utilizations, only a relatively small part is used in various applications, mainly as an admixture in cement and as a building material. Other less common applications include its use in agriculture for soil improvement, as solid waste stabilizer, synthetic zeolites, and industrial waste decontamination. The main problem arising from fly ash disposal in landfills or even during its utilization, is the transfer of some components from the solid to the liquid phase, when the fly ash interacts with aqueous solutions.

The purpose of this study is to investigate the qualitative and quantitative composition of fly and bottom ash samples from the Agios-Dimitrios Power Plant operated by the Greek Public Power Corporation (DEI S.A.). At the same time, a limited number of samples from the Meliti, Kardias and Megalopolis Power Stations were studied for comparative reasons. Laboratory methods included proximate, ultimate, mineralogical, geochemical and organic petrographical analyses.

The results show that the mineralogical composition of the samples includes amorphous material, quartz, calcite, plagioclase, ghemelinite and in small quantities hematite, natrolite, mica and anhydrite. Chemical analysis revealed that the elements Si, Ca, Al, Mg, Fe, and S are contained as major phases, whereas Ti and K as secondary, indicating high slagging tendency within the thermal chambers. Based on the geochemical and mineralogical characteristics of the bottom ash, a possible use in concrete production is proposed, considering nevertheless certain limitations. From the petrographic study of the samples, the effects of heating on the residual particles of organic material were obvious as they showed characteristic heat cracks, while the presence of unburned organic material was quite significant. More specifically, on average, the studied ash samples (in vol.%, mineral matter free) contain 12% huminite, 13.5% inertinite, 3.5% liptinite, whereas the chars amount to 71%. It is concluded that the material is not completely burned in the power plants, resulting in a significant percentage of unburned organic components.

The contribution of palynofacies analysis in archeological studies

Paula A. Gonçalves^{1,2*}, Mónica Corga³, Silvia Aires^{2,4}, Joalice de Oliveira Mendonça¹,
João G. Mendonça Filho¹, Deolinda Flores^{2,5}

(1) Laboratório de Palinofácies & Fácies Orgânica, Departamento de Geologia, Instituto de Geociências, Universidade Federal do Rio de Janeiro, Rio de Janeiro, Brazil; (2) Instituto de Ciências da Terra - Polo da Universidade do Porto, Porto, Portugal; (3) Dryas/Octopetala, Lda., Coimbra, Portugal; (4) Morph/Octopetala, Lda, Coimbra, Portugal; (5) Departamento de Geociências, Ambiente e Ordenamento do Território da Faculdade de Ciências da Universidade do Porto, Porto, Portugal

* Corresponding Author: paula@lifo.geologia.ufrj.br; paula.goncalves@fc.up.pt

Palynofacies analysis is a powerful tool for the study of organic matter (OM) dispersed in sediments and sedimentary rocks, currently applied in diverse areas from geology (stratigraphy, sedimentology, paleoenvironmental studies) to petroleum exploration and environmental studies. However, despite the potential to contribute to the reconstruction of paleoenvironmental conditions and of the cultural processes in the archaeological record, its use in archaeological studies remains rare. In the present study, palynofacies analysis has been applied to investigate the OM preserved in ceramic potsherds recovered from the 3rd millennium collective graves of Horta do João da Moura 1 (Ferreira do Alentejo, Portugal). The studied potsherds, found in association with the deposition of human remains, were probably votive offerings (which by comparison to coeval sites could include cereals, milk, pigments, etc.). In addition to palynofacies, total organic carbon (TOC) and insoluble residue (IR) analyses were performed.

Geochemical results show that the TOC values varied from 0.14% to 0.36%, indicating a low OM recovery. As for the IR, the values vary between 59% and 87%. These values refer not only to the soil of the inner surface of the potsherds but also to the material that constitutes the potsherds themselves (ceramics). All three main groups of OM were observed, with the Phytoclast group dominating in all samples and being represented by both opaque and non-opaque phytoclasts, as well as fungal hyphae. Among the phytoclasts, the opaque ones predominate over non-opaques, probably due to the cooking of ceramic pots and/or food. Cuticles from various plants were observed in varying degrees of degradation. Fungal hyphae of the genus *Glomus* were identified in two samples. This type of fungus occurs in all continental environments and forms symbiotic, mycorrhiza-like relationships with plant roots. The Amorphous group is represented by amorphous organic matter, with different fluorescent colors, derived from microbiological reworking of the particulate organic components. The Palynomorph group is represented by the Sporomorph subgroup and some undifferentiated components. Palynomorphs, when present, occur in small quantities.

While the use of these analyses in the field of prehistoric Archaeology demands for further methodological research, and the specific case of Horta do João da Moura is still at a preliminary stage, it already shows potential to assess the vegetational environment of archaeological sites and the cultural use of the organic resources.

Acknowledgments: This work has been partially supported by national funds through FCT, projects UIDB/04683/2020 and UIDP/04683/2020.

**The behaviour of Kolubara and Kostolac lignite during devolatilisation process:
A petrographical approach**

Miodrag Životić¹, Dragoslava Stojiljković², Nenad Nikolić³, Danica Bajuk-Bogdanović⁴,
Dragana Životić^{5*}

(1) Ludan Engineering, Belgrade, Serbia; (2) University of Belgrade, Faculty of Mechanical Engineering, Belgrade, Serbia; (3) Institute for Multidisciplinary Research, University of Belgrade, Belgrade, Serbia; (4) University of Belgrade, Faculty of Physical Chemistry, Belgrade, Serbia; (5) University of Belgrade, Faculty of Mining and Geology, Belgrade, Serbia

* Corresponding Author: dragana.zivotic@rgf.bg.ac.rs

The devolatilization process is the initial step in the coal combustion. Devolatilization research was performed on a wire-mesh reactor in inert gas, at the atmospheric pressure. Two different sets of feed coal samples of various particle diameters ($0.50 < x < 1.00$ mm; $0.25 < x < 0.50$ mm; $0.1 < x < 0.25$ mm; $x < 0.1$ mm) from the Kolubara and Kostolac mines were used for research. Lignite samples were spread in a thin layer a few particles thick, over electrically heated stainless steel wire mesh and rapidly heated at four different temperature stages (300°C, 500°C, 700°C, 900°C). Maceral analysis and rank determination were performed on 32 combustion residues and 8 lignite samples following the classification developed by ICCP for lignite, bituminous coal and coal chars.

Huminite reflectance (0.27-0.28% R_r) confirms the low rank of all the coal samples. Residues of all particle diameters, devolatilized at 300°C and 500°C, showed very small changes in the reflectance value and still lignite rank. A significant increase in reflectance is observed in residues of all particle diameters, devolatilized at 700°C and 900°C. Measured vitrinite reflectance confirms the High (at 700°C) and the Medium volatile bituminous rank (at 900°C).

Lignite samples showed a relatively high content of huminite (64.7-77.6 vol.%), a low inertinite (3.1-7.2 vol.%) and a low liptinite content in the Kostolac (3.0-6.2 vol.%) and a slightly higher liptinite content in the Kolubara samples (4.2-11.3 vol.%). The mineral matter content ranges from 12.2 to 23.8 vol.%. The solid residue heated at 300°C and 500°C shows a slight decrease in huminite and liptinite contents and a slight increase of altered coal, which corresponds to vitrinite macerals. The major increase of vitrinite macerals was at 700°C, while char content is the highest in residues heated at 900°C. The content of liptinite is lower than in the raw coal, while inertinite displayed a low decrease with temperature change. FTIR spectral data for both Kolubara and Kostolac coal samples reveals a decrease in water, aliphatic- and oxygen-containing structures with increase in combustion temperatures from 300 to 700°C. The absence of aliphatic and oxygen-containing structures, breakdown of clay mineral component and negligible amount of water is detected in samples devolatilized at 900°C where aromatic structures dominate.

The maceral analyses of coal and devolatilized residues, as well as other experimental research (TGA, FTIR) provide information of the large changes of huminite and liptinite macerals at the higher temperatures and the decrease of volatiles with the increase of the devolatilization temperature in all samples from both basins.

Applied organic petrography to spent lithium-ion batteries (LiB) recycling

Bruno Valentim^{1*}, Charlotte Badenhorst¹, Alexandra Guedes¹, Elsayed Mousa^{2,3},
Karen Moreira¹, Ana C. Santos¹, Guozhu Ye²

(1) Earth Science Institute – Porto pole, Department of Geosciences, Environment and Spatial Plannings, Faculty of Sciences, University of Porto, Rua do Campo Alegre s/n, 4169 – 007 Porto, Portugal; (2) SWERIM AB, Aronstorpsvägen 1, SE-974 37 Luleå, Sweden; (3) Central Metallurgical Research and Development Institute (CMRDI), Cairo 12422, Egypt

* Corresponding Author: bvvalent@fc.up.pt

The global market for e-consumers and e-vehicles is exponentially growing, which in turn, is forcing the exponential production of LiB while simultaneously generating increasing amounts of spent LiB. Thus, landfilling, environmental issues and raw materials sustainability are key issues to be addressed. Actually, in Europe, spent LiB recycling at industrial scale applies high-temperature pyrometallurgical processes to recover cobalt and nickel, but graphite and most of Li are being lost in the smelting process.

So, alternative pyrometallurgic and hydrometallurgical processes are needed to decrease the energy consumption and also recover Li and graphite. For this purposes, detailed characterization of the spent LiB components and raw materials should be considered to assist in the improvement of the separation and transformation processes.

Advanced organic petrography, i.e. a combination of the techniques of optical microscopy, SEM-EDS and microscope assisted Raman spectroscopy (MARS), may play a role in the description, quantification and assessment of oil-derived materials, graphite, lithium metal oxides (LMO) and other materials. In this sense, advanced organic petrography was applied, under the scope of project NEXT-LIB aiming at recovering valuable materials from spent LiB.

The results included the identification of Al and Cu foils associations with the black mass, to find and track the binder, to identify and assess anode graphite and LMO transformations, and to assess a hydrometallurgical pathway aiming at separating and recovering all the materials.

For the characterization of a black mass sample rich in lithium manganese oxides, a reflectance microscope with white- and UV-light sources, a polarizer and a 1λ retarder plate, were used, and the following materials were identified: bended Al and Cu foils fragments (white to pale grey and reddish, respectively; non-fluorescent); discrete particles or chunks of flake and dense anode graphite (anisotropic; non-fluorescent); three different types of LMO (non-fluorescent), i.e. white and pale blue spheres composed of submicrometric grains, and rectangular, lilac-twined and dense crystals; fluorescent PVDF binder surrounding anode graphite and LMO. The shape, size and chemical composition were confirmed using SEM-EDS, and the transformations suffered after pyrolysis and roasting were assessed via the combination of advanced organic petrography techniques.

Acknowledgements: ERA-MIN2 programme (2018) and the respective national financier: VINNOVA, Sweden (Project no. 2019-03473), FCT-Portugal (ref. ERA-MIN/0003/2018; project COMPETE 2020 (UIDB/04683/2020); POCI-01-0145-FEDER-007690).

Distinguishing fossil inertinite from modern charcoal in microscope images

Zbigniew Jelonek^{1,3*}, Iwona Jelonek^{1,3}, Agnieszka Drobnik^{1,2,3}, Maria Mastalerz^{2,3}

(1) University of Silesia in Katowice, Institute of Earth Sciences, ul. Będzińska 60, 41-200 Sosnowiec, Poland

(2) Indiana Geological and Water Survey, Indiana University, 1001 E. 10th St., Bloomington, IN, 47405, USA

(3) Centre for Biomass Energy Research and Education, ul. Będzińska 60, 41-200 Sosnowiec, Poland

* Corresponding Author: zbigniew.jelonek@us.edu.pl

The requirements and testing methods for charcoal briquettes and lump charcoal used for barbecuing are regulated by norms EN 1860-2:2005 and ISO 7404-3 with the purpose of implementing quality standards to reduce the risks associated with using solid fuels for grilling. Nowadays, with high manufacturing standards, charcoal contamination during the production phase is rather rare. However, contamination can occur during product packing, transport, and storage. Inorganic matter, petroleum products, slag, metals, rust, coke, and coal are among the most common impurities. While most of these undesired components are easily identified applying incident light microscopy, distinguishing inertinite from coal and modern charcoal can be challenging. Since the addition of coal in charcoal-based BBQ fuels increases emissions of harmful substances and gases, qualitative-quantitative identification of coal is extremely important.

During the microscopic analysis of coal, three groups of macerals (vitrinite, liptinite, and inertinite) can be distinguished. If these macerals occur in association in a single coal fragment (Figs 1a,b), identification of coal does not pose difficulties. The challenge arises when a single fragment of inertinite is encountered (Fig. 1c), as it appears indistinguishable from the image of modern charcoal fragments (Fig. 1d).

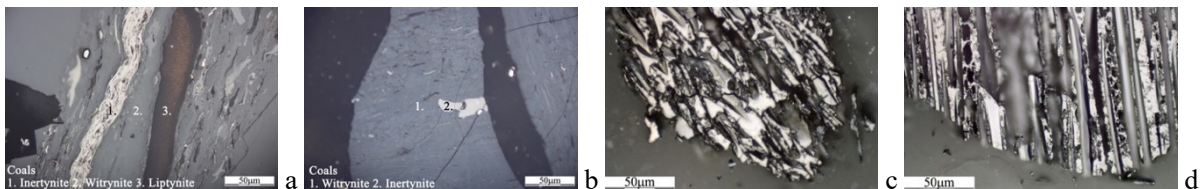


Figure 1. Photomicrographs of coal (a, b, c), and modern charcoal (d) under incident white light microscope.

In this preliminary study, an attempt was made to distinguish coal inertinite from modern charcoal using white light combined with Differential Interference Contrast (DIC) and fluorescent filters. The examination was made on 10 samples of Carboniferous coal from the Upper Silesian Basin in Poland and 10 samples of modern charcoal (grilling fuels). The DIC filter produced an apparent relief and depth of field effect. Its application made it possible to see numerous cracks, scratches, and small and larger pores in coal inertinite fragments; these features were absent from modern charcoal. Coal inertinite also showed rather blurry edges, while charcoal demonstrated sharp outlines typical for modern hardwoods. The use of the fluorescence filter allowed us to clearly see the preserved cellular structure in charcoal. Analyzed fossil inertinite did not have the characteristic structure of modern wood due to the different precursors and the sedimentary and diagenetic processes.

This experimental comparative analysis with the application of filters indicated a potential for developing effective tools to distinguish coal from charcoal during microscopic analysis. The work is ongoing to acquire better ways to enhance the description of their morphological and optical characteristics.

Characterization of the Highveld coal's macromolecular structure and their float products using Raman spectroscopy

Itumeleng Matlala*, Marvin Moroeng, Nicola Wagner

DSI-NRF CIMERA, Department of Geology, University of Johannesburg, Johannesburg, South Africa

* Corresponding Author: imatlala@uj.ac.za

Coal macromolecular structure is generally complex due to the variety of macerals present. The present study focuses on five run of mine (ROM) coal samples collected across the No.4 seam from different collieries in the Highveld Coalfield, and their respective float products (at relative density of 1.7 and 1.9 g/cm³). The purpose is to assess the differences in macromolecular structure per ROM and density fractionation. Organic petrography was undertaken to understand changes to the maceral composition between the samples, and to relate the impact of these differences to the macromolecular structure using Raman Spectroscopy. The mean random vitrinite reflectance (%RoV) values ranges between 0.57 and 0.60% (medium rank D bituminous). The ROM coals are inertinite-rich, enriched mainly in semifusinite and inertodetrinite. The changes in maceral composition following density fractionation noted as reactive macerals are enriched in the float products. The impact of maceral differentiation between the samples was noted in the Raman parameters (Fig. 1). The Raman bands for the ROM coals are narrower than those for F1.7 but slightly broader than those for the F1.9 samples, indicative of increased aliphaticity in the F1.7 samples and increased aromaticity in the F1.9 samples. The F1.9 samples record comparative G FWHM values to those for the ROM samples, but lower values compared to F1.7 samples due to large differences in maceral composition. In contrast, the D FWHM values for the float products are slightly higher than the ROM samples, reflecting the presence of a highly disordered aromatic character, mainly attached with long aliphatic chains.

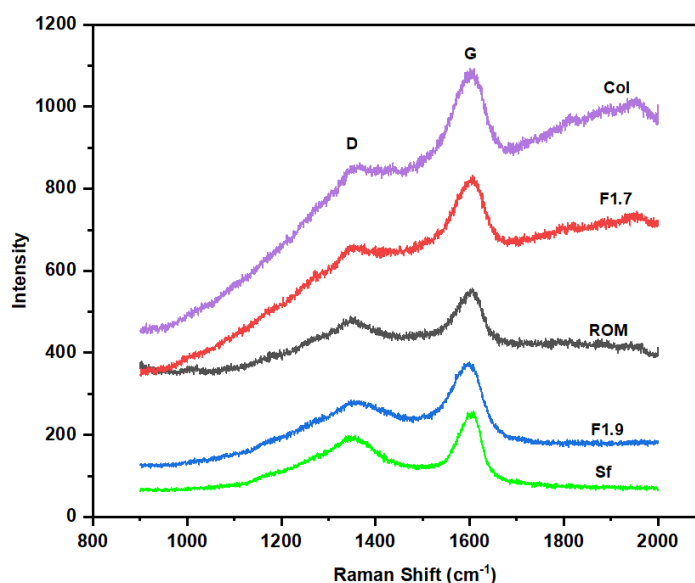


Figure 1. Raman Spectra for ROM, F1.7, F1.9 (F denotes float products), collotelinite (Col) and semifusinite (Sf), baseline not corrected.

Investigations of structural and chemical changes during pyrolysis of biomass by means of optical, spectroscopic and porosimetric methods

Maja Mroczkowska-Szerszeń^{1*}, Konrad Ziemianin¹, Lidia Dudek¹, Bartosz Adamczyk²,
Magdalena Dudek²

(1) Oil and Gas Institute – National Research Institute, Cracow, Poland; (2) AGH University of Science and Technology, Cracow, Poland

* Corresponding Author: mroczkowska@inig.pl

Samples of biomass pyrolysed at temperature range from 300 to 650°C, were characterized in terms of thermal transformations and their carbonisation level using optical, spectroscopic and porosimetric methods. Considering the time and manner of conducting the pyrolysis process and the method of preparing the substrates, an attempt to indicate how these factors affect the transformation of the analyzed samples, was made. The method of application of the obtained biochar samples for solid oxide fuel cells was presented. The influence of the biochar physical and chemical properties on the operating parameters of solid oxide fuel cells was also determined.

During the pyrolysis process a secondary porosity of biomass was formed. The pyrolysis process also led to an increase of the degree of carbonization and ordering of the internal structure, which is manifested by an increased reflectance values. The reflectance measurement was carried out for a walnut samples carbonised at different temperatures (350, 400, 450, 600 and 650°C). An increase in the temperature of pyrolysis from 350 to 450°C, causes an increase in measured mean random reflectance. In comparison, a further temperature rise (600 and 650°C) did not deepen this effect. Moreover, the high standard deviations obtained during the reflectance measurements suggest a broad spectrum of the population. Even with the homogeneous raw material and the imposed thermal & time conditions during the experiment, the pyrolysis process did not occur uniformly and the individual observed fragments of the same material underwent transformations at different rates. Perhaps the duration of the experiment is responsible for this.

The same samples were characterized spectroscopically using the FTIR ATR method. Significant variability of the spectra obtained at higher temperatures was demonstrated due to the gradual thermal decomposition of individual components of the initial raw materials, i.e. hemicelluloses, celluloses and lignocelluloses degradation. It was possible to record the spectra characteristic for the separate stages of transformation and to correlate them with the reflectance measurements performed for these samples. After statistical processing of spectroscopic results, it is possible to obtain groups clustered around patterns indicating the tested samples' transformation degree using the PCA and HCA methods. The level of carbonisation is of fundamental importance for the further use of the obtained biochars, including their use as fuel for efficient and clean energy sources, which are SOFC fuel cells. Assessing the degree of transformation is also essential for using biochar to produce CO+H₂ synthesis gas, which is a further substrate in the production of synthetic methane or methanol.

Impact of pyrite-sourced sulfur on catagenesis in gilsonite undergoing hydrous pyrolysis

Javin Hatcherian^{1*}, Tushar Adsul², Paul Hackley¹, Santanu Ghosh³, Atul Kumar Varma²

(1) U.S. Geological Survey, Reston, VA, USA; (2) Indian Institute of Technology (Indian School of Mines), Dhanbad, Jharkhand, IN, USA; (3) Department of Geology, Mizoram University, MZ, IN, USA

* Corresponding Author: jhatcherian@usgs.gov

Hydrocarbon generation occurs within thermally mature, organic-rich sediments and is influenced by a variety of mineral assemblages and relative mineral abundances. Some elements sourced from minerals have been shown to act as strong catalysts during hydrocarbon generation. Previous laboratory experiments conducted by Ma et al. (2016) suggested that the lone electron pair of sulfur bonded to iron(II) in synthetic pyrite enhanced free radical formation through hydrogen transfer from kerogen to sulfur. In this work, we examine the impact of sulfur in catalysis by conducting a series of hydrous pyrolysis (HP) experiments at varying temperatures and pyrite abundances to investigate how sulfur sourced from pyrite facilitates early hydrocarbon generation and thermal maturation.

To examine the impact of sulfur in catagenesis over a range of temperatures, 1 g of gilsonite (a solid hydrocarbon) was mixed with 0.1 to 10 g of reagent-grade pyrite. Aliquots of these mixtures and aliquots of untreated gilsonite underwent HP at temperatures of 320°C, 350°C, and 370°C for 72 hours. Aliquots of untreated gilsonite and the HP residues of gilsonite/pyrite mixtures were analyzed by reflectance measurements, LECO carbon analyzer for total organic carbon (TOC) and programmed temperature pyrolysis via Hydrocarbon Analyzer with Kinetics (HAWK).

The results indicated solid bitumen reflectance was higher in HP residues with greater pyrite concentrations for the lower temperature HP residues (320°C and 350°C), while reflectance values were similar in the 370°C residues, regardless of pyrite concentration. This result may suggest a greater catalytic effect at lower thermal conditions influenced by C-S and S-S bond dissociation. Samples with the highest concentration of pyrite consistently contained the lowest Hydrogen Index (HI) values among samples undergoing similar HP conditions. Conversely, Production Index (PI) values were higher in samples with higher concentrations of pyrite. These results from gilsonite reflectance, HI, and PI support the hypothesis that the presence of catalytic sulfur enhances thermal maturation through a free radical mechanism. However, HP residues with the highest concentrations of pyrite had lower T_{max} values. These results will be discussed with respect to the relative abundance of pyritic sulfur in source rocks and its potential to act as a catalytic agent during burial maturation.

Reference

Ma, X., Zheng, J., Zheng, G., Xu, W., Qian, Y., Xia, Y., ... Ye, X., 2016. Influence of pyrite on hydrocarbon generation during pyrolysis of type-III kerogen. *Fuel* 167, 329–336.
<https://doi.org/10.1016/j.fuel.2015.11.069>

Composition verification of biofuels produced from herbaceous and woody biomass using petrographic analysis

Iwona Jelonek^{1,3*}, Zbigniew Jelonek^{1,3}, Agnieszka Drobniak^{1,2,3}, Maria Mastalerz^{2,3}

- (1) University of Silesia in Katowice, Institute of Earth Sciences, ul. Będzińska 60, 41-200 Sosnowiec, Poland;
(2) Indiana Geological and Water Survey, Indiana University, 1001 E. 10th St., Bloomington, IN, 47405, USA;
(3) Centre for Biomass Energy Research and Education, ul. Będzińska 60, 41-200 Sosnowiec, Poland

* Corresponding Author: iwona.jelonek@us.edu.pl

The utilization of herbaceous biomass as a potential source of low-cost energy can benefit the environment and contribute to the economical use of renewable energy sources. Increasing the use of various types of grasses (meadow grass, hay, miscanthus, or fescue) could be a possible solution to the problem of dwindling woody biomass resources. Currently, approximately 95% of pellet production is based on material derived from cuttings and tree waste. Given the limited supply of woody biomass, pellets produced from herbaceous biomass could be essential to ensure the sustainable use of forest resources. Not only will this type of production help to reduce the environmental impact of wood harvesting and transportation, it also would increase resource efficiency. For example, grass cuttings acquired during mowing are typically composted, often leading to material decay and, consequently, the release of methane. To minimize the emission impact of this greenhouse gas on the environment, the utilization of green waste for energy purposes seems a more desirable option.

However, the production of pellets from herbaceous biomass requires different shredding and pressing techniques than woody biomass, making the process more complex. Most importantly, herbaceous pellet biomass manufacturing requires maintaining appropriate proportions of the material mix due to the differing nature of the components and, subsequently, controlling the combustion emissions they generate (especially nitrogen and chlorine). Composition control of the pellets by physico-chemical methods at the qualitative-quantitative level is often challenging. Therefore, the goal of our project was to check if such a control would be enhanced by implementing petrographic analysis.

Conducted tests showed that reflected-light microscopy can be an excellent tool to distinguish between herbaceous and woody plants and to determine the component proportions of the pellets. The tests also indicated that the optimal pellet blend should contain about 40% of herbaceous and 60% (by weight) woody material, as such proportions reduce the negative environmental impacts of excessive emissions. Our results showed that combusting such samples yields from 300 to 350 mg/m³ of CO, the VOC ranged between 20 and 25 mg/m³, PM 10 and PM 2.5 contents were about 15 mg/m³, and chlorine-based chemicals (HCl) about 10 mg/m³.

Microscopic Assessment of Some Biomass Chars

Georgeta Predeanu^{1*}, Valerica Slăvescu¹, Marius F. Drăgoescu¹, Petrișor Samoilă²,
Alexandru Fiti³

(1) University Politehnica of Bucharest, Bucharest, Romania; (2) Institute of Macromolecular Chemistry “Petru Poni”, Iași, Romania; (3) SC Cosfel Actual SRL, Bucharest, Romania

* Corresponding Author: gpredeanu@gmail.com

Char-type carbon materials (CCM) are precursors for making activated carbons, products with increased added value. The microscopic assessment of CCM made from waste biomass shells aims at the qualitative determination of structural composition and intragranular porosity in case of some samples obtained in a 3.3 kW microwave heating laboratory equipment.

The study of microstructure highlights several aspects regarding microwave synthesis as evolution and efficiency, and characteristics of the obtained CCM. The microstructure is correlated with the adsorption capacity towards iodine and S_{BET} developed during degassing at 600–700°C. The porosity depends on the initial raw material, temperature, and heating rate during microwave heating (Predeanu et al., 2023).

CCM has a specific microstructure, characterized by a small porosity created in the wider pore walls, with a cellular structure of round pores. The photomicrographs highlight both the characteristics of porous texture and types of carbon matrix, which can contribute, to the size of adsorption surface given by the iodine index and surface area, such as: 455 mg/g, S_{BET} 295 m²/g for sample A, and iodine index 469 mg/g and S_{BET} 251 m²/g for sample B (Fig. 1).

The results are very promising about CCM utilization for purification purposes in case of some organic pollutants such as phenols and 4-chloraniline.

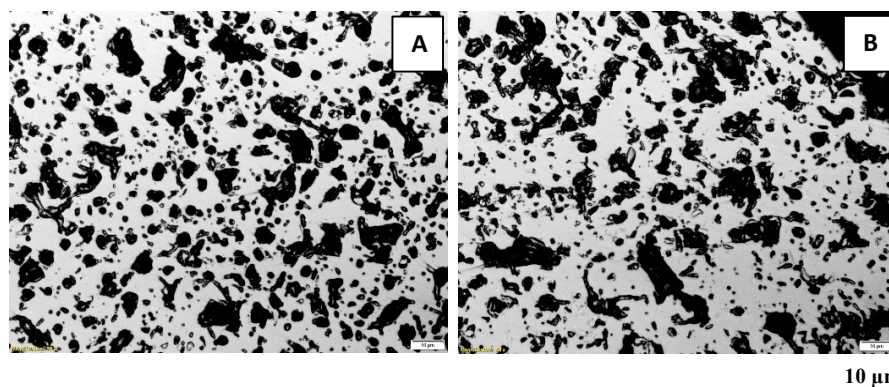


Figure 1. Photomicrographs of fine porosity of CCM obtained from walnut shells char, RL, imm., 500X.

Acknowledgments: Present research received funding from POC 163/1/3, grant agreement 386/390062/4.10.2021, MySMIS: 120696

Reference

Predeanu, G., Slăvescu, V., Drăgoescu, M.F., Bălănescu, N.M., Fiti, A., Meghea, A., Samoila, P., Harabagiu, V., Ignat, M., Manea-Saghin, A.M., Vasile, B.S., Badea, N., 2023. Green Synthesis of Advanced Carbon Materials Used as Precursors for Adsorbents Applied in Wastewater Treatment. *Materials* 16, 1036. <https://doi.org/10.3390/ma16031036>

Microscopic characterization of carbon materials derived from coal and biomass and their interaction phenomena in making high grade products

G. Predeanu¹, M. Wojtaszek-Kalaitzidi², I. Suárez Ruiz³, M. Bălănescu¹, A. Gómez Borrego³, M.A. Diez³, L. Garcia³, M. D. Ghiran⁴, P. Hackley⁵, S. Kalaitzidis⁶, J. Kus⁷, D. Mancisidor³, M. Mastalerz⁸, M. Misz-Kennan⁹, S. Pusz¹⁰, S. Rodriguez¹¹, G. Siavalas¹², A.K. Singh¹³, P. Tomillo³, A. Varma¹⁴, A. Zdravkov¹⁵, D. Životić¹⁶

(1) University Politehnica of Bucharest, Bucharest, Romania; (2) Institute of Energy and Fuel Processing Technology, Zabrze, Poland; (3) Instituto Nacional del Carbón, Oviedo, Spain; (4) ICPMT - OMV Petrom, Câmpina, Romania; (5) U.S. Geological Survey, Reston, USA; (6) University of Patras, Patras, Greece; (7) Federal Institute for Geosciences and Natural Resources, Hannover, Germany; (8) Indiana University, Indiana, USA; (9) University of Silesia, Sosnowiec, Poland; (10) Centre of Polymer and Carbon Materials, Zabrze, Poland; (11) University of Queensland, Brisbane, Australia; (12) Shell Global Solutions International, The Hague, The Netherlands; (13) TATA Iron & Steel Comp. Ltd, Jamshedpur, India; (14) Indian School of Mines, Dhanbad, India; (15) University of Mining and Geology “St. Ivan Rilski”, Sofia, Bulgaria; (16) University of Belgrade, Belgrade, Serbia

* Corresponding Author: gpredeanu@gmail.com

This work presents the results of the Microscopy of Carbon Materials Working Group in Commission III of the International Committee for Coal and Organic Petrology between the years 2016 and 2022. The round robin exercises were run on photomicrograph samples and over 20 active participants totally were involved, who were asked to assess raw coals, coal by-products and biomass-based carbons and to identify the morphological differences, as optical texture (isotropic/anisotropic), optical type (punctiform, mosaic, fiber, ribbon, domain), size and origin. The samples obtained during laboratory experimental trials in Romania, Spain and Poland were focused on the following raw materials and intermediary/final products and technological steps: a) coal/lignite, xylite char, physical activation/activated carbon; b) coal/semianthracite/anthracite/oxidation, pyrogenation, physical & chemical activation, activated carbon; c) coal tar pitch/pitch coke obtained from oxidative polymerization of an industrial anthracene oil (AO)/chemical activation, microwave-derived precursors for graphene-like materials; d) biomass/biomass pyrogenation, char physical activation, activated carbons. Four sets of digital color and black & white photomicrographs comprising 158 photos containing over 400 fields of different types of organic matter such as 22 types of chars/coke and 7 types of activated carbons were examined. Based on the unique ability of carbon to form a wide range of textures, the results showed an increased number of carbon occurrences, which have crucial role in the chosen industrial applications using conventional and microwave heating technologies to make adsorbents used for purification purposes and precursors for graphene-like materials. The original character of the round robin exercises is emphasized by the attempt to correlate different types of coals/biomasses/chars/coke with their higher or smaller susceptibility and/or selectivity *versus* the technologies applied to obtain high grade products. The statistical method applied to evaluate the results, was based on the “raw agreement indices”. It gave a new and original view of the analysts' opinion by not only counting the correct answers, but also all the knowledge and experience of the participants. Comparative analyses of the average values of the level of overall agreement performed by each analyst in the exercises during 2016–2022 showed a rather homogeneity in the results with a satisfactory 82.5% for all identified structures, the mean value being of 84% for optical texture, 86% for morphology, 87% for optical shape and 73% for origin of particle.



Study on thermal properties differences of coal from insight of nano carbon structure characteristics

Xin Guo^{1*}, Yuegang Tang², Cortland Eble³, Harold Schobert⁴, Shaoqing Wang²

(1) CCTEG Chinese Institute of Coal Science, Beijing, China; (2) College of Geoscience and Surveying Engineering, China University of Mining and Technology (Beijing), Beijing, China; (3) Kentucky Geological Survey, University of Kentucky, Lexington, USA; (4) The EMS Energy Institute, The Pennsylvania State University, Pennsylvania, United States

* Corresponding Author: guoxin012370@163.com

From the perspective of structural chemistry (nano-scale), coal is an amorphous solid substance with short-range order, long-range disorder, hierarchical structure. There are significant differences in the macroscopic thermal properties between caking coal and non-caking coal, and the nano-structure differences that affect the macroscopic properties of coal when analyzed from the perspective of meso-micro dimensions. Ten samples, including four caking coals (three medium volatile, and one low volatile bituminous) and six non-caking coals (one lignite, two subbituminous, one high volatile C, one semianthracite, and one anthracite), were used to study their microscopic structural changes when heated. An optical microscope with microphotometer, FTIR, ¹³C-NMR, Raman, XRD, SEM, HRTEM, and electron paramagnetic/spin resonance (EPR/ESR) was jointly employed to investigate the untreated samples and thermally altered products from the perspective of micro-nano morphology, chemical components, spatial alignment, and free radical types. The bulk chemical testing methods, including FTIR, ¹³C-NMR, and XRD, indicate little change under the same heat-treated environments, even though the parent-coals were of different rank. Microanalysis methods, such as SEM, HRTEM, and semiquantitative results of the samples demonstrated that the optical and structural parameters of the heat-treated products derived from the caking and non-caking coals were significantly different. The reflectance of the heat-treated products derived from the non-caking coals showed a smaller distribution range compared to that from the caking coals, while the A_D/A_G ratio showed a contrary trend; the A_D/A_G of the heat-treated products derived from the non-caking coals showed a relative larger distribution range compared to that from the caking coals. The results of the EPR/ESR revealed that free radical types in the heat-treated products derived from the caking coals and non-caking coals were diverse. Microscopic characteristics of the nanocarbon structure are the essential factors affecting the differences in coal thermal properties. If structural arrangement can be determined, based on the characteristics of nanocarbon structure, it may be possible to accurately predict the thermally-altered properties of coal-based materials through microscopic structural determination. This study provides insight into using coal as an added-value material in the Energy Transition Era.

Acknowledgments: This study is supported by National Natural Science Foundation of China (42102226, 41872175), and State Key Laboratory of Clean and Efficient Coal Utilization, Taiyuan University of Technology (MJNYSKL202302). The authors express great thanks to Dr. James Hower at the Center for Applied Energy Research, University of Kentucky.



The graphitization characteristics of coal macerals

Shaoqing Wang^{*}, Lei Zhao, Yan Shao, Zeyu Dong

College of Geoscience and Surveying Engineering, China University of Mining & Technology (Beijing),
Beijing, P.R. China

** Corresponding Author: wangzq@cumtb.edu.cn*

In this paper, three coal samples at the same coal ranks from Xiaojihan coal mine, P.R. China, were studied. Inertinite and vitrinite were separated by hand-picking method. The purity of vitrinite and inertinite reached up to 94% and 92%, respectively. The graphitization experiments of each maceral and raw coal were conducted at six different temperature levels: 1800°C, 2000°C, 2200°C, 2600°C, 2800°C, and 3000°C. Titanium dioxide and niobium oxide were added as catalysts. The X-ray diffraction (XRD) method was applied, and some parameters derived from XRD analysis were obtaining, including the crystalline length (L_a), the crystalline height (L_c), and the interlayer distance (d_{002}).

The results showed that the graphitization characteristics of the macerals were influenced by the temperatures and catalysts used. Meanwhile, different macerals revealed different change behavior. For both vitrinite and inertinite, with the temperature increase, the values of d_{002} for all samples generally decreased, whereas the values of L_a and L_c increased. An interesting result was that when temperature exceeded 2800°C, the values of L_a and L_c for vitrinite and inertinite increased sharply. Furthermore, the fast increase in L_a value of inertinite was higher than that of vitrinite. Besides, the catalyst played an important role in promoting the graphitization of the maceral. The addition of both titanium dioxide and niobium oxide led to a d_{002} decrease at the temperature range from 2200-3000°C. For vitrinite, both L_c values increased when adding titanium dioxide and niobium oxide, separately, at up to 2200°C, whereas the characteristic L_a value increase was different. The obvious increase range for L_a values was from 2200-2600°C when adding titanium dioxide and up to 2600°C when adding niobium oxide. For inertinite, when adding niobium oxide, the L_c value decreased when temperature exceeded 2200°C and the L_a value increased sharply at $\geq 2600^\circ\text{C}$. This study can enrich the theory of coal graphitization, which is important for coal clean utilization and efficient conversion.



The Occurrence of Methane in the Deep Parts of the Carboniferous Formations in the Upper Silesian Coal Basin, Poland. Case Study of the Orzesze 1 Deep Exploratory Well

Sławomir Kędzior

University of Silesia in Katowice, Faculty of Natural Sciences, Institute of Earth Sciences, 41-200 Sosnowiec, Będzińska 60, Poland

Corresponding Author: slawomir.kedzior@us.edu.pl

The Orzesze-1 exploratory well was drilled in 2019–2020 by Polish Oil and Gas Company (PGNiG S.A.) and Polish Geological Institute (PGI) in the depocenter of the Upper Silesian Coal Basin (USCB). The main purpose of this well was to identify and investigate the possibility of coal bed methane (CBM) and tight gas occurrence (Report, 2021). The depth of the hole is 3,708 m (TVD) and the deepest level reached was the Malinowice Beds (Carboniferous, Namurian A). The methane content in coal seams has been tested to a depth of 2,840 m and the sorption capacity of coal to a depth of 2,576 m. These are the deepest measurements in the USCB so far.

The vertical distribution of methane content in the borehole shows two depth zones of interest, the first at a depth >900 m to about 1300 m (maximum methane content about 12 m³/t coal^{daf}) and another in the range of 1500–2880 m, i.e. to the maximum depth of measurements, so the actual lower boundary depth of this zone is unknown. The maximum methane content here exceeds 18 m³/t coal^{daf} at a depth of >2,800 m. Both zones are separated by an interval of reduced methane content to about 5 m³/t coal^{daf} at a depth of approximately 1,400 m. The gas composition is dominated by methane (>83%), the content of carbon dioxide increases to approximately 15% at a depth of >2,300 m. The methane-bearing zone between 900–1300 m corresponds to the zone of high and medium volatile coal (second coalification jump), while the highest methane content at a depth of >2800 m was determined in anthracite.

The methane sorption capacity of coal seams oscillates between 16 and 40 m³/t coal^{daf} with a maximum in anthracite at a depth of >2800 m, where the temperature of the rocks approaches 100°C and the deposit pressure exceeds 28 MPa. The highest sorption capacity in anthracites results from their inner structure characterized by the predominance of ordered aromatic lamellas and the dominance of vitrinite macerals (>70%), which contain coal micropores accumulating adsorbed methane. In addition, it has been shown (Jing et al., 2023) that in coal micropores temperature has a weaker effect on methane adsorption at high pressure than at lower pressure. The comparison of the sorption capacity of the tested coal and the measured methane content displays undersaturation of 11–59%, however the methane content exceeding the balance value of 4.5 m³/t coal^{daf} makes the drilling area a prospect for further exploration and development of CBM.

References

- Jing, T., Zhang, J., Zhu, M., Zhao, W., Zhou, J., Yin, Y., 2023. Methane Adsorption in Anthracite Coal under Different Pressures and Temperatures — A Study Combining Isothermal Adsorption and Molecular simulation. *Geofluids*. Article ID 8528359, 15 pages, doi.org/10.1155/2023/8528359
- Report, 2021. Geological documentation of the Orzesze 1 exploration well. National Geological Archives, Warsaw (unpublished report).

CLSM thermal maturity of *Tasmanites*-rich Devonian Ohio Shale, northern Appalachian Basin, USA

Jolanta Kus^{1*}, Paul C. Hackley²

(1) Federal Institute for Geosciences and Natural Resources (BGR), GEOZENTRUM Hannover, Stilleweg 2, 30655 Hannover, Germany; (2) U.S. Geological Survey, Geology, Energy & Minerals Science Center, MS 954 12201 Sunrise Valley Dr., Reston, Virginia, USA

* Corresponding Author: j.kus@bgr.de

Confocal laser scanning microscopy (CLSM)-derived thermal maturity determination of liptinite macerals has been evaluated in a limited number of sedimentary deposits. The application of CLSM-based fluorescence spectroscopy to organic sedimentary matter is a relatively novel qualitative and quantitative analysis method in dispersed organic petrology. It allows petrographer to explore and enhanced understanding of changes in spectral fluorescence (eg.: λ_{\max} , $Q_{650/500}$, and $Q_{\max/500}$) across diverse thermal maturity stages. Furthermore, it provides the foundation for standardization efforts carried out within the International Committee for Coal and Organic Petrology (ICCP). In the current study, *Tasmanites* algae microfossils sourced from nineteen Devonian Ohio Shale (Huron Member) samples collected from the northern Appalachian Basin (Kentucky, Ohio, Virginia, West Virginia) were subjected to spectral fluorescence measurements. A multi-parameter approach involved determination of λ_{\max} , $Q_{650/500}$, and $Q_{\max/500}$ at different locations within the *Tasmanites* microfossils (at fold apices, adjacent to impinging minerals, in the middle of microfossils, and parallel to their centers), at orientations perpendicular and parallel to sedimentary bedding, and examined parameter correlation with conventional thermal maturity indicators (BR_r %). The results display a moderate correlation ($r^2=0.49$) between λ_{\max} perpendicular to the bedding in the middle vs. BR_r (excluding diagenetic solid bitumen) and ($r^2=0.56$) between $Q_{650/500}$ perpendicular to the bedding vs. BR_r (excluding diagenetic solid bitumen), respectively. A much higher correlation coefficient ($r^2=0.91$) was recorded between λ_{\max} perpendicular to the bedding in the middle vs. λ_{\max} parallel to the bedding in the middle, indicating the absence of spectral fluorescence anisotropy in the interior of *Tasmanites* microfossils. A similarly high correlation coefficient ($r^2=0.90$) between λ_{\max} perpendicular at apices and λ_{\max} perpendicular adjacent to impinging minerals suggests a strong interrelation and possibly a genetic covariation due to experiencing a comparable deformational history. High r^2 values also were recorded between individual CLSM-based spectral fluorescence parameters (e.g., 0.94 for I_{650} vs. Area under curve). Lastly, variation of individual spectral fluorescence parameters after 5, 10, 15, 20, and 25 cumulative measurements was assessed and evaluated. The encountered range and variance of individual parameters is dissimilar and will be utilized for standardization of spectral fluorescence measurements. The results suggest that fluorescence spectroscopy measurements are a valid approach in deriving CLSM-based thermal maturity from *Tasmanites* algae microfossils. In addition, this work provides a practical methodology to define and document the comparability and quality of CLSM fluorescence spectroscopy data sets.

Acknowledgements: The study forms part of a larger research project “CLSM (spectral fluorescence) for thermal maturity derivation in marine mudstones” and is published with the permission of the Federal Institute for Geosciences and Natural Resources (BGR, Germany).

Origin and thermal maturity of organic matter in Lower-Middle Jurassic rocks from the Lusitanian Basin (Portugal): A case study from the São Pedro de Moel-2 well

Alejandro Ortiz-Loaiza¹, Paula A. Gonçalves^{2,3*}, João G. Mendonça Filho², Deolinda Flores^{1,3}

(1) Departamento de Geociências, Ambiente e Ordenamento do Território da Faculdade de Ciências da Universidade do Porto, Porto, Portugal; (2) Laboratório de Palinofácies & Fácies Orgânica, Departamento de Geologia, Instituto de Geociências, Universidade Federal do Rio de Janeiro, Rio de Janeiro, Brazil; (3) Instituto de Ciências da Terra - Polo da Faculdade de Ciências da Universidade do Porto, Porto, Portugal

* Corresponding Author: paula@lafo.geologia.ufrj.br; paula.goncalves@fc.up.pt

In the last decade, the São Pedro de Moel region (Lusitanian Basin, Portugal) has been considered an interesting area for the study of dispersed organic matter (DOM), with some outcrops being considered international references in the study of the Mesozoic. This study aims to characterize the DOM, based on the identification of maceral groups, and to evaluate its thermal maturation. It was also intended to identify secondary products and to compare the data obtained with existing data from outcrops. For this purpose, a total of 16 cutting samples were collected from the Lower-Middle Jurassic of São Pedro de Moel - 2 (SPM-2) well for basic geochemical analysis by total organic carbon (TOC) and insoluble residue (IR), and organic petrology microscopy (incident white light and blue-light excitation).

The TOC and RI values of 0.19-2.74 wt.% and 3-51 wt.% (respectively) indicate a poor to good organic matter content in carbonate rocks. Petrographic analysis revealed the presence of all major maceral groups. Inertinite particles are the main organic component identified, with the prevalence of fusinite, semifusinite, and inertodetrinite macerals, and minor macrinite. Some inertinite particles have devolatilization pores. The liptinite group includes sporinite (spores and pollen grains of the genus *Classopollis*), cutinite, resinite, and minor bituminite and alginite. Vitrinite is not present in all samples and, when identified, is usually small in size. Its mean random reflectance varied between 0.52 and 0.61%VR₀. In terms of secondary products, solid bitumen was identified in some samples from the Dagorda and Coimbra formations. Under reflected white light, the bitumen shows a grey color and appears to fill voids and fractures among the inorganic matter (mainly carbonates).

The presence of liptinite and terrestrial material indicates a mixture of type III-II kerogen. Vitrinite reflectance results suggest that the samples are mature in terms of hydrocarbon generation. While the kerogen type is consistent with the outcrop data, the thermal maturity data is not (immature *versus* early mature). In addition, solid bitumen has never been identified in outcrop samples. This feature may be important to understand basin evolution, as it suggests that, in this sector of the basin, the crustal uplift occurred prior to bitumen production and migration.

Acknowledgments: This work has been partially supported by national funds through FCT, projects UIDB/04683/2020 and UIDP/04683/2020.

Understanding the effects of heating rate, stress and fluids in maturation of carbonaceous materials by Raman spectroscopy

Andrea Schito^{1*}, David Muirhead¹, Paul Hackley², John Parnell¹,
Roberto Galimberti³, Luca Mascheroni³

(1) Department of Geology and Geophysics, University of Aberdeen, Aberdeen, UK; (2) U.S. Geological Survey, Reston, VA, USA; (3) Geolog Technologies S.r.l, Milan, Italy

* Corresponding Author: andrea.schito@abdn.ac.uk

Raman spectroscopy of carbonaceous material (CM) has recently become one of the most commonly used geothermometers in Earth Science studies. However, the effects of heating rate, stress, and fluid composition on the aromatization path are not yet fully understood. A recent review suggested that different maturation paths could be detected according to their heating rate and stress/fluids conditions. However, this result needs to be systematically tested using additional sample types and the same fitting approach for spectral deconvolution. In this work, the Raman spectra of two sets of coals and a type III kerogen matured under different natural (regional metamorphism vs. around shallow intrusion) or artificial (isothermal closed-system hydrous vs. high heating rate open-system anhydrous) conditions, were analysed and compared. Natural samples that matured around a shallow intrusion were from vitrinite-rich nearshore marine siltstones deposited during the middle Jurassic and then intruded by a 7-m thick doleritic dyke in the Paleogene in the Skye Island (UK). Vitrinite reflectance (%R_o) of these samples increases from about 0.6% to about 4.5% at distances corresponding to 100% down to 10% of the intrusion thickness (i.e., from 7 to 0.7 m). A background (0.36% R_o) sample unaffected by the intrusion was used to perform open-system pyrolysis under anhydrous conditions while coals from the Paleocene-Eocene Wilcox group in Texas (USA) were analysed after hydrous pyrolysis experiments. Maximum temperatures in the open-anhydrous system vary between 300 and 550°C and were reached between 2 and 15 minutes and kept for 30-120 seconds, while hydrous pyrolysis maximum temperatures vary between 320-360°C and were held between 1 and 100 days. The maturity of the samples post-pyrolysis ranged from immature up to the wet gas window. Finally, several coals from different Carboniferous basins in the UK represent CM matured under a diagenetic/regional metamorphism regime in a thermal range between 0.4% up to 3.27% R_o. One naturally matured solid bitumen-rich shale and one graptolitic-shale from the Southern Uplands Paleozoic accretionary prism were also used. When compared against R_o values, the Raman band separation, full-width at half maximum height of the G band and the R1 Raman parameters of the different sample series follow a similar path up to a thermal maturity of ~1.0% R_o. Beyond that, a mismatch occurs, with samples matured under regional metamorphism conditions showing Raman parameters associated with greater aromatization than the intruded or pyrolyzed samples, probably due to lithostatic pressure, as previously observed in literature. Hydrous pyrolysis seems to better reproduce the maturation path around intrusions compared to open-system pyrolysis, suggesting that the hydrous pyrolysis technique could be used to develop a Raman-based kinetics model for CM maturation at low maturities and/or high heating rate conditions.

Origin of organic matter and hydrocarbon generation potential of Early-Mid Jurassic argillaceous rocks from North Bulgaria

Alexander Zdravkov^{1*}, Nikola Botoucharov², Doris Groß³, Irena Kostova², Achim Bechtel³, Denitsa Apostolova²

(1) University of Mining and Geology, Sofia, Bulgaria; (2) Sofia University, Sofia, Bulgaria;
(3) Montanuniversität, Leoben, Austria

* Corresponding Author: alex_zdravkov@mgu.bg

Three intervals of Early-Mid Jurassic black argillaceous rocks belonging to the Southern Margin of the Moesian Platform and western Fore-Balkan units, are traditionally considered the main hydrocarbon source charging numerous small oil and gas deposits along the Bulgarian sector of the Moesian Platform (Georgiev, 2000). Petrological data indicates that organic matter (OM) in these rocks is composed of micrometer-sized hydrocarbon residues (HR) and solid bitumens (SB), whereas vitrinite and inertinite are scarce. HR are typically scattered within the mineral matrix, but also infill stripes and small fractures together with SB, or line up with clastic grains. Based on the measured SB reflectance (BRo), three broad populations of solid bitumens, i.e. SB-I (BRo=0.2–0.8%), SB-II (BRo=0.9–2.2%), and SB-III (BRo=2.2–2.6%), were distinguished. These are considered to represent thermal alteration products from the transformation of Type II marine organic matter during the initial-, peak- and late-oil phases (Sanei, 2020). Type II kerogen is further evidenced from biomarker analysis, denoting predominance of short-chain *n*-alkanes, *n*-fatty acids and *n*-alkanols, as well as C₂₇ steranes. For most of the samples, a sterane/hopane ratio >2 along with rare tasmanite algal remains detected in few samples recovered from lower burial depths, argue for a dominant role of phytoplankton and algae for OM accumulation. Minor amounts of oleanane detected in five of the samples, argue for a possible mixing with oils from a post Jurassic source. Rock Eval pyrolysis data reveals poor hydrocarbon generation potential of the rocks with average total organic carbon contents (TOC) of 1.2 wt.%, average total petroleum potential (S1+S2) of 0.7 mg HC/g rock, and average Hydrogen index (HI) of 42 mg HC/g TOC. T_{max} values in the range from 430 to over 600°C (avg. 485°C) are compatible with the SB reflectance and indicate the predominance of mature to over-mature organic matter, currently capable of generation of limited amounts of thermogenic gas. Reconstructed geochemical parameters (following the approach of Jarvie et al., 2007) indicate average OM transformation ratio of 0.94, initial HI of 448 mg HC/g TOC, initial TOC (avg. 1.6 wt.%) and initial S2 (avg. 7.4 mg HC/g TOC), thus denoting fair to good hydrocarbon generation capabilities of the rocks at their immature state.

Acknowledgements: Financial support from the BNSF through contract № KP-06-PN-34/9 is greatly appreciated.

References

- Georgiev, G., 2000. Oil-oil and oil-source correlation for the major crude oils in Bulgaria. *Annuare de l'Universite de Sofia "St. Kliment Ohridski"* 92, 39–60.
- Jarvie, D.M., Hill, R.J., Ruble, T.E., Pollastro, R.M., 2007. Unconventional shale-gas systems: The Mississippian Barnett Shale of north-central Texas as one model for thermogenic shale-gas assessment. *Bulletin* 91, 475–499. <https://doi.org/10.1306/12190606068>
- Sanei, H., 2020. Genesis of solid bitumen. *Sci Rep* 10, 15595. <https://doi.org/10.1038/s41598-020-72692-2>

Enumeration of RockEval and organic petrography results from artificially matured core samples with varying TOC and S contents

Julito Reyes^{1*}, Levi J. Knapp^{2#}, Omid H. Ardakani^{1,3}, Kazuaki Ishikawa²

(1) Natural Resources Canada, Geological Survey of Canada, Calgary, Canada; (2) Japan Oil, Gas and Metals National Corporation (JOGMEC), Chiba, Japan; (3) Department of Geoscience, University of Calgary, Calgary, Canada; #Now at Alberta Energy Regulator, Edmonton, Canada

* Corresponding Author: julito.reyes@nrca-nrcan.gc.ca

Five thermally immature marine deposited core samples with varying lithology and organic and sulphur contents were artificially matured using hydrous pyrolysis (HP). The samples were collected from middle late Miocene Onnagawa Formation (Japan), early Jurassic Gordondale member of the Fernie Formation (Canada), and late Devonian Duvernay Formation (Canada) (Fig. 1). Both T_{max} (403-431°C) and vitrinite reflectance ($VR = 0.49-0.65\%Ro$) confirm that all samples are immature. Hydrous pyrolysis was conducted using four different isothermal temperature and duration (310, 340 and 350°C for 3 days, and 350°C for 9 days). These combinations simulate physicochemical transformation of kerogen during peak hydrocarbon to early gas generation as confirmed by multiple previously published studies.

Post HP RockEval and VR analyses show that all samples were artificially matured. The T_{max} increases to 430-438°C after the first stage and 470-504°C after the last stage. These values have a VR equivalent ($VR_{equiv.}$) of 0.58-0.72%Ro to 1.19-1.32%Ro respectively, which are comparable to the measured VR of 0.66-0.74%Ro to 1.35-1.47%Ro. Petrographic analysis of the pyrolyzate shows significant evidence of the thermal degradation and transformation of kerogen as well as the generation and evolution of pore spaces. Moreover, some pore spaces were observed partially filled with produced solid bitumen. The results presented herein are part of a multidisciplinary study to determine the porosity generation and evolution in sedimentary rocks during oil to early phase of gas generation (Knapp et al., 2003).

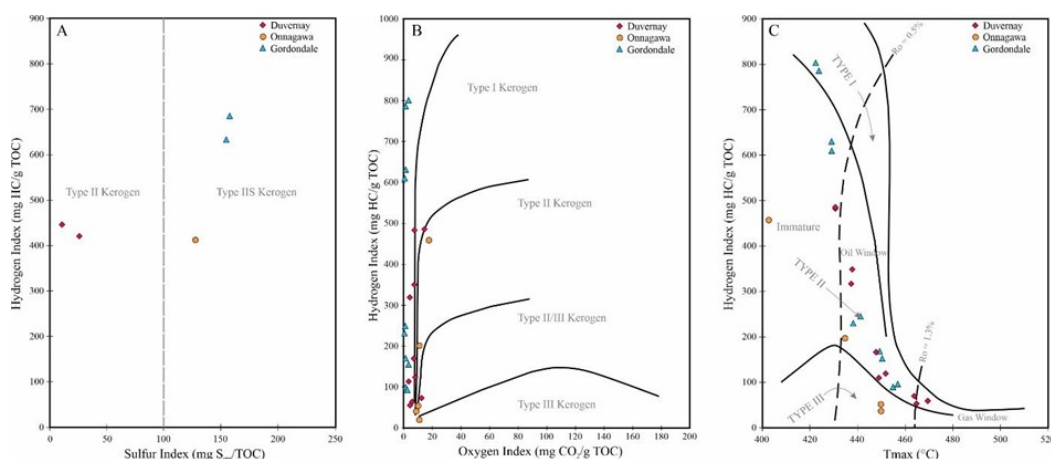


Figure 1. (A) Hydrogen Index (HI) versus Sulfur Index based on sulfur speciation using Rock-Eval 7S. (B) Hydrogen index (HI) versus oxygen (OI), and (C) HI versus Tmax plots. (from Knapp et al., 2023).

Reference

Knapp, L.J., Ardakani, O.H., Reyes, J., et al., 2023. Early porosity generation in organic-sulfur-rich mudstones. *Sci Rep* 13, 9904. <https://doi.org/10.1038/s41598-023-35259-5>

Author Index

Adamczyk B.	69	Erdenetsogt B.-O.	54
Adsul T.	44, 70	Esterle J.S.	7
Aggelopoulos M.	55	Fabiańska M.J.	35, 36, 62
Aires S.	64	Fike D.	44
Apostolova D.	80	Fiti A.	72
Ardakani O.H.	81	Flores D.	20, 64, 78
Aubrecht R.	36	Fonseca C.	27, 45, 59
Bachmann Ørberg S.	33	Font E.	56
Badenhorst C.	66	Galimberti R.	79
Bajuk-Bogdanović D.	65	Galleo J.L.R.	51
Bălănescu M.	73	Ganzorig R.	54
Bechtel A.	52, 53, 80	Garcia L.	73
Bian L.	24	Garcia-Gonzalez M.	23
Birdwell J.E.	21	Gentzis T.	26, 29
Biswas S.	47	Ghiran M.D.	73
Borghi L.	27	Ghosh S.	44, 70
Borrego A.G.	51, 73	Gilhooly III W.P.	44
Botoucharov N.	80	Gonçalves P.A.	45, 64, 78
Büçkün Z.	48	Goodarzi F.	26
Carvajal-Ortiz H.	29	Groß D.	52, 53, 80
Chatziapostolou A.	4	Guedes A.	61, 66
Christanis K.	49, 55, 63	Guo X.	74
Chrysakopoulou C.	58	Guo Xx.	16
Ciesielczuk J.	62	Guo Z.	19
Çolak M.	48	Hackley P.C.	21, 44, 70, 73, 77, 79
Corga M.	64	Hatcherian J.J.	44, 70
Costa M.	20	Havelcová M.	43
Damodhar Kamble A.	14	Heimhofer U.	7
de Lima D.M.	45	Houghton J.	44
de Oliveira A.D.	27, 45	Iliopoulos G.	49
de Oliveira Mendonça J.	27, 45, 64	Iordanidis A.	63
Demberelsuren B.	54	Ishikawa K.	81
Deskur H.	33	Jargal L.	54
Diez M.A.	73	Jelonek I.	15, 37, 67, 71
Dong Z.	75	Jelonek Z.	37, 67, 71
Drăgoescu M.F.	72	Johnson L.	6, 41
Drobniak A.	37, 67, 71	Jubb A.M.	21
Duarte L.V.	59	Kalaitzidis S.	34, 46, 49, 55, 58, 63, 73
Dudek L.	69	Kantiranis N.	58
Dudek M.	69	Kędzior S.	76
Eble C.	74	Khanaqa P.	46
Ejeh O.I.	55	Khash-Erdene T.	54
Engle M.A.	17	Knapp L.J.	81
Erbolato Filho J.	57	Kojić I.	53

**Organic Petrology in the Energy Transition Era:
Challenges ahead**

Bulletin of the Geological Society of Greece, Sp. Publ. 12

Kokkinopoulou K.	22	Ortiz J.E.	51
Kostova I.	80	Ortiz-Loaiza A.	78
Kouvtrakidis N.	63	Otgonbaatar J.	54
Krause-Jensen D.	33	Palmera-Henao T.S.	23
Křibek B.	43	Pandey S.	12, 39
Książek M.	34	Papadopoulou L.	58
Kumar Varma A.	44, 70, 73	Papadopoulou P.	49
Kus J.	73, 77	Parnell J.	79
Kuźniarska-Biernacka I.	61	Pasadakis N.	22
Kyriazaki E.	55	Pedersen P.K.	26
Larikova T.	43	Perleros K.	49, 55, 58
Larsen S.Y.	34	Petersen H.I.	28, 32, 33, 40
Li P.	17	Pinto de Jesus A.	20
Li W.	9	Plašienka D.	36
Li Y.	11, 16	Potočný T.	36
Lis G.P.	15	Predeanu G.	72, 73
Littke R.	7	Pusz S.	73
Liu A.	24	Rejdak M.	34
Liu C.	10	Ren Z.	16
Liu Y.	42	Reolid M.	59
Lkhagva-Ochir S.	54	Reyes J.	81
Louwye S.	59	Ribeiro J.	56, 57
Makri N.	63	Ribeiro M.	57
Makri V.I.	22	Riegel W.	46
Mancisidor D.	73	Rodriguez S.	73
Mascheroni L.	79	Rudra A.	28, 32, 33
Mastalerz M.	15, 37, 67, 71, 73	Sadd I.	6, 41
Matlala I.	68	Samoilă P.	72
McAleer R.J.	21	Sánchez-Palencia Y.	51
Melo R.	56	Sanei H.	24, 28, 32, 33, 40
Mendhe V.A.	12, 38, 39	Santos A.C.	61, 66
Mendonça Filho J.G.	27, 45, 59, 64, 78	Schito A.	79
Mertens K.N.	59	Schobert H.	74
Meyvisch P.	59	Schovsbo N.H.	24, 28
Milakovska Z.	35	Shao L.	8
Misz-Kennan M.	35, 36, 62, 73	Shao Y.	75
Mohebati S.	26	Shukla P.	12, 39
Molčan Matejová M.	36	Siavalas G.	73
Moreira K.	66	Singh A.K.	73
Moroeng O.M.	47, 68	Slăvescu V.	72
Moura H.	20	Smith G.	6, 41
Mousa E.	66	Song D.	11, 16
Mroczkowska-Szerszeń M.	69	Stefanova M.	35
Muirhead D.	79	Stefatos A.	3
Nikolić N.	65	Stenshøj R.Ø.	40
O'Beirne M.D.	44	Stojanović K.	52, 53
Ogala J.E.	55	Stojilković D.	65
Oikonomopoulos I.	29	Suárez Ruiz I.	73



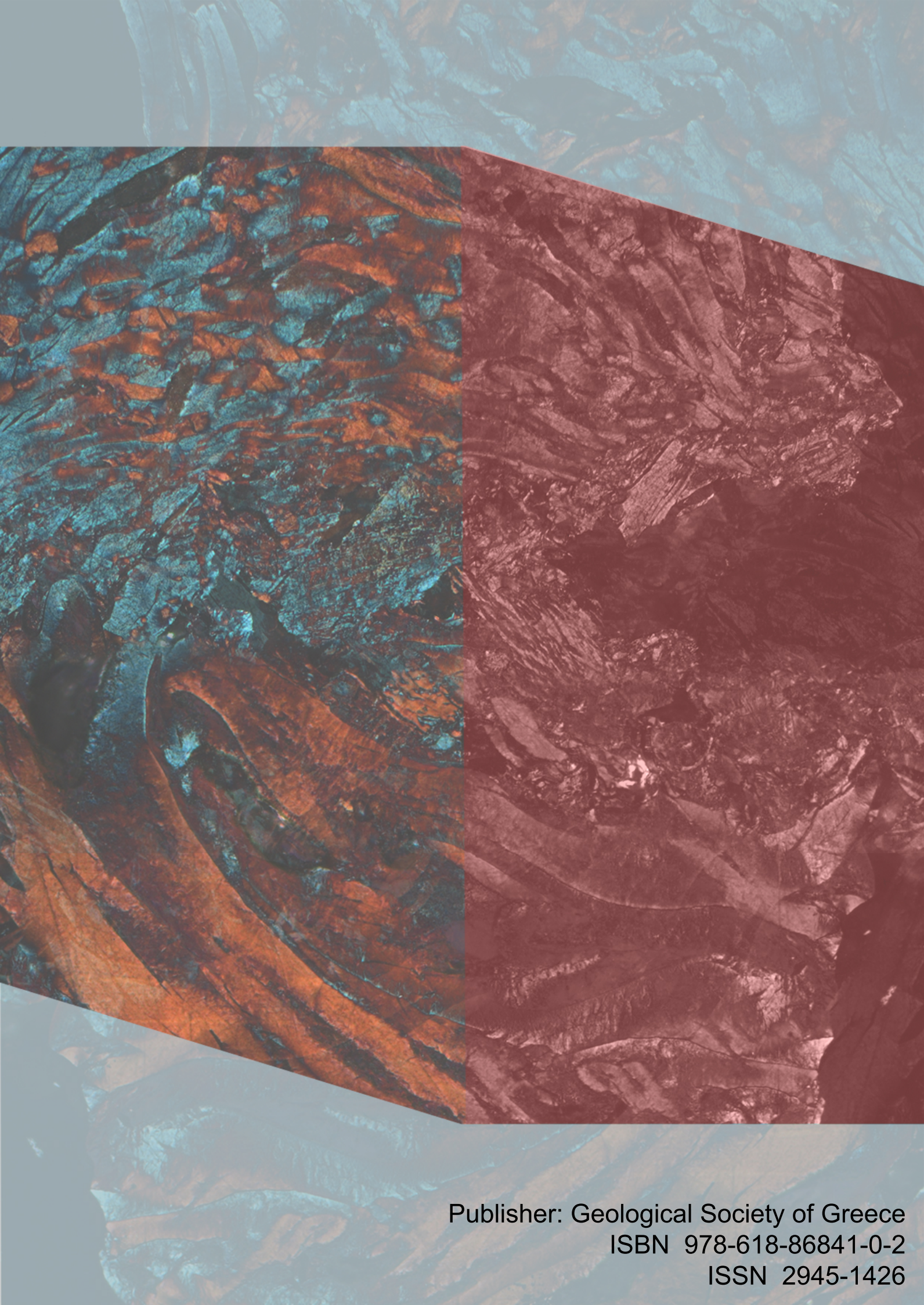
Joint 74th ICCP and 39th TSOP Meeting
17th – 24th September 2023, Patras, Greece



**Organic Petrology in the Energy Transition Era:
Challenges ahead**

Bulletin of the Geological Society of Greece, Sp. Publ. 12

Sun B.	10, 19
Sýkorová I.	43
Szram E.	36, 62
Tang Y.	74
Tomillo P.	73
Topór T.	15
Torres Souza J.	27
Torres T.	51
Tripsanas E.	29
Tugj O.	54
Valentim B.	61, 66
Valentine B.J.	21
Vladislavov G.	35
Wagner N.J.	47, 68
Wang H.	16
Wang J.	60
Wang Q.	17
Wang S.	74, 75
Werne J.P.	44
Wheeler A.	7
Więclaw D.	35, 62
Wojtaszek-Kalaitzidi M.	34, 58, 73
Xenakis M.	4
Xiao R.	60
Xie X.	42
Xu N.	17
Xu Y.	42
Yang W.	9
Ye G.	66
Zdravkov A.	52, 53, 73, 80
Zhai Y.	11
Zhang J.	60
Zhao L.	75
Zhao Y.	60
Zheng X.	24, 40
Zhou Z.	28
Zielińska M.	36
Ziemianin K.	69
Životić D.	65, 73
Životić M.	65
Zorigbold T.	54
Zouros N.	49



Publisher: Geological Society of Greece
ISBN 978-618-86841-0-2
ISSN 2945-1426